Characterisation of reactive species in the Fenton reaction:

$^{\bullet}OH$ vs. Fe^{IV}

Dissertation

zur Erlangung des akademischen Grades eines

Doktors der Naturwissenschaften

− Dr. rer. nat. −

vorgelegt von

Hanna Laura Wiegand

geboren in Essen

Institut für Instrumentelle Analytische Chemie

der

Universität Duisburg-Essen

2018

Die vorliegende Arbeit wurde im Zeitraum von April 2014 bis Februar 2018 im Arbeitskreis von Prof. Dr. Torsten C. Schmidt am Institut für Instrumentelle Analytische Chemie der Universität Duisburg-Essen durchgeführt.

Tag der Disputation: 12.04.2019

Gutachter: Prof. Dr. Torsten C. Schmidt

Prof. Dr. Malte Behrens

Vorsitzender: Prof. Dr. Eckhard Hasselbrink

DOI: 10.17185/duepublico/70144
URN: urn:nbn:de:hbz:464-20200407-072932-8

DANKSAGUNG

Mein besonderer Dank gilt Prof. Dr. Torsten C. Schmidt, der mir die Möglichkeit gab, diese Arbeit in seiner Arbeitsgruppe anzufertigen. Wissenschaftlich ließ er mir stets den Freiraum eigene Ideen umzusetzen und stand mir bei Bedarf immer mit Rat und Tat zur Seite. Prof. Dr. Malte Behrens danke ich für die Übernahme des Zweitgutachtens.

Ausdrücklich möchte ich mich auch bei Dr. Holger Lutze bedanken für die vielen hilfreichen Diskussionen, die Unterstützung und die konstruktive Kritik. Dank gebührt außerdem Timon Orths, Katharina Hupperich und Mischa Jütte, deren Master- bzw. Bachelorarbeiten ich betreuen durfte und die mit ihrer Arbeit maßgeblich zum Gelingen dieser Arbeit beigetragen haben. Ebenfalls möchte ich Michelle Lüling danken für die Unterstützung im Labor.

Bei allen derzeitigen und ehemaligen Mitarbeitern der Instrumentellen Analytischen Chemie möchte ich mich bedanken für die angenehme Arbeitsatmosphäre, die gute Zusammenarbeit, für die guten Gespräche und die schöne gemeinsame Zeit. Insbesondere möchte ich der AOP-Gruppe (Dr. Holger Lutze, Alexandra Beermann, Alexandra Fischbacher, Jens Terhalle, Sarah Willach und Vanessa Wirzberger) für den hilfreichen, fachlichen Austausch, das angenehme Miteinander im Büro und die vielen gemeinsamen Ausflüge danken.

Dank gebührt ebenfalls der Deutschen Forschungsgemeinschaft, deren Förderung der Bearbeitung dieses Projekts den finanziellen Rahmen gab.

Ganz besonders bedanken möchte ich mich bei meinen Eltern Silke und Bernd und meiner Schwester Isabel für die immerwährende Unterstützung, den Glauben an mich und dafür, dass sie immer hinter mir gestanden haben. Meinen Freunden, ganz besonders Florian Metzelder, danke ich ebenfalls für die Unterstützung in den letzten Jahren.

ABSTRACT

The term Fenton reaction describes the reaction of divalent iron (Fe^{II}) with hydrogen peroxide (H_2O_2) leading to formation of highly reactive species. Even though the reaction is known for more than 100 years, its mechanism is no fully resolved yet. In literature formation of an intermediate iron-peroxo-complex ($Fe(H_2O_2)^{2+}$) is suggested, which is supposed to lead to formation of hydroxyl radicals ($^{\bullet}OH$) at acidic pH and to a tetravalent iron species (Fe^{IV}) at neutral or alkaline conditions. However, no experimental evidence for the formation of this intermediate could be found, yet. Elucidation of the Fenton mechanism is not only of scientific interest but also with regard to the use of the Fenton reaction in oxidative water treatment or pollutant degradation.

Accordingly, the present study aims to further elucidate the Fenton mechanism. For this purpose, the influence of various reaction conditions on existence, formation and stability of the postulated $Fe(H_2O_2)^{2+}$-complex and resulting reactive products will be investigated. Additionally, the influence of different reaction conditions on the degradation of a model compound (bisphenol S) will be investigated. Finally, an alternative reaction leading to the formation of Fe^{IV} will be examined in order to investigate if Fe^{IV} is a relevant oxidant in the Fenton reaction.

This thesis presents the first kinetic indication for the existence of the postulated $Fe(H_2O_2)^{2+}$-complex. Regardless of the Fe^{II}-concentration, at pH 3 the complex reveals constant stability, which is neither affected by the presence of an $^{\bullet}OH$-scavenger. When the pH is increased from 1 to 4 decreasing decay rates of the intermediate are observed (ca. 70 s^{-1} at pH 1 and 2 and ca. 50 s^{-1} at pH 3 and 4). Furthermore, regardless of the pH determined $^{\bullet}OH$-yields of ~100% based on the applied Fe^{II}-concentration did not reveal any indication for the formation of Fe^{IV}.

Examination of the pH-dependent influence of various organic chelating ligands indicates that even in the presence of these ligands an intermediate $Fe(H_2O_2)^{2+}$-complex is formed, which forfeits stability with increasing pH. The quantification of •OH-concentrations again does not reveal any indication of the formation of Fe^{IV} even in ligand-assisted Fenton reactions.

Investigations on the Fenton-based degradation of bisphenol S (BPS) shows that degradation can be influenced by applied reactant concentrations. However, it must be considered that too high concentrations of Fe^{II} and H_2O_2 may also cause •OH-scavenging effects, which compete with degradation of contaminants. The optimum pH for BPS degradation was pH 3. Additionally, it could be shown that the Fenton-based degradation of contaminants in absence of ligands keeping Fe^{III} dissolved is not restricted to acidic pH as it is hitherto assumed. Even at pH 7 BPS was completely degraded. At pH values < 3, BPS degradation was observed to be restricted by insufficient Fe-recycling. The presence of •OH-consuming matrix components also limits BPS degradation. Comparative experiments dealing with the Fenton degradation of *para*-chlorobenzoic acid at pH 3 and 7, again did not show any indication for the formation of Fe^{IV} in the Fenton reaction, which could be involved in the degradation of the investigated pollutants.

The reaction described in literature for the generation of Fe^{IV} from Fe^{II} and ozone (O_3) could not be reproduced. Instead, the results suggest that Fe^{III} is directly formed.

In summary, the first kinetic indication for the existence of the hitherto postulated intermediate $Fe(H_2O_2)^{2+}$-complex was obtained, which was observed to exclusively yield •OH at all reaction conditions investigated. Gained information can be used to make the application of the Fenton reaction more efficient in terms of wastewater treatment and remediation of contaminated sites. Nevertheless, further research is required to fully understand the whole Fenton process.

ZUSAMMENFASSUNG

Charakterisierung reaktiver Spezies in der Fenton Reaktion: $^{\bullet}OH$ vs. Fe^{IV}

Der Begriff Fenton Reaktion beschreibt die Reaktion von zweiwertigem Eisen (Fe^{II}) mit Wasserstoffperoxid (H_2O_2), die zur Bildung hoch reaktiver Spezies führt. Obwohl die Reaktion bereits seit über 100 Jahren bekannt ist, ist ihr Mechanismus noch nicht vollständig aufgeklärt. Postuliert wird die Bildung eines intermediären Eisen-Peroxo-Komplexes ($Fe(H_2O_2)^{2+}$), der bei der Reaktion von Fe^{II} mit H_2O_2 entsteht und in saurem Millieu zu Hydroxylradikalen ($^{\bullet}OH$) und bei neutralem bis alkalischem pH-Wert zu tetravalentem Eisen (Fe^{IV}) reagiert. Einen experimentellen Nachweis für die Bildung dieses Komplexes gibt es bisher nicht. Die Aufklärung des Fenton-Mechanismus ist dabei nicht nur von wissenschaftlichem Interesse, sondern auch im Hinblick auf den Einsatz der Fenton Reaktion in der Wasseraufbereitung.

Entsprechend ist es das Ziel der vorliegenden Arbeit, den Mechanismus der Fenton Reaktion weiter aufzuklären. Zu diesem Zweck soll der Einfluss verschiedener Reaktionsbedingungen auf Existenz, Bildung und Stabilität des postulierten $Fe(H_2O_2)^{2+}$-Komplexes untersucht werden, sowie auf die entstehenden reaktiven Produkte. Zusätzlich soll der Abbau einer Modellverbindung (Bisphenol S) betrachtet werden. Final soll eine alternative Reaktion zur Bildung von Fe^{IV} untersucht werden, um auf diese Weise herauszufinden, ob Fe^{IV} als reaktive Spezies in der Fenton Reaktion tatsächlich relevant ist.

Die vorliegende Arbeit zeigt den ersten kinetischen Hinweis auf die Existenz des postulierten $Fe(H_2O_2)^{2+}$-Komplexes. Unabhängig von der eingesetzten Fe^{II}-Konzentration weist dieser bei pH 3 eine gleichbleibende Stabilität auf, die auch durch die Anwesenheit eines $^{\bullet}OH$-Scavengers nicht beeinflusst wird. Im pH-Bereich von 1 bis 4 wurden bei gleichbleibender Fe^{II}-Konzentration mit steigendem pH-Wert geringer werdende Zerfallsraten des $Fe(H_2O_2)^{2+}$-Komplexes beobachtet (ca. 70 s^{-1} bei pH 1 und 2 und ca. 50 s^{-1} bei pH 3 und 4). Außerdem konnten anhand der bestimmten $^{\bullet}OH$-Ausbeuten von ~100 % bezogen auf die eingesetzte Fe^{II}-Konzentration bei pH 1 bis 4 keine Hinweise auf die Bildung von Fe^{IV} beobachtet werden.

Die Untersuchung des pH-abhängigen Einflusses von verschiedenen organischen Chelatliganden weist darauf hin, dass es auch in Anwesenheit der chelatisierenden Liganden zur Ausbildung eines intermediären Eisen-Peroxo-Komplexes kommt, der mit zunehmendem pH-Wert an Stabilität verliert. Die Quantifizierung der •OH-Konzentrationen lässt erneut nicht auf die Bildung von Fe^{IV} in der Fenton Reaktion schließen.

Die Untersuchung des Abbaus von Bisphenol S (BPS) mit Hilfe der Fenton Reaktion zeigt, dass sich die Abbaugeschwindigkeit durch die eingesetzten Fe^{II}- und H_2O_2-Konzentrationen beeinflussen lässt. Dabei ist zu beachten, dass durch eine zu starke Erhöhung der Fe^{II}- und H_2O_2-Konzentrationen auch •OH-zehrende Effekte auftreten können, die mit dem Abbau von Schadstoffen konkurrieren. Der optimale pH-Wert für den BPS-Abbau lag bei pH 3. Gleichzeitig konnte gezeigt werden, dass der Abbau von Schadstoffen mit Hilfe der Fenton Reaktion nicht wie bisher angenommen auf den sauren pH-Bereich beschränkt ist. Auch bei pH 7 konnte BPS vollständig abgebaut werden. Bei pH-Werten < 3 wurde beobachtet, dass der BPS-Abbau durch unzureichendes Fe-Recycling eingeschränkt wird. Durch die Anwesenheit •OH-zehrender Matrixbestandteile wurde der BPS-Abbau ebenfalls eingeschränkt. Vergleichende Experimente mit *para*-Chlorbenzoesäure ergaben sowohl bei pH 3 als auch bei pH 7 erneut keinerlei Hinweise auf die Bildung von Fe^{IV} in der Fenton Reaktion, die am Abbau der untersuchten Schadstoffe beteiligt sein könnten.

Die in der Literatur beschriebene Reaktion zur Synthese von Fe^{IV} aus Fe^{II} und O_3 konnte nicht reproduziert werden. Stattdessen lassen die Ergebnisse darauf schließen, dass es in der beschriebenen Reaktion zur direkten Bildung von Fe^{III} kommt.

Insgesamt konnten in der vorliegenden Arbeit der erste kinetische Hinweise auf die Existenz des zuvor nur postulierten intermediären $Fe(H_2O_2)^{2+}$-Komplexes gewonnen werden, der unter allen untersuchten Reaktionsbedingungen quantitativ zu •OH reagiert. Diese mechanistischen Erkenntnisse können genutzt werden, um die Anwendung der Fenton Reaktion zur Aufbereitung von Abwässern und zur Entfernung von Schadstoffen effizienter zu gestalten. Trotzdem sind weitergehende Untersuchungen nötig, um die Fenton Reaktion vollständig verstehen zu können.

TABLE OF CONTENTS

Chapter 1 -

INTRODUCTION

1.1 WATER & WASTE WATER TREATMENT

According to the European water framework directive 2000/60/EC (WFD) rivers, lakes, transitional waters, coastal waters as well as ground waters should achieve good qualitative and quantitative status at the latest by the year 2027. In this context increased protection and improvement of the environment is aimed among others by a stepwise reduction of discharge and emission of priority and priority hazardous substances.[1] Thereby, the good status of raw water sources is not only important with respect to ecological soundness of water bodies. Additionally, it is the basis for safe drinking water. In this regard, effective wastewater treatment is important in order to avoid contamination of receiving raw waters by residual pollutants.

Methods recently applied for the removal of trace contaminants include physical treatment (e.g. sorption with activated carbon or membrane filtration), biological treatment (e.g. biological filtration) and chemical treatment (e.g. advanced oxidation processes). Contaminant removal by physical treatment is based on physical separation of pollutants from the water to be purified. Biological treatment requires biodegradability of pollutants. A major drawback of biological pollutant control is that the biological community needs time to adapt to current conditions prior to biodegradation. Hence, it is not able to cope with spontaneous events. In terms of chemical treatment oxidative water treatment with ozone as well as so-called advanced oxidation processes (AOPs) are most commonly used. AOPs are defined as those processes, "which involve the generation of hydroxyl radicals (•OH) in sufficient quantity to affect water purification"[2].

According to the definition of AOPs given by Glaze, *et al.* (1987)[2] many different processes can be rated as such. All these processes have in common that mostly a combination of a strong

oxidant (e.g. ozone (O_3) or hydrogen peroxide (H_2O_2)), a catalyst (e.g. transition metal ions or photo-catalysts) and/or irradiation (e.g. ultraviolet (UV)) is used.[3] In the following, typical AOPs mentioned in literature are listed: photolysis of H_2O_2, peroxone process ($O_3 + H_2O_2$), O_3 + natural organic matter (NOM), O_3 + UV, O_3 + activated carbon, ionising radiation, vacuum + UV, Fenton reaction ($Fe^{II} + H_2O_2$), and photo-Fenton reaction ($Fe^{III} + H_2O_2 + UV$).[4]

As this thesis focusses on the Fenton reaction, the present Chapter 1 - will compare different AOPs frequently applied for wastewater treatment and demonstrate why especially the Fenton reaction is suitable to treat highly contaminated industrial wastewaters. Additionally, the relevance of the Fenton reaction in fields other than wastewater treatment will be explained. This will reveal the importance of fully understanding underlying mechanisms in the Fenton reaction. For although, the Fenton reaction is known for more than 100 years, as well as intensively studied and applied for oxidation of various compounds, the exact reaction mechanism is still a subject of controversial discussion and not fully understood yet. Especially, the question concerning involved reactive species could not be entirely elucidated up to now.

1.2 CHARACTERISTICS OF ˙OH

1.2.1 KINETICS AND MECHANISMS OF ˙OH-REACTIONS

˙OH are way more reactive and nonselective than other oxidising species which are used for oxidative treatment of drinking and wastewater.[4] They can react with various organic contaminants via three different mechanisms: (1) addition to C=C, C=N and S=O double bonds, (2) H-abstraction, and (3) electron-transfer.

Usually, the addition to double bonds is almost diffusion controlled ($k \approx 10^9$ M^{-1} s^{-1}). Nevertheless, the side of attack is controlled by the electrophilic character of •OH, resulting in region selective reactions.[4]

In contrast, the rate of H-abstraction depends on the R-H bond dissociation energy (BDE). S-H bonds are attacked very fast, C-H bonds notably slower taking into account that it is important whether the relevant C-atom is tertiary, secondary, or primary. The attack on O-H bonds can almost be neglected.[4]

•OH induced electron transfer reactions only take place when the addition to double bonds or H-abstraction are kinetically disfavoured, e.g. for steric reasons.[5] Thus, the high oxidation-reduction potential (E^0) of 2.02 V according to which •OH is one of the strongest oxidants, is not directly connected with its high reactivity.[4, 6]

1.2.2 DETECTION OF •OH

In order to compare different AOPs with regard to their capability to degrade contaminants it is important to quantify •OH generated under certain conditions. Several methods suitable to quantify •OH-yields in various systems are described in literature including electron paramagnetic resonance (EPR) spectroscopy, spectrophotometric methods, chromatographic methods or electrochemical methods.[7-23]

Electron paramagnetic resonance spectroscopy

EPR (also called electron spin resonance) spectroscopy is a technique, which can be used to detect paramagnetic species. In the presence of an external magnetic field, these species absorb microwave energy resulting in the transition of spin states.[7]

In combination with spin trapping EPR spectroscopy enables detection of unstable and highly reactive radicals such as ˙OH or perhydroxyl radicals (HO_2˙), which are undetectable under normal conditions.[7-8] During spin trapping such short-lived radicals react with spin traps to form more stable radical adducts which are detectable by EPR.[7-8] For each spin adduct a characteristic EPR spectrum can be detected enabling differentiation of various radicals. A molecule frequently used as spin trapping agent in liquids is 5,5-dimethyl-1-pyrroline N-oxide (DMPO).[7-8] However, in presence of ferric ion (Fe^{III}) spin trapping of ˙OH with DMPO can lead to false positive results. The Fe^{3+} can catalyse the nucleophilic addition of water to DMPO and subsequent oxidation of the EPR-active nitroxide resulting in the formation of the DMPO-OH adduct.[7] Furthermore, EPR is not well suitable to quantify ˙OH as the generated spin-adduct is not stable.[9]

Tertiary butanol (t-BuOH) as ˙OH-trap

t-BuOH is a molecule frequently used as ˙OH-trap in terms of radical quantification.[16, 19, 23] In the primary reaction of ˙OH with *t*-BuOH ($k = 3 \times 10^8$ M^{-1} s^{-1})[24] the radical abstracts an H-atom mainly from carbon (95%) or from oxygen (5%). The product of the latter reaction, the tertiary butoxyl radical immediately decomposes into acetone and a methyl radical via β-fragmentation. In the presence of molecular oxygen (O_2) the carbon centred radical yields a perhydroxyl radical, which finally yields acetone, formaldehyde (CH_2O), 2-hydroxy-2-methylpropanal, and 2-hydroxy-2-methylpropanol via different chain reactions.[16, 19] The generated CH_2O can then be quantified either by the Hantzsch method or after derivatisation with 2,4-dinitrophenyl-hydrazine (DNPH) via high performance liquid chromatography (HPLC) coupled with an UV detector.[16, 19, 23] However, the CH_2O-yield depends on the ˙OH-generating system. In case of a radiolytic system, ~ 25% of ˙OH were converted into CH_2O whereas in ozonolysis the CH_2O-

yield corresponds to 48% of the ˙OH-yield.[16, 19] Nothing is known about CH_2O-yields in other ˙OH-generating systems.

Dimethyl sulfoxide (DMSO) as ˙OH-trap

Another molecule frequently utilised as ˙OH-trap is DMSO. The reaction of ˙OH with DMSO is effectively diffusion controlled ($k = 7 \times 10^9\ M^{-1}\ s^{-1}$)[24] and leads to the formation of methyl radicals (˙CH_3) and methane sulfinic acid (MSIA) (Figure 1.1). Thereby, the yield of MSIA corresponds to 92% of ˙OH available.[25] In presence of O_2 MSIA is further oxidised to methane sulfonic acid (MSOA) (Figure 1.1).[21] Hence, combined detection of MSIA and MSOA (in Figure 1.1 both highlighted in red) is essential for reliable quantification of ˙OH-yields and can be achieved by ion chromatography (IC).[19]

Alternatively, CH_2O (highlighted in green), which is also quantitatively produced during ˙OH-based oxidation of DMSO (Figure 1.1) is used to quantify ˙OH.[9, 18, 22]

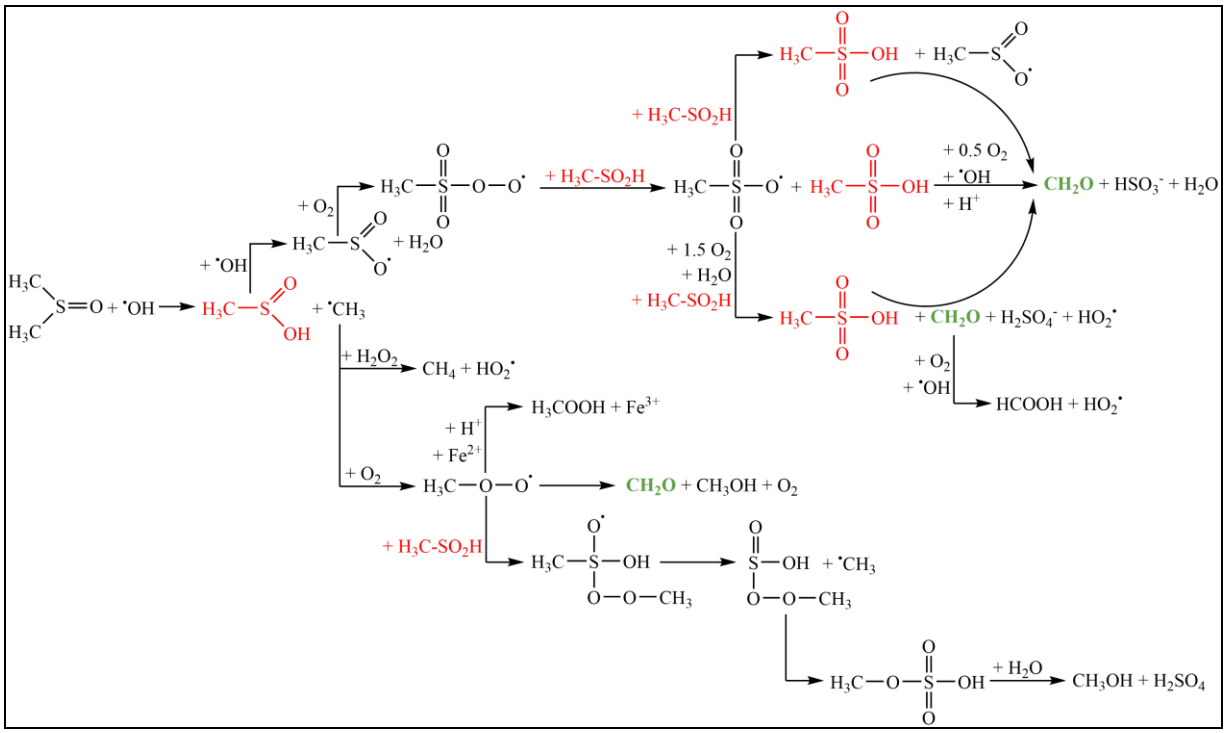

Figure 1.1: Sequence of reactions occurring in ˙OH-based oxidation of DMSO based on reactions given by Flyunt et al. (2001/2003).[19, 21]

1.3 AOPS FREQUENTLY APPLIED FOR WATER TREATMENT

As mentioned above, the definition of AOPs given by Glaze, *et al.* (1987)[2] comprises several processes. In the following, some important AOPs will be described in more detail.

1.3.1 PHOTOLYSIS OF H_2O_2

In the photolysis of H_2O_2 two $^{\bullet}OH$ are generated per H_2O_2-molecule, at least in the gas phase.

$$H_2O_2 + h\nu \rightarrow 2\ ^{\bullet}OH \qquad (1.1)$$

In aqueous solution the two radicals are held together by a so-called solvent cage for a certain time. In this time, the radicals can either recombine and re-form H_2O_2 or diffuse out of the solvent cage. This leads to a $^{\bullet}OH$-yield of only 50%.[26] Additionally, the low absorption coefficient of H_2O_2 limits the efficiency of H_2O_2-photolysis. As H_2O_2 only absorbs at wavelengths below 280 nm and has a molar extinction coefficient (ε) of 20 M^{-1} cm^{-1} at 254 nm, for high absorption either high concentrations of H_2O_2 or long path lengths are required. On the other hand an increased H_2O_2-concentration will increase the frequency of reactions between $^{\bullet}OH$ and H_2O_2 and therefore, lower the efficiency of the whole process.[4]

1.3.2 PEROXONE PROCESS

The peroxone process describes the reaction of O_3 with H_2O_2. This reaction strongly depends on the pH as the reaction of H_2O_2 itself with O_3 is very slow (k < 0.01 M^{-1} s^{-1}) whereas the reaction of the anion HO_2^- is fast ($k = 5.5 \times 10^6$ M^{-1} s^{-1}) (reaction 1.2).[4, 27-28] Due to competing reactions (1.3, 1.4), the $^{\bullet}OH$-yield is only 50% with respect to O_3 consumption as only $O_3^{\bullet-}$ yields $^{\bullet}OH$ (reaction 1.5).[23] For applications of the peroxone process in real water matrices $^{\bullet}OH$-formation from O_3-reactions with NOM (see chapter 1.3.3) must be taken into account.[29]

$$O_3 + HO_2^- \rightleftharpoons HO_5^- \qquad (1.2)$$

$HO_5^- \rightarrow 2\ {}^3O_2 + OH^-$ (1.3)

$HO_5^- \rightarrow O_3^{\bullet-} + HO_2^{\bullet}$ (1.4)

$O_3^{\bullet-} + H_2O \rightleftharpoons O_2 + OH^- + {}^{\bullet}OH$ (1.5)

1.3.3 O_3 + NOM

In natural waters O_3 reacts with NOM under $^{\bullet}OH$-formation. In a first step O_3 reacts with NOM to form a $NOM^{\bullet+}$ molecule and $O_3^{\bullet-}$ (reaction 1.6).[30] will react with H_2O yielding O_2, $^{\bullet}OH$ and OH^- (reaction 1.5).[4]

$O_3 + NOM \rightarrow O_3^{\bullet-} + NOM^{\bullet+}$ (1.6)

For wastewater the $^{\bullet}OH$-yield has been determined to be about 10% with respect to the dosed O_3-concentration.[29]

1.4 THE FENTON REACTION

1.4.1 HISTORY OF THE FENTON REACTION

The reaction of divalent iron (Fe^{II}) with H_2O_2 is known as Fenton reaction. In the 1890**s**, Henry J. H. Fenton was the first who systematically investigated the activating effect of Fe^{II} on H_2O_2 enabling oxidation of polyhydric alcohols and organic acids.[31-33] In 1926, Walton and Christensen (1926)[34] were the first who used the term "Fenton reaction" as such when they investigated "the catalytic influence of Fe^{III} on the oxidation of ethanol by H_2O_2".[34] In that time, nothing was known about the background of such oxidation reactions.

In the 1930s, different approaches were developed to explain the catalytic effect of Fe^{II} on H_2O_2 based oxidations. Bray and Gorin (1932)[35] suggested that a tetravalent iron species (Fe^{IV}), possibly the ferryl ion (FeO^{2+}), might be the reactive product of the Fenton reaction (reaction 1.7).[35]

$$Fe^{II} + H_2O_2 \rightarrow FeO^{2+} + H_2O \qquad (1.7)$$

At the same time, Haber and Weiss developed a mechanism involving the formation of $^{\bullet}OH$ (reactions 1.8 – 1.11).[36-38]

$$Fe^{II} + H_2O_2 \rightarrow Fe^{III} + OH^- + {}^{\bullet}OH \qquad k = 40 - 80\ M^{-1}\ s^{-1} \qquad (1.8)^{39}$$

$^{\bullet}OH$ generated via reaction 1.8 can be quenched either by H_2O_2 or Fe^{II} (reactions 1.9 and 1.10) depending on experimental conditions. This leads to a reduced amount of radicals, which can oxidise target compounds.

$$^{\bullet}OH + H_2O_2 \rightarrow H_2O + HO_2^{\bullet} \qquad k = 2.7 \times 10^7\ M^{-1}\ s^{-1} \qquad (1.9)^{24}$$

$$^{\bullet}OH + Fe^{II} \rightarrow Fe^{III} + OH^- \qquad k = 3 \times 10^8\ M^{-1}\ s^{-1} \qquad (1.10)^{24}$$

$$HO_2^{\bullet} + H_2O_2 \rightarrow O_2 + H_2O + {}^{\bullet}OH \qquad k = 3\ M^{-1}\ s^{-1} \qquad (1.11)^{40}$$

The radical chain mechanism proposed by Haber and Weiss was revised and expanded by Barb, *et al.* (1951)[41] in the early 1950s (reactions 1.12 – 1.15). $HO_2^{\bullet}$ formed in reactions 1.9 and 1.12 also participate in the Fenton chain reaction. They can either react with Fe^{III}, Fe^{II} or another $HO_2^{\bullet}$ (reactions 1.13 – 1.15). Their proposed mechanism involving catalytic cycling between Fe^{II} and Fe^{III} is nowadays referred to as “classical” or “free radical” Fenton chain reaction.[39]

$$Fe^{III} + H_2O_2 \rightarrow Fe^{II} + HO_2^{\bullet} + H^+ \qquad \text{(see below)} \qquad (1.12)$$

$$HO_2^{\bullet} + Fe^{II} + H^+ \rightarrow Fe^{III} + H_2O_2 \qquad k = 1.2 \times 10^6\ M^{-1}\ s^{-1} \qquad (1.13)^{42}$$

$HO_2^{\bullet} + Fe^{III} \rightleftharpoons Fe^{II} + O_2 + H^+$ $k = 1.5 \times 10^5\ M^{-1}\ s^{-1}$ (1.14)[43-44]

$HO_2^{\bullet} + HO_2^{\bullet} \rightarrow H_2O_2 + O_2$ $k = 1 \times 10^6\ M^{-1}\ s^{-1}$ (1.15)[45]

Actually, the Fenton-like reaction (reaction 1.12) is a twostep process. At first, Fe^{III} and H_2O_2 form a complex (reactions 1.12-1a – 1.12-1b), which in the following decomposes into Fe^{II} and $HO_2^{\bullet}$ (reactions 1.12-2a – 1.12-2b). Whereas Fe^{II}-speciation remains constant at pH values relevant for Fenton chemistry[46] Fe^{III}-speciation changes in this pH range.[47] At pH ≤ 2.2 Fe^{3+} is the dominant Fe^{III}-species and changes into $Fe(OH)^{2+}$ in the pH range 2.2 – 3.5. At pH ≥ 3.5 $Fe(OH)_2^+$ becomes prevalent (see Figure 1.2). These species show differences in the complex formation equilibrium of about one order of magnitude, whereas in case of the decay of the complex it cannot be differentiated kinetically between $Fe(OOH)^{2+}$ and $Fe(OH)(OOH)^+$.[48-49]

$Fe^{3+} + H_2O_2 \rightleftharpoons Fe(OOH)^{2+} + H^+$ $K = 3.1 \times 10^{-3}$ (1.12-1a)[48]

$FeOH^{2+} + H_2O_2 \rightleftharpoons Fe(OH)(OOH)^+ + H^+$ $K = 2 \times 10^{-4}$ (1.12-1b)[48]

$Fe(OOH)^{2+} \rightarrow Fe^{2+} + HO_2^{\bullet}$ $k = 2.7 \times 10^{-3}\ s^{-1}$ (1.12-2a)[49]

$Fe(OH)(OOH)^+ \rightarrow FeOH^+ + HO_2^{\bullet}$ $k = 2.7 \times 10^{-3}\ s^{-1}$ (1.12-2b)[49]

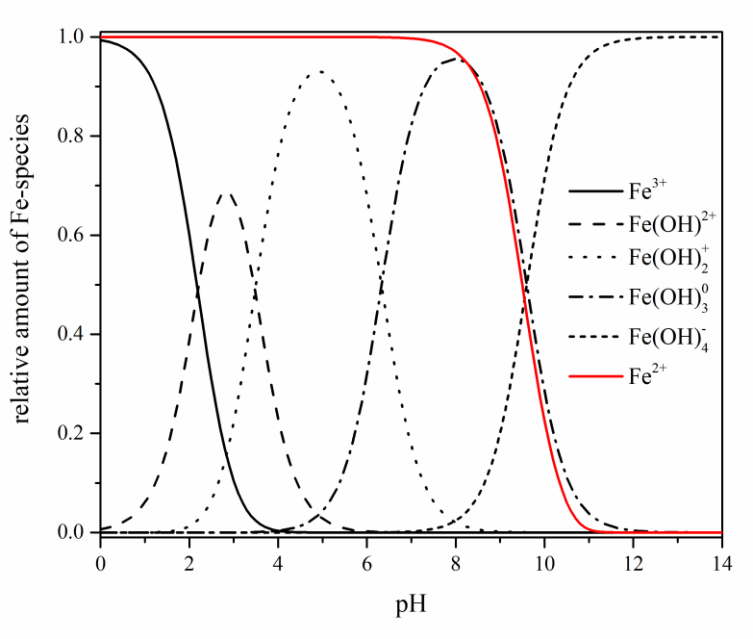

Figure 1.2: pH-dependent speciation of Fe^{II} (red) and Fe^{III} (black). The plot was created based on complex stability data published by [50].

According to comparison of experimental and calculated rate constants for the Fe^{II} + H_2O_2 reaction Goldstein, *et al.* (1993)[51] concluded that the oxidation of Fe^{II} by H_2O_2 is unlikely to occur via an outer sphere electron transfer mechanism, which would require the formation of $H_2O_2^{\bullet-}$ as transient radical anion. They found that calculated rate constants were much lower than experimental ones. Hence, the primary step in the reaction of Fe^{II} with H_2O_2 is widely accepted to occur via an inner sphere electron transfer mechanism.[51] In analogy to the reaction of Fe^{III} and H_2O_2 in which at first a labile water molecule of $Fe(H_2O)^{3+}$ is exchanged by H_2O_2,[48] in case of Fe^{II} also the exchange of a water ligand by H_2O_2 leading to the formation of a hydrated Fe^{II}-H_2O_2-complex ($Fe(OOH)(H_2O)_5^+$) is thermodynamically favoured (reaction 1.16). To simplify reaction equations, in the following water ligands are neglected.

$$Fe^{II} + H_2O_2 \rightleftharpoons FeOOH^+ + H^+ \qquad (1.16)$$

According to von Sonntag (2008)[4] the complex is formulated as $FeOOH^+$.[4] Rachmilovich-Calis, *et al.* (2009)[52] suggested a pH-dependent equilibrium of $FeOOH^+$ as formulated in reaction 1.17.

$$FeOOH^+ + H^+ \rightleftharpoons Fe(H_2O_2)^{2+} \quad (1.17)$$

Hence, reaction (1.16) can also be expressed as

$$Fe^{II} + H_2O_2 \rightleftharpoons Fe(H_2O_2)^{2+} \quad (1.18)$$

The formation of this intermediate is nowadays widely accepted,[51, 53-55] even though experimental evidence for its existence is still missing.[4, 39] Experimental evidence for the existence of $FeOOH^+$ would finally confirm that the reaction between Fe^{II} and H_2O_2 occurs via an inner sphere electron transfer[39] as an outer sphere electron transfer would require the formation of $H_2O_2^{-\bullet}$ as transient radical ion.[51]

Additionally, there is a still ongoing controversial discussion concerning the type of oxidant involved in the Fenton reaction. Up to now the exact mechanism of the Fenton reaction could not be fully elucidated, even though it has been subject of numerous studies in the past decades regarding fundamentals of the Fenton reaction itself[41, 52-53, 56-60] and pollutant degradation by means of Fenton[61-66] or modified Fenton reaction (e.g. photo-Fenton[67-69], electro-Fenton[70-73], photoelectro-Fenton[74], ligand-assisted Fenton[75-81]). It is assumed that the formed complex could either react further via a one-electron transfer to form Fe^{III} and $^\bullet OH$ (reaction 1.19) or via a two-electron transfer yielding Fe^{IV} (reaction 20). [4, 82-85]

$$Fe(H_2O_2)^{2+} \rightarrow Fe^{III} + OH^- + {}^\bullet OH \quad (1.19)$$

$$Fe(H_2O_2)^{2+} \rightarrow FeO^{2+} + H_2O \quad (1.20)$$

FeO^{2+} generated via reaction 1.20 might further react with Fe^{II} to form Fe^{III} without yielding any $^{\bullet}OH$ (reaction 1.21).

$$FeO^{2+} + Fe^{II} + 2\ H^{+} \rightarrow 2\ Fe^{III} + H_2O \qquad (1.21)$$

Reaction 1.19 is likely to be dominant at acidic conditions whereas reaction 1.20 is supposed to be dominant at circumneutral pH.[4] This is confirmed by Hug and Leupin (2003)[82]. They observed that oxidation of trivalent arsenic (As^{III}) by Fe^{II} and H_2O_2 could effectively be quenched by classical $^{\bullet}OH$-scavengers at acidic (pH 3.5) but not at circumneutral pH (pH 7.5). They concluded that there must be a mechanistic changeover in the Fenton reaction from $^{\bullet}OH$ to Fe^{IV} with increasing pH. Similar conclusions were drawn by Bataineh, *et al.* (2012)[84] based on reactions of Fenton's reagent with DMSO at acidic to neutral pH. They found that at acidic pH the oxidation products of DMSO are MSIA and ethane unambiguously indicating that $^{\bullet}OH$ are the generated reactive species in the Fenton reaction at applied conditions. In contrast, at circumneutral pH DMSO was oxidised into dimethyl sulfone ($DMSO_2$) strongly supporting formation of Fe^{IV}.[84]

In the meantime, on the basis of experiments Kremer (1999)[56] developed a complex Fenton mechanism involving formation of Fe^{IV} even at acidic pH (pH 2.43) (reactions 1.22 – 1.27).[56]

$$Fe^{II} + H_2O_2 \rightleftharpoons \{Fe^{2+} \bullet H_2O_2\} \qquad (1.22)$$

$$\{Fe^{2+} \bullet H_2O_2\} \rightarrow FeO^{2+} + H_2O \qquad (1.23)$$

$$FeO^{2+} + H_2O_2 \rightarrow Fe^{2} + O_2 + H_2O \qquad (1.24)$$

$$FeO^{2+} + Fe^{II} + H_2O \rightarrow 2\ Fe^{III} + 2\ OH^{-} \qquad (1.25)$$

$$FeO^{2+} + Fe^{3+} \rightleftharpoons \{FeOFe\}^{5+} \qquad (1.26)$$

$$\{FeOFe\}^{5+} + H_2O_2 \rightarrow Fe^{2+} + Fe^{3+} + O_2 + H_2O \qquad (1.27)$$

In contrast, most of the recent publications concerning the Fenton mechanism and involved reactive species again confirm the idea of Gallard, *et al.* (1998)[54] that there is a mechanistic changeover from •OH to Fe^{IV} with increasing pH. Depending on the pH the transient iron-peroxo-complex decomposes either via a one-electron transfer from Fe to the peroxo-ligand to form •OH or via a two-electron transfer to form Fe^{IV}.[82-85]

1.4.2 RELEVANCE OF FENTON CHEMISTRY IN DIFFERENT FIELDS

Application of Fenton reactions for oxidative treatment of contaminated waters

Fenton reactions have already been investigated for oxidative treatment of a variety of target compounds including aromatic amines,[86] phenols and substituted phenols,[64, 87-92] *para*-hydroxybenzoic acid,[66] or different dyes[62, 93]. Besides those studies, in which Fenton chemistry has been applied to synthetic samples in laboratory scale, it has also been applied to wastewaters of various industries (such as chemical, pharmaceutical, pulp and paper, textile, food, or cork processing industries)[94] as well as for the treatment of landfill leachate[65] or contaminated soil[95] leading to marked reduction of toxicity, enhanced biodegradability, decolourisation, and removal of odour causing compounds.

Naturally occurring Fenton reactions

Fenton chemistry is also relevant in natural systems. As both, Fe and H_2O_2, are present in atmospheric, terrestrial or aquatic environments as well as in living organisms, these are all possible sites for Fenton reactions to occur.[96-101] The mutual presence of Fe, H_2O_2 and halides results in abiotic halogenation of organic matter.[96] Products of such reactions are important with respect to stratospheric and tropospheric chemistry and pose a risk to terrestrial ecosystems.[96] Furthermore, Fe-catalysed oxidation of humic acids is reported.[96]

Fenton reactions *in vivo* necessarily require free intracellular Fe. However, at usual conditions Fe-regulation ensures that no free Fe is released.[102] In case of stress conditions, elevated concentrations of superoxide ($O_2^{\bullet-}$), which can be produced from endogenous as well as exogenous substances, cause the release of free Fe^{II} from Fe-containing enzymes.[102-103] Liberated Fe^{II} can than react with H_2O_2 leading to formation of highly reactive $^{\bullet}OH$.[104-105] Due to their short half-live[106] $^{\bullet}OH$ react close to their site of generation where they can react with enzymes or deoxyribonucleic acid (DNA). Reactions of $^{\bullet}OH$ with DNA bases or the DNA backbone result in damaged bases or strand breaks and finally in apoptosis or cancerogenesis.[102]

Undesired Fenton reactions in technical systems

In technical systems (e.g. fuel cells) Fenton reactions may also occur undesirably. Oxygen reduction reactions lead to formation of H_2O_2.[107] Fe ions are supplied by fuel cell end plates.[108] In combination this leads to formation of $^{\bullet}OH$, which can attack and finally degrade the membrane inside fuel cells. That is why the Fenton reaction is frequently used to evaluate membrane stability and determine membrane degradation products under stress conditions.[109]

1.4.3 COMPARISON OF FENTON-TYPE REACTIONS WITH OTHER AOPS

An important factor, which should be applied to compare economic feasibility of different AOPs with respect to pollutant degradation is the $^{\bullet}OH$-yield. In case of Fenton reactions $^{\bullet}OH$-yields strongly depend on reaction conditions such as pH, temperature or reactant concentrations.[110] Furthermore, Fe^{IV} is discussed as alternative oxidant and there are still controversies concerning the conditions leading to Fe^{IV}-formation.[39] Considerable formation of Fe^{IV} would largely limit the efficiency of Fenton-based oxidation of contaminants as it is a rather mild oxidant and much more selective compared to $^{\bullet}OH$.[4, 39] Whereas $^{\bullet}OH$ can react with contaminants via various mechanisms (see chapter 1.2.1), Fe^{IV} is only able to react with organic compounds via electron transfer.[94]

Without further modification, the Fenton reaction is limited to acidic pH due to formation of Fe^{III}-sludge at pH > 3, which would have to be disposed separately. Additionally, formation of insoluble Fe^{III}-hydroxides terminates catalytic recycling of Fe^{III} to Fe^{II} so that the amount of Fe^{II} must be increased to achieve the same treatment efficiency.[39] Otherwise, the pH-optimum of the Fenton reaction in the acidic range is advantageous with respect to the treatment of acidic industrial wastewaters. In such cases, other AOPs would require preceding neutralisation to achieve optimum treatment conditions. Fenton reactions are not restricted to a certain temperature range but in principle, an increase in temperature should lead to accelerated kinetics of the reactions.[94] However, one must bear in mind that increasing temperatures favour the rate of decomposition of H_2O_2 into O_2 and water (H_2O) by a factor of about 2.3 per 10 °C.[111]

With respect to required chemicals as well as with respect to energy demand, the Fenton reaction can be viewed as environmental friendly. Applied chemicals (Fe and H_2O_2) are comparably inexpensive, easy to store and safe to handle. Furthermore, they are readily available and non-threatening to the environment.[39, 94, 110] As oxidant formation is catalytically in Fe, its utilised amount can be kept minimal and hence, also eventual sludge formation minimised.[39]

Fenton-type reactions possess diverse opportunities of modifications, which on the one hand enhance the treatment efficiency and on the other hand enlarge the field of application. These comprise photo-Fenton, solar photo-Fenton, sono-Fenton, electro-Fenton, Fenton-type reactions with metal cations other than Fe, and ligand-assisted Fenton reactions and will be described in detail in chapter 1.4.4.[39, 110, 112]

1.4.4 MODIFICATIONS OF FENTON REACTIONS

Photo-Fenton reaction

The photolytic enhancement of the Fenton reaction is mainly based on the photochemistry of Fe^{III}. Fe^{III}-species, which are present at mildly acidic conditions (Figure 1.2), can be reduced photolytically leading to the formation of Fe^{II} and $^{\bullet}OH$ according to reaction 1.28.[113]

$$Fe(OH)^{2+} + h\nu \rightarrow Fe^{II} + {}^{\bullet}OH \qquad (1.28)$$

Thus, on the one hand catalytic recycling of Fe^{II} is accelerated and on the other hand further $^{\bullet}OH$ are produced, both leading to a higher oxidation efficiency.[114] Furthermore, as mentioned in chapter 1.3.1 photolysis of H_2O_2 results in the formation of $^{\bullet}OH$ (reaction 1.1). In case of solar photo-Fenton chemistry, no additional energy source would be required.

Sonochemical Fenton reaction

The application of ultrasound to a water sample leads to the formation of cavitation bubbles. When these bubbles explosively collapse, a pressure of several hundred atmosphere and a temperature of several thousand Kelvin can be reached. At such conditions, sonolysis of water molecules occurs yielding $^{\bullet}OH$ (reaction 1.29).

$$H_2O +))) \rightarrow {}^{\bullet}OH + {}^{\bullet}H \qquad (1.29)$$

with))) = ultrasound.

Hence, ultrasonic treatment in combination with Fenton reactions increases the amount of radicals available.[115] Besides, sono-Fenton treatment supports mineralisation of pollutants due to enhanced mixing and contact between $^{\bullet}OH$ and pollutants and by accelerating the regeneration of Fe^{II} (reaction 1.30).[116-117]

$$FeOOH^{2+} +))) \rightarrow Fe^{2+} + HO_2^{\bullet} \qquad (1.30)$$

However, sono-Fenton processes also have some disadvantages. On the one hand, stoichiometric quantities of ferrous ions are required.[112] This can somehow be compensated by the application of zero valent iron (ZVI).[118] In such ZVI systems, zero valent iron metals are corroded in the presence of H_2O_2 leading to formation of Fe^{2+} (reaction 1.31)[119], which can then react with H_2O_2 according to reaction 1.8. Generated Fe^{3+} is subsequently reduced by Fe^0 to re-form Fe^{2+} (reaction 1.32).

$$Fe^0 + 2\ H^+ \rightarrow Fe^{2+} + H_2 \qquad (1.31)$$

$$Fe^0 + 2\ Fe^{3+} \rightarrow 3\ Fe^{2+} \qquad (1.32)$$

On the other hand, the high energy consumption of ultrasound systems limits the applicability of sono-Fenton processes.[112]

Electrochemical Fenton reaction

In electro-Fenton processes, one or both reagents can be generated in situ depending on the cell potential, reaction conditions and type of electrodes.[39] Fe^{II} can either be produced by oxidative dissolution of sacrificial anodes (reaction 1.33) or by reduction of Fe^{III} at in inert cathode (reaction 1.34).[120-121]

$$Fe^0 \rightarrow Fe^{II} + 2\ e^- \qquad (1.33)$$

$$Fe^{III} + e^- \rightarrow Fe^{II} \qquad (1.34)$$

In situ production of H_2O_2 can be obtained by reduction of O_2 at the cathode (reaction 1.35).[122]

$$O_2 + 2\ H^+ + 2\ e^- \rightarrow H_2O_2 \qquad (1.35)$$

However, several drawbacks limit the applicability of electro-Fenton reactions, such as the slow production of H_2O_2 due to the low solubility of O_2 in water, corrosion of electrodes, and the formation of insoluble Fe^{III}-hydroxides at pH > 3.[39, 123]

Ligand-assisted Fenton reaction

A possibility to keep Fe^{III} soluble at pH > 3 and hence, enlarge the range of applicability of Fenton chemistry, is the addition of ligands, which form soluble complexes with Fe^{III}. Organic chelates, which have two or more Lewis base groups, are especially suitable to complex metal ions. The effective complexation of iron with such chelates is expressed by the high complex formation constants (see Table 1.1). Thereby, complex stability depends on the 3-dimensional structure of the ligand and the number of functional groups. According to the Dewar-Chatt-Dunkanson-model complexation preferably occurs via the double bonded O-atoms of carboxylic groups, as such bonds allow formation of highly stable π-backbonds,[124-125] and via the free electron pair of amino groups.

Table 1.1: Selection of organic chelating ligands and their complex formation constants with Fe^{II} and Fe^{III}.

Type of ligand	**No. of funct. groups**	**log *K*(Fe^{II})[126]**	**log *K*(Fe^{III})[126]**
Citrate	0 (-NH_2) 3 (-CO_2H)	15.5	25.0
DCTA (*trans*-1,2-diaminecyclohexane-tetraacetic acid)	2 (-NH_2) 4 (-CO_2H)	18.2	29.3
DTPA (diethylenetriaminepentaacetic acid)	3 (-NH_2) 5 (-CO_2H)	16.0	27.5
EDTA (ethylenediaminetetraacetic acid)	2 (-NH_2) 4(-CO_2H)	14.3	25.1
HEDTA (hydroxyethylenediaminetriacetic acid)	2 (-NH_2) 3 (-CO_2H)	12.2	19.8
NTA (nitrilotriacetic acid)	1 (-NH_2) 3 (-CO_2H)	8.8	15.9
Oxalate	0 (-NH_2) 2 (-CO_2H)	3.0 [127]	8.0

The influence of organic chelates on Fenton chemistry is intensively discussed in literature.[76, 79-80, 128] Indeed, it is coherently described that the Fenton reaction is accelerated in presence of such ligands, but inconclusive results were reported regarding the extent of this effect. The increase in second order reaction rate constants of the reaction of Fe^{II} and H_2O_2 caused by ligands such as DTPA, EDTA, HEDTA, and NTA presumably results from the lowered reduction potential of the complexed Fe^{II}/Fe^{III} redox couple compared to $Fe(H_2O)_6^{2+}$ by decreasing its positive charge.[39, 129]

Iron usually forms hexadentate complexes, but also heptadentate complexes of iron are known. In case of a Fe^{II}-EDTA complex a water molecule occupies a seventh coordination site at the central Fe^{2+}.[130-131] It was proposed that Fe requires a coordination site, which is open or occupied by a labile ligand such as water to be substituted by H_2O_2 to enable the Fenton reaction.[130] However, this is contradicted by the reported generation of $^{\bullet}OH$ in DTPA-assisted Fenton reactions, even though DTPA is an octadentate ligand, which should not leave any coordination site open at the Fe-centre.[132-137] On the other hand, some researchers also ruled out the formation of $^{\bullet}OH$ in the presence of EDTA or other hexa- or less dentate ligands based on product identification of the reaction between the reactive species formed and classical $^{\bullet}OH$-scavengers.[75, 129, 138-139] These contradictory results might be ascribed to differences in experimental conditions as Yamazaki and Piette (1991)[137] described an effect of increasing $[H_2O_2]$ on the type of generated reactive species. They found out that at pH 7.4 the dominant oxidant changes from ferryl to $^{\bullet}OH$ when $[H_2O_2]$ is increased.[137] For many ligands (e.g. DCTA, DTPA, EDTA, NTA) generation of $^{\bullet}OH$ as well as of Fe^{IV}-species is stated by different researchers.[75, 129-130, 132-141]

Also in case of wastewater treatment by means of Fenton reaction the influence of chelating ligands must be taken into account. Several anthropogenic chelating agents are present in

wastewaters and may reach high concentrations in particular in some industrial wastewaters.[142-144] Additionally, humic acids of organic matter (OM) in wastewaters may have several functional groups (e.g. carboxylic groups or amines), which could also complex metal ions and hence, might influence Fenton chemistry. Several researchers already investigated the effect of NOM (e.g. Suwannee river fulvic acids (SRFA)) on ˙OH-yields in Fenton reactions. They reported that ˙OH are formed at circumneutral pH. However, information on ˙OH-yields in ligand-assisted Fenton reactions is largely scattering with respect to the type of generated oxidants.[79, 145-150]

Fenton-type reactions with metal cations other than Fe

Besides Fe, several elements with multiple redox states, such as chromium (Cr), cerium (Ce), copper (Cu), cobalt (Co), and ruthenium (Ru), are able to decompose H_2O_2 into ˙OH.[151] However, even if these metals possess some advantages compared to Fe when used as Fenton catalyst, as e.g. stability at neutral to alkaline pH, there are practical limitations influencing their environmental applicability. There are for instance, the cytotoxic effects of Cr, Ce, and Co, which confine their use for practical applications.[151] In case of Ru, optimum oxidation efficiency was observed in the neutral and near-alkaline pH range. Furthermore, Ru is a very stable Fenton catalyst so that it can be used for several catalytic cycles. Thus, it can somehow be compensated that Ru is a very rare and expensive element.[151] Cu exhibits a quite similar redox behaviour compared to Fe. Cu^+ as well as Cu^{2+} are able to react with H_2O_2. However, Cu^+ requires strict anaerobic conditions as it is easily oxidised by O_2 to Cu^{2+}.[151] The latter, which is indeed stable as $Cu(H_2O)_6^{2+}$ at neutral pH, requires a large excess of H_2O_2 to achieve pollutant degradation, which then in turn scavenges generated ˙OH.[152]

The present chapter 1 demonstrates the large complexity of Fenton chemistry. Indeed, the Fenton reaction has frequently been investigated in terms of pollutant degradation in the last

decades, but the exact mechanism and type of oxidant ($^{\bullet}OH$ vs. Fe^{IV}) generated at certain conditions is still contentious. Nevertheless, the Fenton process has shown to be a promising tool to degrade organic contaminants. However, applicability of the Fenton reaction for effective treatment of real waters strongly depends on the type of reactive species formed at prevailing conditions as Fe^{IV} is a much more selective oxidant compared to $^{\bullet}OH$.

1.5 REFERENCES

1. European Water Framework Directive 2000/60/EG. **2000**

2. Glaze, W. H.; Kang, J. W.; Chapin, D. H., The chemistry of water treatment processes involving ozone, hydrogen peroxide and ultraviolet radiation. *Ozone Sci. Eng.* **1987,** *9* (4), 335-352.

3. Huang, C. P.; Dong, C.; Tang, Z., Advanced chemical oxidation: Its present role and potential future in hazardous waste treatment. *Waste Manage. (Oxford)* **1993,** *13* (5-7), 361-377.

4. von Sonntag, C., Advanced oxidation processes: Mechanistic aspects. *Water Sci. Technol.* **2008,** *58* (5), 1015-1021.

5. Fang, X.; Schuchmann, H. P.; Von Sonntag, C., The reaction of the OH radical with pentafluoro-, pentachloro-, pentabromo- and 2,4,6-triiodophenol in water: Electron transfer vs. addition to the ring. *J Chem Soc Perkin Trans 2* **2000,** (7), 1391-1398.

6. Vanysek, P., Electrochemical series. In *CRC Handbook of Chemistry and Physics*, 90th (internet version) ed.; Lide, D. R.; Hynes, W. M. M., Eds. CRC Press/Taylor and Francis: Boca Raton, FL, **2010**.

7. Villamena, F. A.; Zweier, J. L., Detection of Reactive Oxygen and Nitrogen Species EPR Spin Trapping. *Antioxid. Redox Signal.* **2004,** *6* (3), 619-629.

8. Azman, N. A. M.; Peiró, S.; Fajarí, L.; Julià, L.; Almajano, M. P., Radical scavenging of white tea and its flavonoid constituents by electron paramagnetic resonance (EPR) spectroscopy. *J. Agric. Food. Chem.* **2014,** *62* (25), 5743-5748.

9. Tai, C.; Peng, J. F.; Liu, J. F.; Jiang, G. B.; Zou, H., Determination of hydroxyl radicals in advanced oxidation processes with dimethyl sulfoxide trapping and liquid chromatography. *Anal. Chim. Acta* **2004,** *527* (1), 73-80.

10. Babbs, C. F.; Gale, M. J., Colorimetric assay for methanesulfinic acid in biological samples. *Anal. Biochem.* **1987,** *163* (1), 67-73.

11. Babbs, C. F.; Griffin, D. W., Scatchard analysis of methane sulfinic acid production from dimethyl sulfoxide: A method to quantify hydroxyl radical formation in physiologic systems. *Free Radical Biol. Med.* **1989,** *6* (5), 493-503.

12. Babbs, C. F.; Steiner, M. G., Detection and quantitation of hydroxyl radical using dimethyl sulfoxide as molecular probe. *Methods Enzymol.* **1990,** *186*, 137-147.

13. Steiner, M. G.; Babbs, C. F., Quantitation of the hydroxyl radical by reaction with dimethyl sulfoxide. *Arch. Biochem. Biophys.* **1990,** *278* (2), 478-481.

14. Peralta, E.; Roa, G.; Hernandez-Servin, J. A.; Romero, R.; Balderas, P.; Natividad, R., Hydroxyl Radicals quantification by UV spectrophotometry. *Electrochim. Acta* **2014,** *129*, 137-141.

15. Zhao, H.; Gao, J.; Zhou, W.; Wang, Z.; Wu, S., Quantitative detection of hydroxyl radicals in Fenton system by UV-vis spectrophotometry. *Anal. Methods* **2015,** *7* (13), 5447-5453.

16. Schuchmann, M. N.; Von Sonntag, C., Hydroxyl radical-induced oxidation of 2-methyl-2-propanol in oxygenated aqueous solution. A product and pulse radiolysis study. *The Journal of Physical Chemistry* **1979,** *83* (7), 780-784.

17. Klein, S. M.; Cohen, G.; Cederbaum, A. I., Production of formaldehyde during metabolism of dimethyl sulfoxide by hydroxyl radical generating systems. *Biochemistry* **1981,** *20* (21), 6006-6012.

18. Tai, C.; Gu, X.; Zou, H.; Guo, Q., A new simple and sensitive fluorometric method for the determination of hydroxyl radical and its application. *Talanta* **2002,** *58* (4), 661-667.

19. Flyunt, R.; Leitzke, A.; Mark, G.; Mvula, E.; Reisz, E.; Schick, R.; Von Sonntag, C., Determination of $^{\bullet}OH$, $O_2^{\bullet-}$, and hydroperoxide yields in ozone reactions in aqueous solution. *J. Phys. Chem. B* **2003,** *107* (30), 7242-7253.

20. Scaduto Jr, R. C., Oxidation of DMSO and methanesulfinic acid by the hydroxyl radical. *Free Radical Biol. Med.* **1995,** *18* (2), 271-277.

21. Flyunt, R.; Makogon, O.; Schuchmann, M. N.; Asmus, K. D.; Von Sonntag, C., OH-radical-induced oxidation of methanesulfinic acid. The reactions of the methanesulfonyl radical in the absence and presence of dioxygen. *J. Chem. Soc. Perkin Trans. 2* **2001,** (5), 787-792.

22. Lee, Y.; Lee, C.; Yoon, J., Kinetics and mechanisms of DMSO (dimethylsulfoxide) degradation by UV/H_2O_2 process. *Water Res.* **2004,** *38* (10), 2579-2588.

23. Fischbacher, A.; Von Sonntag, J.; Von Sonntag, C.; Schmidt, T. C., The $^{\bullet}OH$ radical yield in the $H_2O_2 + O_3$ (peroxone) reaction. *Environ. Sci. Technol.* **2013,** *47* (17), 9959-9964.

24. Buxton, G. V.; Greenstock, C. L.; Helman, W. P.; Ross, A. B., Critical review of rate constants for reactions of hydrated electrons, hydrogen atoms and hydroxyl radicals (•OH/•O⁻) in aqueous solution. *J. Phys. Chem. Ref. Data* **1988,** *17* (2), 513-886.

25. Veltwisch, D.; Janata, E.; Asmus, K. D., Primary processes in the reaction of •OH-radicals with sulphoxides. *J. Chem. Soc. Perkin Trans. 2* **1980,** (1), 146-153.

26. Legrini, O.; Oliveros, E.; Braun, A. M., Photochemical Processes for Water Treatment. *Chem. Rev.* **1993,** *93* (2), 671-698.

27. Sein, M. M.; Golloch, A.; Schmidt, T. C.; Von Sonntag, C., No marked kinetic isotope effect in the peroxone (H2O 2/D2O2 + O3) reaction: Mechanistic consequences. *ChemPhysChem* **2007,** *8* (14), 2065-2067.

28. Staehelin, J.; Holgné, J., Decomposition of Ozone in Water: Rate of Initiation by Hydroxide Ions and Hydrogen Peroxide. *Environ. Sci. Technol.* **1982,** *16* (10), 676-681.

29. Nöthe, T.; Fahlenkamp, H.; Von Sonntag, C., Ozonation of wastewater: Rate of ozone consumption and hydroxyl radical yield. *Environ. Sci. Technol.* **2009,** *43* (15), 5990-5995.

30. von Gunten, U., Ozonation of drinking water: Part I. Oxidation kinetics and product formation. *Water Res.* **2003,** *37* (7), 1443-1467.

31. Fenton, H. J. H., LXXIII. - Oxidation of tartaric acid in presence of iron. *J. Chem. Soc., Trans.* **1894,** *65*, 899-910.

32. Fenton, H. J. H.; Jackson, H. J., I. - The oxidation of polyhydric alcohols in presence of iron. *J. Chem. Soc., Trans.* **1899,** *75*, 1-11.

33. Fenton, H. J. H.; Jones, H. O., VII. - The oxidation of organic acids in presence of ferrous iron. Part I. *J. Chem. Soc., Trans.* **1900,** *77*, 69-76.

34. Walton, J. H.; Christensen, C. J., The catalytic influence of ferric ions on the oxidation of ethanol by hydrogen peroxide. *J. Am. Chem. Soc.* **1926,** *48* (8), 2083-2091.

35. Bray, W. C.; Gorin, M. H., Ferryl ion, a compound of tetravalent iron. *J. Am. Chem. Soc.* **1932,** *54*, 2124-2125.

36. Haber, F.; Weiss, J., Über die Katalyse des Hydroperoxydes. *Naturwissenschaften* **1932,** *20* (51), 948-950.

37. Haber, F.; Weiss, J., The catalytic decomposition of hydrogen peroxide by iron salts. *P. Roy. Soc. Lond. A Mat.* **1934,** *147* (861), 332-351.

38. Weiss, J., Reaction mechanism of oxidation-reduction processes [6]. *Nature* **1934,** *133* (3365), 648-649.

39. Pignatello, J. J.; Oliveros, E.; MacKay, A., Advanced oxidation processes for organic contaminant destruction based on the Fenton reaction and related chemistry. *Crit. Rev. Environ. Sci. Technol.* **2006,** *36* (1), 1-84.

40. Koppenol, W. H.; Butler, J.; van Leeuwen, J. W., The Haber-Weiss cycle. *Photochem. Photobiol.* **1978,** *28* (4-5), 655-658.

41. Barb, W. G.; Baxendale, J. H.; George, P.; Hargrave, K. R., Reactions of ferrous and ferric ions with hydrogen peroxide. Part I. - The ferrous ion reaction. *Trans. Faraday Soc.* **1951,** *47*, 462-500.

42. Rush, J. D.; Bielski, B. H. J., Pulse radiolytic studies of the reactions of $HO_2^{\bullet}/O_2^{\bullet -}$ with Fe(II)/Fe(III) ions. The reactivity of $HO_2^{\bullet}/O_2^{\bullet -}$ with ferric ions and its implication on the occurrence of the Haber-Weiss reaction. *J. Phys. Chem.* **1985,** *89* (23), 5062-5066.

43. Allen, A. O.; Hogan, V. D.; Rothschild, W. G., Studies in the radiolysis of ferrous sulfate solutions. II. Effect of acid concentration in solutions containing oxygen. *Radiat. Res.* **1957,** *7* (6), 603-608.

44. Sehested, K.; Bjergbakke, E.; Rasmussen, O. L.; Fricke, H., Reactions of H_2O_3 in the pulse-irradiated Fe(II)-O_2 system. *J. Chem. Phys.* **1969,** *51* (8), 3159-3166.

45. Christensen, H.; Sehested, K., HO_2 and O_2^- radicals at elevated temperatures. *J. Phys. Chem.* **1988,** *92* (10), 3007-3011.

46. Fischbacher, A.; Von Sonntag, C.; Schmidt, T. C., Hydroxyl radical yields in the Fenton process under various pH, ligand concentrations and hydrogen peroxide/Fe(II) ratios. *Chemosphere* **2017,** *182*, 738-744.

47. Stefánsson, A., Iron(III) hydrolysis and solubility at 25°C. *Environ. Sci. Technol.* **2007,** *41* (17), 6117-6123.

48. Gallard, H.; de Laat, J.; Legube, B., Spectrophotometric study of the formation of iron(III)-hydroperoxy complexes in homogeneous aqueous solutions. *Water Res.* **1999,** *33* (13), 2929-2936.

49. de Laat, J.; Gallard, H., Catalytic decomposition of hydrogen peroxide by Fe(III) in homogeneous aqueous solution: Mechanism and kinetic modeling. *Environ. Sci. Technol.* **1999,** *33* (16), 2726-2732.

50. Turner, D. R.; Whitfield, M.; Dickson, A. G., The equilibrium speciation of dissolved components in freshwater and sea water at 25°C and 1 atm pressure. *Geochim. Cosmochim. Acta* **1981,** *45* (6), 855-881.

51. Goldstein, S.; Meyerstein, D.; Czapski, G., The Fenton reagents. *Free Radical Biol. Med.* **1993,** *15* (4), 435-445.

52. Rachmilovich-Calis, S.; Masarwa, A.; Meyerstein, N.; Meyerstein, D.; van Eldik, R., New mechanistic aspects of the Fenton reaction. *Chem. Eur. J.* **2009,** *15* (33), 8303-8309.

53. Bossmann, S. H.; Oliveros, E.; Göb, S.; Siegwart, S.; Dahlen, E. P.; Payawan Jr, L.; Straub, M.; Wörner, M.; Braun, A. M., New evidence against hydroxyl radicals as reactive intermediates in the thermal and photochemically enhanced Fenton reactions. *J. Phys. Chem. A* **1998,** *102* (28), 5542-5550.

54. Gallard, H.; de Laat, J.; Legube, B., Effect of pH on the oxidation rate of organic compounds by Fe^{II}/H_2O_2. Mechanisms and simulation. *New J. Chem.* **1998,** *22* (3), 263-268.

55. Buda, F.; Ensing, B.; Gribnau, M. C. M.; Baerends, E. J., DFT study of the active intermediate in the Fenton reaction. *Chem. Eur. J.* **2001,** *7* (13), 2775-2783.

56. Kremer, M. L., Mechanism of the Fenton reaction. Evidence for a new intermediate. *Phys. Chem. Chem. Phys.* **1999,** *1* (15), 3595-3605.

57. Kremer, M. L., The Fenton reaction. Dependence of the rate on pH. *J. Phys. Chem. A* **2003,** *107* (11), 1734-1741.

58. Walling, C., Fentons reagent revisited. *Acc. Chem. Res.* **1975,** *8* (4), 125-131.

59. Barb, W. G.; Baxendale, J. H.; George, P.; Hargrave, K. R., Reactions of ferrous and ferric ions with hydrogen peroxide. Part II. - The ferric ion reaction. *Trans. Faraday Soc.* **1951,** *47*, 591-616.

60. Wells, C. F.; Salam, M. A., The effect of pH on the kinetics of the reaction of iron(II) with hydrogen peroxide in perchlorate media. *J. Chem. Soc. A* **1968**, 24-29.

61. Walling, C.; Amarnath, K., Oxidation of mandelic acid by Fenton's reagent. *J. Am. Chem. Soc.* **1982,** *104* (5), 1185-1189.

62. Kuo, W. G., Decolorizing dye wastewater with Fenton's reagent. *Water Res.* **1992,** *26* (7), 881-886.

63. Liou, M. J.; Lu, M. C.; Chen, J. N., Oxidation of explosives by Fenton and photo-Fenton processes. *Water Res.* **2003,** *37* (13), 3172-3179.

64. Kavitha, V.; Palanivelu, K., Degradation of nitrophenols by Fenton and photo-Fenton processes. *J. Photochem. Photobiol. A Chem.* **2005,** *170* (1), 83-95.

65. Zhang, H.; Heung, J. C.; Huang, C. P., Optimization of Fenton process for the treatment of landfill leachate. *J. Hazard. Mater.* **2005,** *125* (1-3), 166-174.

66. Rivas, F. J.; Beltran, F. J.; Frades, J.; Buxeda, P., Oxidation of p-hydroxybenzoic acid by Fenton's reagent. *Water Res.* **2001,** *35* (2), 387-396.

67. Pérez, M.; Torrades, F.; Domènech, X.; Peral, J., Fenton and photo-Fenton oxidation of textile effluents. *Water Res.* **2002,** *36* (11), 2703-2710.

68. Méndez-Arriaga, F.; Esplugas, S.; Giménez, J., Degradation of the emerging contaminant ibuprofen in water by photo-Fenton. *Water Res.* **2010,** *44* (2), 589-595.

69. Klamerth, N.; Malato, S.; Agüera, A.; Fernández-Alba, A., Photo-Fenton and modified photo-Fenton at neutral pH for the treatment of emerging contaminants in wastewater treatment plant effluents: A comparison. *Water Res.* **2013,** *47* (2), 833-840.

70. Brillas, E.; Sirés, I.; Oturan, M. A., Electro-Fenton process and related electrochemical technologies based on Fenton's reaction chemistry. *Chem. Rev.* **2009,** *109* (12), 6570-6631.

71. Barhoumi, N.; Labiadh, L.; Oturan, M. A.; Oturan, N.; Gadri, A.; Ammar, S.; Brillas, E., Electrochemical mineralization of the antibiotic levofloxacin by electro-Fenton-pyrite process. *Chemosphere* **2015,** *141*, 250-257.

72. Olvera-Vargas, H.; Cocerva, T.; Oturan, N.; Buisson, D.; Oturan, M. A., Bioelectro-Fenton: A sustainable integrated process for removal of organic pollutants from water: Application to mineralization of metoprolol. *J. Hazard. Mater.* **2016,** *319*, 13-23.

73. Rocha, R. S.; Silva, F. L.; Valim, R. B.; Barros, W. R. P.; Steter, J. R.; Bertazzoli, R.; Lanza, M. R. V., Effect of Fe^{2+} on the degradation of the pesticide profenofos by electrogenerated H_2O_2. *J. Electroanal. Chem.* **2016,** *783*, 100-105.

74. Babuponnusami, A.; Muthukumar, K., A review on Fenton and improvements to the Fenton process for wastewater treatment. *J. Environ. Chem. Eng.* **2014,** *2* (1), 557-572.

75. Rush, J. D.; Koppenol, W. H., Reactions of Fe^{II}NTA and Fe^{II}EDDA with hydrogen peroxide. *J. Am. Chem. Soc.* **1988,** *110* (15), 4957-4963.

76. Szulbiński, W. S., Fenton reaction of iron chelates involving polyazacyclononane. The ligand structure effect. *Pol. J. Chem.* **2000,** *74* (1), 109-124.

77. Bossmann, S. H.; Oliveros, E.; Kantor, M.; Niebler, S.; Bonfill, A.; Shahin, N.; Wörner, M.; Braun, A. M., New insights into the mechanisms of the thermal Fenton reactions occurring using different iron(II)-complexes. In *Water Sci. Technol.*, 2004; Vol. 49, 75-80.

78. Remucal, C. K.; Sedlak, D. L., The role of iron coordination in the production of reactive oxidants from ferrous iron oxidation by oxygen and hydrogen peroxide. In *ACS Symp. Ser.*, American Chemical Society: 2011; Vol. 1071, 177-197.

79. Miller, C. J.; Rose, A. L.; Waite, T. D., Hydroxyl radical production by H_2O_2-mediated oxidation of Fe(II) complexed by suwannee river fulvic acid under circumneutral freshwater conditions. *Environ. Sci. Technol.* **2013,** *47* (2), 829-835.

80. Salgado, P.; Melin, V.; Contreras, D.; Moreno, Y.; Mansilla, H. D., Fenton reaction driven by iron ligands. *J. Chilean Chem. Soc.* **2013,** *58* (4), 2096-2101.

81. Zhang, Y.; Klamerth, N.; Chelme-Ayala, P.; Gamal El-Din, M., Comparison of classical fenton, nitrilotriacetic acid (NTA)-Fenton, UV-Fenton, UV photolysis of Fe-NTA, UV-NTA-Fenton, and UV-H_2O_2 for the degradation of cyclohexanoic acid. *Chemosphere* **2017,** *175*, 178-185.

82. Hug, S. J.; Leupin, O., Iron-catalyzed oxidation of arsenic(III) by oxygen and by hydrogen peroxide: pH-dependent formation of oxidants in the Fenton reaction. *Environ. Sci. Technol.* **2003,** *37* (12), 2734-2742.

83. Katsoyiannis, I. A.; Ruettimann, T.; Hug, S. J., pH dependence of Fenton reagent generation and As(III) oxidation and removal by corrosion of zero valent iron in aerated water. *Environ. Sci. Technol.* **2008,** *42* (19), 7424-7430.

84. Bataineh, H.; Pestovsky, O.; Bakac, A., pH-induced mechanistic changeover from hydroxyl radicals to iron(IV) in the Fenton reaction. *Chem. Sci.* **2012,** *3* (5), 1594-1599.

85. Lee, H.; Lee, H. J.; Sedlak, D. L.; Lee, C., pH-Dependent reactivity of oxidants formed by iron and copper-catalyzed decomposition of hydrogen peroxide. *Chemosphere* **2013,** *92* (6), 652-658.

86. Casero, I.; Sicilia, D.; Rubio, S.; Pérez-Bendito, D., Chemical degradation of aromatic amines by Fenton's reagent. *Water Res.* **1997,** *31* (8), 1985-1995.

87. Zazo, J. A.; Casas, J. A.; Mohedano, A. F.; Gilarranz, M. A.; Rodríguez, J. J., Chemical pathway and kinetics of phenol oxidation by Fenton's reagent. *Environ. Sci. Technol.* **2005,** *39* (23), 9295-9302.

88. Beltran De Heredia, J.; Torregrosa, J.; Dominguez, J. R.; Peres, J. A., Kinetic model for phenolic compound oxidation by Fenton's reagent. *Chemosphere* **2001,** *45* (1), 85-90.

89. Barbeni, M.; Minero, C.; Pelizzetti, E.; Borgarello, E.; Serpone, N., Chemical degradation of chlorophenols with Fenton's reagent (Fe^{2+} + H_2O_2). *Chemosphere* **1987,** *16* (10-12), 2225-2237.

90. Basu, S.; Wei, I. W., Advanced chemical oxidation of 2,4,6-trichlorophenol in aqueous phase by Fenton's Reagent-part I: Effects of the amounts of oxidant and catalyst on the treatment reaction. *Chem. Eng. Commun.* **1998,** *164*, 111-137.

91. Basu, S.; Wei, I. W., Advanced chemical oxidation of 2,4,6-trichlorophenol in aqueous phase by Fenton's Reagent-part II: Effects of various reaction parameters on the treatment reaction. *Chem. Eng. Commun.* **1998,** *164*, 139-151.

92. Lipczynska-Kochany, E., Degradation of aqueous nitrophenols and nitrobenzene by means of the Fenton reaction. *Chemosphere* **1991,** *22* (5-6), 529-536.

93. Wang, S., A Comparative study of Fenton and Fenton-like reaction kinetics in decolourisation of wastewater. *Dyes Pigment.* **2008,** *76* (3), 714-720.

94. Bautista, P.; Mohedano, A. F.; Casas, J. A.; Zazo, J. A.; Rodriguez, J. J., An overview of the application of Fenton oxidation to industrial wastewaters treatment. *J. Chem. Technol. Biotechnol.* **2008,** *83* (10), 1323-1338.

95. Usman, M.; Hanna, K.; Haderlein, S., Fenton oxidation to remediate PAHs in contaminated soils: A critical review of major limitations and counter-strategies. *Sci. Total Environ.* **2016,** *569-570*, 179-190.

96. Comba, P.; Kerscher, M.; Krause, T.; Schöler, H. F., Iron-catalysed oxidation and halogenation of organic matter in nature. *Environmental Chemistry* **2015,** *12* (4), 381-395.

97. Kok, G. L., Measurements of hydrogen peroxide in rainwater. *Atmos. Environ. Part A Gen. Top.* **1980,** *14* (6), 653-656.

98. Olszyna, K. J.; Meagher, J. F.; Bailey, E. M., Gas-phase, cloud and rain-water measurements of hydrogen peroxide at a high-elevation site. *Atmos. Environ. Part A Gen. Top.* **1988,** *22* (8), 1699-1706.

99. Yoshizumi, K.; Aoki, K.; Nouchi, I.; Okita, T.; Kobayashi, T.; Amakura, S. K.; Tajima, M., Measurements of the concentration in rainwater and of the Henry's law constant of hydrogen peroxide. *Atmos. Environ. Part A Gen. Top.* **1984,** *18* (2), 395-401.

100. Zuo, Y.; Deng, Y., Evidence for the production of hydrogen peroxide in rainwater by lightning during thunderstorms. *Geochim. Cosmochim. Acta* **1999,** *63* (19-20), 3451-3455.

101. Taylor, S. R., Abundance of chemical elements in the continental crust: a new table. *Geochim. Cosmochim. Acta* **1964,** *28* (8), 1273-1285.

102. Valko, M.; Rhodes, C. J.; Moncol, J.; Izakovic, M.; Mazur, M., Free radicals, metals and antioxidants in oxidative stress-induced cancer. *Chem. Biol. Interact.* **2006,** *160* (1), 1-40.

103. Liochev, S. I.; Fridovich, I., The role of $O_2^{\bullet-}$ in the production of $HO^{\bullet}$: in vitro and in vivo. *Free Radical Biol. Med.* **1994,** *16* (1), 29-33.

104. Leonard, S. S.; Harris, G. K.; Shi, X., Metal-induced oxidative stress and signal transduction. *Free Radical Biol. Med.* **2004,** *37* (12), 1921-1942.

105. Stohs, S. J.; Bagchi, D., Oxidative mechanisms in the toxicity of metal ions. *Free Radical Biol. Med.* **1995,** *18* (2), 321-336.

106. Pastor, N.; Weinstein, H.; Jamison, E.; Brenowitz, M., A detailed interpretation of OH radical footprints in a TBP-DNA complex reveals the role of dynamics in mechanism of sequence-specific binding. *J. Mol. Biol.* **2000,** *304* (1), 55-68.

107. Ramaswamy, N.; Hakim, N.; Mukerjee, S., Degradation mechanism study of perfluorinated proton exchange membrane under fuel cell operating conditions. *Electrochim. Acta* **2008,** *53* (8), 3279-3295.

108. Pozio, A.; Silva, R. F.; De Francesco, M.; Cardellini, F.; Giorgi, L., A novel route to prepare stable Pt-Ru/C electrocatalysts for polymer electrolyte fuel cell. *Electrochim. Acta* **2002,** *48* (3), 255-262.

109. Zedda, M.; Tuerk, J.; Peil, S.; Schmidt, T. C., Determination of polymer electrolyte membrane (PEM) degradation products in fuel cell water using electrospray ionization tandem mass spectrometry. *Rapid Commun. Mass Spectrom.* **2010,** *24* (24), 3531-3538.

110. Oturan, M. A.; Aaron, J. J., Advanced oxidation processes in water/wastewater treatment: Principles and applications. A review. *Crit. Rev. Environ. Sci. Technol.* **2014,** *44* (23), 2577-2641.

111. Jones, C. W.; Clark, J. H., Introduction to the Preparation and Properties of Hydrogen Peroxide. In *Applications of Hydrogen Peroxide and Derivatives*, The Royal Society of Chemistry: Cambridge, UK, **1999**; 1-36.

112. Pliego, G.; Zazo, J. A.; Garcia-Muñoz, P.; Munoz, M.; Casas, J. A.; Rodriguez, J. J., Trends in the Intensification of the Fenton Process for Wastewater Treatment: An Overview. *Crit. Rev. Environ. Sci. Technol.* **2015,** *45* (24), 2611-2692.

113. Faust, B. C.; Hoigné, J., Photolysis of Fe (III)-hydroxy complexes as sources of OH radicals in clouds, fog and rain. *Atmospheric Environment Part A, General Topics* **1990,** *24* (1), 79-89.

114. Pignatello, J. J., Dark and photoassisted Fe^{3+}-catalyzed degradation of chlorophenoxy herbicides by hydrogen peroxide. *Environ. Sci. Technol.* **1992,** *26* (5), 944-951.

115. Neppolian, B.; Jung, H.; Choi, H.; Lee, J. H.; Kang, J. W., Sonolytic degradation of methyl tert-butyl ether: The role of coupled fenton process and persulphate ion. *Water Res.* **2002,** *36* (19), 4699-4708.

116. Liang, J.; Komarov, S.; Hayashi, N.; Kasai, E., Improvement in sonochemical degradation of 4-chlorophenol by combined use of Fenton-like reagents. *Ultrason. Sonochem.* **2007,** *14* (2), 201-207.

117. Adityosulindro, S.; Barthe, L.; González-Labrada, K.; Jáuregui Haza, U. J.; Delmas, H.; Julcour, C., Sonolysis and sono-Fenton oxidation for removal of ibuprofen in (waste)water. *Ultrason. Sonochem.* **2017,** *39*, 889-896.

118. Segura, Y.; Martinez, F.; Melero, J. A.; Molina, R.; Chand, R.; Bremner, D. H., Enhancement of the advanced Fenton process (Fe-0/H2O2) by ultrasound for the mineralization of phenol. *Appl. Catal. B-Environ.* **2012,** *113*, 100-106.

119. Chakinala, A. G.; Bremner, D. H.; Gogate, P. R.; Namkung, K. C.; Burgess, A. E., Multivariate analysis of phenol mineralisation by combined hydrodynamic cavitation and heterogeneous advanced Fenton processing. *Appl. Catal. B-Environ.* **2008,** *78* (1-2), 11-18.

120. Pratap, K.; Lemley, A. T., Electrochemical Peroxide Treatment of Aqueous Herbicide Solutions. *J. Agric. Food. Chem.* **1994,** *42* (1), 209-215.

121. Oturan, M. A.; Aaron, J. J.; Oturan, N.; Pinson, J., Degradation of chlorophenoxyacid herbicides in aqueous media, using a novel electrochemical method. *Pestic. Sci.* **1999,** *55* (5), 558-562.

122. Foller, P. C.; Bombard, R. T., Processes for the production of mixtures of caustic soda and hydrogen peroxide via the reduction of oxygen. *J. Appl. Electrochem.* **1995,** *25* (7), 613-627.

123. Savall, A., Electrochemical treatment of industrial organic effluents. *Chimia* **1995,** *49* (1-2), 23-27.

124. Dewar, J. S., A review of the π-complex theory. *Bull. Soc. Chim. Fr.* **1951,** *18* (3-4), C71-C79.

125. Chatt, J.; Duncanson, L. A., Olefin co-ordination compounds. 3. infra-red spectra and structure - attempted preparation of ecetylene complexes. *J. Chem. Soc.* **1953,** (OCT), 2939-2947.

126. Ringbom, A., Complexation in analytical chemistry: a guide for the critical selection of analytical methods based on complexation reactions. In *Chemical Analysis*, Elving, P. J.; Kolthoff, I. M., Eds. Interscience Publishers: New York/London, **1963**; Vol. 16.

127. Sedlak, D. L.; Hoigné, J., The role of copper and oxalate in the redox cycling of iron in atmospheric waters. *Atmospheric Environment Part A, General Topics* **1993,** *27* (14), 2173-2185.

128. Engelmann, M. D.; Bobier, R. T.; Hiatt, T.; Cheng, I. F., Variability of the Fenton reaction characteristics of the EDTA, DTPA, and citrate complexes of iron. *BioMetals* **2003,** *16* (4), 519-527.

129. Rush, J. D.; Koppenol, W. H., Oxidizing intermediates in the reaction of ferrous EDTA with hydrogen peroxide. Reactions with organic molecules and ferrocytochrome c. *J. Biol. Chem.* **1986,** *261* (15), 6730-6733.

130. Graf, E.; Mahoney, J. R.; Bryant, R. G.; Eaton, J. W., Iron-catalyzed hydroxyl radical formation. Stringent requirement for free iron coordination site. *J. Biol. Chem.* **1984,** *259* (6), 3620-3624.

131. Mizuta, T.; Yamamoto, T.; Miyoshi, K.; Kushi, Y., The ligand field stabilization effect on the metal-ligand bond distances in octahedral metal complexes with EDTA-type ligands. Redetermination of the molecular structure of (ethylenediaminetriacetatoacetic acid)-(aqua)iron(III), [Fe(HEDTA)(H_2O)]. *Inorg. Chim. Acta* **1990,** *175* (1), 121-126.

132. Sutton, H. C.; Winterbourn, C. C., Chelated iron-catalyzed $^{\bullet}OH$ formation from paraquat radicals and H_2O_2: Mechanism of formate oxidation. *Arch. Biochem. Biophys.* **1984,** *235* (1), 106-115.

133. Sutton, H. C., Efficiency of chelated iron compounds as catalysts for the Haber-Weiss reaction. *J. Free Radic. Biol. Med.* **1985,** *1* (3), 195-202.

134. Croft, S.; Gilbert, B. C.; Lindsay Smith, J. R.; Whitwood, A. C., An E.S.R. investigation of the reactive intermediate generated in the reaction between Fe^{II} and H_2O_2 in aqueous solution. Direct evidence for the formation of the hydroxyl radical. *Free Radical Res.* **1992,** *17* (1), 21-39.

135. Šnyrychová, I.; Pospíšil, P.; Nauš, J., The effect of metal chelators on the production of hydroxyl radicals in thylakoids. *Photosynth. Res.* **2006,** *88* (3), 323-329.

136. Cohen, G.; Sinet, P. M., The Fenton reaction between ferrous-diethylenetriaminepentaacetic acid and hydrogen peroxide. *FEBS Lett.* **1982,** *138* (2), 258-260.

137. Yamazaki, I.; Piette, L. H., EPR spin-trapping study on the oxidizing species fomed in reaction of the ferrous ion with hydrogen peroxide. *J. Am. Chem. Soc.* **1991,** *113* (20), 7588-7593.

138. Koppenol, W. H., The reaction of ferrous EDTA with hydrogen peroxide: Evidence against hydroxyl radical formation. *J. Free Radic. Biol. Med.* **1985,** *1* (4), 281-285.

139. Rahhal, S.; Richter, H. W., Reaction of hydrogen peroxide with low molecular weight iron complexes. *International Journal of Radiation Applications and Instrumentation. Part* **1988,** *32* (1), 129-135.

140. Rahhal, S.; Richter, H. W., Reduction of hydrogen peroxide by the ferrous iron chelate of diethylenediamine-N,N,N',N",N"-pentaacetate. *J. Am. Chem. Soc.* **1988,** *110* (10), 3126-3133.

141. Egan, T. J.; Barthakur, S. R.; Aisen, P., Catalysis of the Haber-Weiss reaction by iron-diethylenetriaminepentaacetate. *J. Inorg. Biochem.* **1992,** *48* (4), 241-249.

142. James, A. C.; Taylor, D. M., DTPA therapy for chelation of ^{239}Pu in bone: The influence of bone remodelling. *Health Phys.* **1971,** *21* (1), 31-39.

143. Smith, V. H., Therapeutic removal of internally deposited transuranium elements. *Health Phys.* **1972,** *22* (6), 765-778.

144. Means, J. L.; Kucak, T.; Crerar, D. A., Relative degradation rates of NTA, EDTA and DTPA and environmental implications. *Environ. Pollut. Ser. B Chem. Phys.* **1980,** *1* (1), 45-60.

145. Georgi, A.; Schierz, A.; Trommler, U.; Horwitz, C. P.; Collins, T. J.; Kopinke, F. D., Humic acid modified Fenton reagent for enhancement of the working pH range. *Appl. Catal. B Environ.* **2007,** *72* (1-2), 26-36.

146. Paciolla, M. D.; Davies, G.; Jansen, S. A., Generation of hydroxyl radicals from metal-loaded humic acids. *Environ. Sci. Technol.* **1999,** *33* (11), 1814-1818.

147. White, E. M.; Vaughan, P. P.; Zepp, R. G., Role of the photo-Fenton reaction in the production of hydroxyl radicals and photobleaching of colored dissolved organic matter in a coastal river of the southeastern United States. *Aquatic Sci.* **2003,** *65* (4), 402-414.

148. Southworth, B. A.; Voelker, B. M., Hydroxyl radical production via the photo-fenton reaction in the presence of fulvic acid. *Environ. Sci. Technol.* **2003,** *37* (6), 1130-1136.

149. Vermilyea, A. W.; Voelker, B. M., Photo-fenton reaction at near neutral pH. *Environ. Sci. Technol.* **2009,** *43* (18), 6927-6933.

150. Lindsey, M. E.; Tarr, M. A., Quantitation of hydroxyl radical during Fenton oxidation following a single addition of iron and peroxide. *Chemosphere* **2000,** *41* (3), 409-417.

151. Bokare, A. D.; Choi, W., Review of iron-free Fenton-like systems for activating H_2O_2 in advanced oxidation processes. *J. Hazard. Mater.* **2014,** *275*, 121-135.

152. Bali, U.; Karagozoglu, B., Performance comparison of Fenton process, ferric coagulation and H_2O_2/pyridine/Cu(II) system for decolorization of Remazol Turquoise Blue G-133. *Dyes Pigment.* **2007,** *74* (1), 73-80.

Chapter 2 -

SCOPE

Due to formation of oxidative species, the Fenton reaction, i.e. the reaction of ferrous iron (Fe^{II}) with hydrogen peroxide (H_2O_2), is a promising tool in terms of oxidative wastewater treatment. Compared with oxidation techniques as e.g. ozonation, which is nowadays frequently applied for pollutant control in water treatment, Fenton chemistry offers quite a few advantages in terms of required chemicals, energy demand and pH conditions. However, even though the Fenton reaction is already known for more than a century, some mechanistic aspects are still subject of controversial discussions.

The present work provides a systematic survey of the Fenton mechanism at selected reaction conditions. Reaction kinetics are addressed as well as identification and quantification of reactive species.

In literature formation of an intermediate iron-peroxo-complex prior to oxidant generation is postulated without any experimental evidence. In chapter 3, observed pseudo first order reaction rate constants of Fe^{III}-formation in the Fenton reaction determined at increasing concentrations of H_2O_2 might provide kinetic indication for the existence of such an intermediate. Experiments are based on stopped-flow measurements as this technique enables investigation of fast kinetics. Formation of Fe^{III} is followed spectrophotometrically. Kinetic data obtained at pH 1 to 4 are used to derive decay rates of the iron-peroxo-complex and linked to hydroxyl radical ($^{\bullet}OH$) yields.

Especially the influence of iron chelating ligands on the type of reactive species formed during the Fenton reaction is intensively discussed in literature. In a previous work the influence of inorganic ligands was investigated. As to our knowledge chapter 3 provides first kinetic indication for formation of an intermediate iron-peroxo-complex in Fenton chemistry and further insight into the Fenton mechanism, chapter 4 aims at the investigation of observed pseudo first order reaction rate constants of Fe^{III}-formation in presence of selected chelating

agents. Again decay rates of the iron-peroxo-complex are derived and correlated with •OH-yields at selected pH-values.

In chapter 5 the Fenton reaction is applied to degrade bisphenol S (BPS). BPS is chosen as model pollutant as it gains increasing interest due to restrictions made on its structural analogue bisphenol A. Reaction conditions are varied with respect to reactant concentrations, pH and matrix components in order to determine optimum conditions for Fenton based degradation of pollutants. Coincidently, results are interpreted focussing on reactive species being responsible for BPS degradation.

Overall, results presented in chapters 3 to 5 cannot provide any indication for the formation of tetravalent iron (Fe^{IV}) as reactive species involved in the Fenton reaction at investigated reaction conditions. Thus, in chapter 6 an alternative reaction described in literature to yield a reactive Fe^{IV} species, i.e. the reaction of Fe^{II} with ozone, is surveyed at selected reaction conditions. This chapter should provide insight into the question whether Fe^{IV} really is relevant as reactive species in the Fenton process.

In chapter 7, the main results of this study are combined and an outlook is given regarding further research requirements.

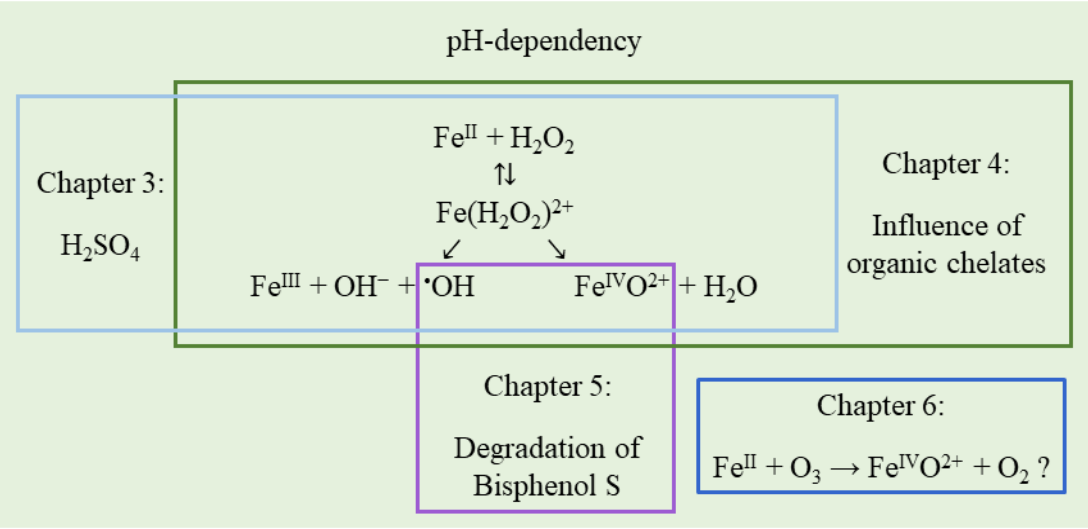

Figure 2.1: Graphic illustration of the scope of the thesis.

Chapter 3 -

INVESTIGATION OF THE IRON-PEROXO-COMPLEX IN THE FENTON REACTION: KINETIC INDICATION, DECAY KINETICS AND HYDROXYL RADICAL YIELDS

Adapted with permission from: Wiegand , H.L.; Orths, C.T.; Kerpen, K.; Lutze, H.V.; Schmidt, T.C., Investigation of the iron peroxo-complex in the Fenton reaction: Kinetic indication, decay kinetics and hydroxyl radical yields, *Environmental Science and Technology*, **2017**, 51(24), pp. 14321-14329

3.1 ABSTRACT

The Fenton reaction describes the reaction of Fe^{II} with hydrogen peroxide. Several researchers proposed the formation of an intermediate iron-peroxo-complex but experimental evidence for its existence is still missing.

The present study investigates formation and life time of this intermediate at various conditions such as different Fe^{II}-concentrations, absence vs. presence of a hydroxyl radical scavenger (dimethylsulfoxide, DMSO), and different pH values.

Obtained results indicate that the iron-peroxo-complex is formed under all experimental conditions. Based on these data, stability of the iron-peroxo-complex could be examined. At pH 3 regardless of $[Fe^{II}]_0$ decay rates for the iron-peroxo-complex of about 50 s^{-1} were determined in absence and presence of DMSO. Without DMSO and $[Fe(II)]_0$ = 300 µM variation of pH yielded decay rates of about 70 s^{-1} for pH 1 and 2 and of about 50 s^{-1} at pH 3 and 4. Hence, the iron-peroxo-complex becomes more stable with increasing pH.

Furthermore, pH-dependent hydroxyl radical yields were determined to investigate whether the increasing stability of the intermediate complex may indicate a different reaction of the iron-peroxo-complex which might yield Fe(IV) instead of hydroxyl radical formation as suggested in literature. However, it was found that hydroxyl radicals were produced proportionally to the Fe(II)-concentration.

3.2 INTRODUCTION

The term Fenton reaction describes the reaction of ferrous iron (Fe^{II}) with hydrogen peroxide (H_2O_2). As described above, different reaction mechanisms can be found in literature, one of them involving formation of an intermediate iron-peroxo-complex ($Fe(H_2O_2)^{2+}$) (reaction 3.1), which could either react further via a one-electron transfer to form Fe^{III} and $^{\bullet}OH$ (reaction 3.2) or via a two-electron transfer yielding Fe^{IV} (reaction 3.3). [1-5]

$$Fe^{II} + H_2O_2 \rightleftharpoons Fe(H_2O_2)^{2+} \quad (3.1)$$

$$Fe(H_2O_2)^{2+} \rightarrow Fe^{III} + OH^- + {}^{\bullet}OH \quad (3.2)$$

$$Fe(H_2O_2)^{2+} \rightarrow FeO^{2+} + H_2O \quad (3.3)$$

Corresponding differential equations for changes in $[Fe^{II}]$, $[Fe(H_2O_2)^{2+}]$, and $[Fe^{III}]$, respectively, can be formulated as follows:

$$\frac{d[Fe^{II}]}{dt} = -k_{3.1}[H_2O_2][Fe^{II}] + k_{-3.1}[Fe(H_2O_2)^{2+}] \quad (3.I)$$

$$\frac{d[Fe(H_2O_2)^{2+}]}{dt} = k_{3.1}[H_2O_2][Fe^{II}] - k_{-3.1}[Fe(H_2O_2)^{2+}] - k_{3.2}[Fe(H_2O_2)^{2+}] \quad (3.II)$$

$$\frac{d[Fe^{III}]}{dt} = k_{3.2}[Fe(H_2O_2)^{2+}] \quad (3.III)$$

Assuming steady-state conditions for equation II $\left(\frac{d[Fe[H_2O_2]^{2+}]}{dt} = 0\right)$ one yields

$$k_{3.1}[Fe^{II}][H_2O_2] = k_{-3.1}[Fe[H_2O_2]^{2+}] + k_{3.2}[Fe[H_2O_2]^{2+}] \quad (3.IV)$$

Furthermore, it is assumed that the total iron concentration $[Fe]_t$ is constant and hence, that $[Fe^{II}]$ remaining in solution at any instant in time after reaction has begun must be equal to the

difference between $[Fe^{II}]_0$ and the sum of $[Fe(H_2O_2)^{2+}]$ and $[Fe^{III}]$. Thus, equation 3.IV changes as follows:

$$[\mathrm{Fe}[\mathrm{H_2O_2}]^{2+}] = \frac{k_{3.1}[\mathrm{Fe^{II}}][\mathrm{H_2O_2}]}{k_{-3.1}+k_{3.2}} = \frac{k_{3.1}[\mathrm{H_2O_2}]\left([\mathrm{Fe^{II}}]_0-([\mathrm{Fe}[\mathrm{H_2O_2}]^{2+}]+[\mathrm{Fe^{III}}])\right)}{k_{-3.1}+k_{3.2}} \quad (3.V)$$

which can be transformed as follows:

$$[Fe(H_2O_2)^{2+}] + \frac{k_{3.1}[H_2O_2][Fe(H_2O_2)^{2+}]}{k_{-3.1}+k_{3.2}} = \frac{k_{3.1}[H_2O_2]\left([Fe^{II}]_0-[Fe^{III}]\right)}{k_{-3.1}+k_{3.2}} \quad (3.VI)$$

$$1 + \frac{k_{3.1}[H_2O_2]}{k_{-3.1}+k_{3.2}} = \frac{k_{3.1}[H_2O_2]\left([Fe^{II}]_0-[Fe^{III}]\right)}{k_{-3.1}+k_{3.2}} \times \frac{1}{[Fe(H_2O_2)^{2+}]} \quad (3.VII)$$

$$[Fe(H_2O_2)^{2+}]\left(1 + \frac{k_{3.1}[H_2O_2]}{k_{-3.1}+k_{3.2}}\right) = \frac{k_{3.1}[H_2O_2]\left([Fe^{II}]_0-[Fe^{III}]\right)}{k_{-3.1}+k_{3.2}} \quad (3.VIII)$$

$$[Fe(H_2O_2)^{2+}]\left(\frac{k_{-3.1}+k_{3.2}+k_{3.1}[H_2O_2]}{k_{-3.1}+k_{3.2}}\right) = \frac{k_{3.1}[H_2O_2]\left([Fe^{II}]_0-[Fe^{III}]\right)}{k_{-3.1}+k_{3.2}} \quad (3.IX)$$

$$[\mathrm{Fe}[\mathrm{H_2O_2}]^{2+}] = \frac{k_{3.1}[\mathrm{H_2O_2}]\left([\mathrm{Fe^{II}}]_0-[\mathrm{Fe^{III}}]\right)}{k_{-3.1}+k_{3.2}+k_{3.1}[\mathrm{H_2O_2}]} \quad (3.X)$$

Inserting equation 3.X in the rate expression for $\frac{\mathrm{d}[\mathrm{Fe^{III}}]}{\mathrm{dt}}$ (equation 3.III) leads to:

$$\frac{\mathrm{d}[\mathrm{Fe^{III}}]}{\mathrm{dt}} = \frac{k_{3.2}k_{3.1}[\mathrm{H_2O_2}]\left([\mathrm{Fe^{II}}]_0-[\mathrm{Fe^{III}}]\right)}{k_{-3.1}+k_{3.2}+k_{3.1}[\mathrm{H_2O_2}]} \quad (3.XI)$$

with $\frac{k_{3.2}k_{3.1}[\mathrm{H_2O_2}]}{k_{-3.1}+k_{3.2}+k_{3.1}[\mathrm{H_2O_2}]}$ being the observed pseudo first order reaction rate constant of the Fenton reaction (k').

At very high $[H_2O_2]$ the expression for k' should simplify to

$$k' = \frac{k_{3.2}k_{3.1}[\mathrm{H_2O_2}]}{k_{-3.1}+k_{3.2}+k_{3.1}[\mathrm{H_2O_2}]} \approx \frac{k_{3.2}k_{3.1}[\mathrm{H_2O_2}]}{k_{3.1}[\mathrm{H_2O_2}]} = k_{3.2} \quad (3.XII)$$

so that at such conditions of high [H_2O_2] *k'* becomes independent of [H_2O_2] and finally equals the rate constant for the decay rate of the intermediate $Fe(H_2O_2)^{2+}$-complex.

Reaction 3.2 is likely to be dominant at acidic conditions whereas reaction 3.3 is supposed to be dominant at circumneutral pH.[5]

The present study gives the first kinetic indication for the existence of the Fe-H_2O_2-complex formed as intermediate in the Fenton reaction, examines its pH-dependent stability and, correlates these findings with corresponding $^{\bullet}OH$-yields to investigate if the decay route of the iron-peroxo-complex is affected by pH ($^{\bullet}OH$- vs. Fe^{IV}-formation).

3.3 MATERIALS AND METHODS

3.3.1 CHEMICALS

Ammonium iron(II) sulfate hexahydrate ($(NH_4)_2Fe(SO_4)_2 \times 6\ H_2O$) (99%) (Sigma Aldrich, Germany), ammonium iron(III) sulfate dodecahydrate ($(NH_4)Fe(SO_4)_2 \times 12\ H_2O$) (≥ 98.5%) (Carl Roth, Germany), H_2O_2 (30%) (AppliChem, Germany), sulfuric acid (H_2SO_4) (> 95%) (Fischer Chemicals, Switzerland), DMSO (99.9%) (VWR, Germany), sodium hydroxide solution (NaOH) (1 M) (Bernd Kraft, Germany), sodium methane sulfinate ($NaCH_3O_2S$) (MSIA) (95%) (Alfa Aesar, Germany), and methane sulfonic acid (CH_4O_3S) (MSOA) (≥ 99.9%) (Merck, Germany) were used as received without further purification. Disodium carbonate (Na_2CO_3) (≥ 99.5%) (Carl Roth, Germany) and sodium bicarbonate ($NaHCO_3$) (99.7%) (Riedel de Haën, Germany) were dried at 80 °C overnight before use. Once dried the two salts were stored in a desiccator. Solutions of $(NH_4)_2Fe(SO_4)_2 \times 6\ H_2O$, $(NH_4)Fe(SO_4)_2 \times 12\ H_2O$ and DMSO were prepared by dissolution of an appropriate amount in milli-Q-filtered

water (PURELAB ultra, ELGA, Germany) acidified with H_2SO_4 to pH 1, 2, 3, or 4, respectively. Stock solutions of MSIA and MSOA were prepared by dissolution of an appropriate amount or volume, in milli-Q-filtered water. A bicarbonate/carbonate buffer stock solution was prepared by dissolution of appropriate amounts of dried salts in milli-Q-filtered water.

3.3.2 KINETIC EXPERIMENTS

Experimental Setup

Kinetic Fenton experiments were carried out with a stopped-flow system (SFM-20, Biologic, France) equipped with a diode array detector (DAD) (TIDAS S 300K, j & m Analytics AG, Germany). The system worked with two 10-mL syringes. One of the syringes contained the Fe^{II}-solution whereas the other syringe contained H_2O_2 and in the respective case DMSO.

For each measurement 100 µL out of each syringe were injected with a flow rate of 3.5 mL min^{-1} per syringe. Before the two solutions reached the measurement cell – a 10-µL quartz cuvette; path length: 10 mm – they were rapidly mixed in a mixing chamber. This led to a dead time of 6.4 ms. Spectroscopic data were recorded every millisecond for 2.5 seconds.

For a schematic figure of the stopped-flow setup see Figure 3.5.

Experimental conditions

Experiments were based on the assumption that the observed pseudo first order rate constant (*k'*) of the reaction between Fe^{II} and H_2O_2 should increase and finally reach a plateau with increasing $[H_2O_2]$, as at very high $[H_2O_2]$ *k'* should not depend on $[H_2O_2]$ anymore but on the decay rate of $Fe(H_2O_2)^{2+}$. Consequently, a plateau in *k'* with increasing $[H_2O_2]$ would yield kinetic indication for the existence of the postulated intermediate complex formed in the

reaction and the value of *k'* reached at the plateau could be interpreted as observed first order reaction rate constant for its decay ($k_{3.2}$).

Kinetics of Fe^{III}-formation from the reaction of Fe^{II} (used as $(NH_4)_2Fe(SO_4)_2 \times 6\ H_2O$) with a surplus of H_2O_2 were followed spectrophotometrically under pseudo first order conditions at pH 3. The whole spectrum ranging from λ = 190 – 700 nm was recorded every millisecond. However, the absorbance maximum at λ = 300 nm was used to follow Fe^{III}-formation whereas at other wavelengths no further maxima could be observed. *k'* was determined at four different $[Fe^{II}]_0$ (50 µM, 135 µM, 300 µM, and 500 µM) and varying $[H_2O_2]$ ranging from 0.005 M to 1.25 M for $[Fe^{II}]_0$ = 50 µM, from 0.0135 M to 1.35 M for $[Fe^{II}]_0$ = 135 µM, from 0.03 M to 1.2 M for $[Fe^{II}]_0$ = 300 µM, and from 0.05 M to 1.25 M for $[Fe^{II}]_0$ = 500 µM.

For the four $[Fe^{II}]_0$ investigated, the influence of DMSO as radical scavenger was examined at pH 3. The required [DMSO] was calculated for each $[H_2O_2]$ by means of a competition kinetic (equation XIII) so that theoretically 99% of all •OH react with DMSO.

$$f(^{\bullet}OH + DMSO) = \frac{[DMSO] \times k(^{\bullet}OH + DMSO)}{[DMSO] \times k(^{\bullet}OH + DMSO) + [Fe^{II}] \times k(^{\bullet}OH + Fe^{II}) + [H_2O_2] \times k(^{\bullet}OH + H_2O_2)}) \qquad (3.XIII)$$

With f(•OH + DMSO) being the fraction of •OH reacting with DMSO. For the calculation, the following rate constants were used.[6]

$k(^{\bullet}OH + Fe^{II}) = 3 \times 10^8\ M^{-1}\ s^{-1}$

$k(^{\bullet}OH + H_2O_2) = 2.7 \times 10^7\ M^{-1}\ s^{-1}$

$k(^{\bullet}OH + DMSO) = 7 \times 10^9\ M^{-1}\ s^{-1}$

For 300 µM Fe^{II}, additionally the influence of the pH on the development of *k'* with increasing $[H_2O_2]$ was studied. pH was adjusted with H_2SO_4 and varied between 1 and 4 in steps of 1 unit. Higher pH values could not be examined due to limited solubility of Fe^{III}.

All experiments were carried out at room temperature (~ 20 °C).

Data evaluation

All calculations and regression analyses described were performed with OriginPro 2015G.

For data evaluation at first absorbance measured at 300 nm (Figure 3.6) during Fenton experiments was corrected for by blank subtraction. Samples containing equal [H_2O_2] and as appropriate [DMSO] compared to the respective Fenton experiment served as blank. Afterwards, the corrected absorbance was converted to the corresponding [Fe^{III}] via calibration with $(NH_4)Fe(SO_4)_2 \times 12\ H_2O$ at the same wavelength (Figure 3.7). Even if the calibration was quite stable (y = 0.00177 (± 6.05×10^{-5}) x – 0.00312 (± 0.0034)) it was performed every measurement day in order to correct for random variations of the detector. Calibration standards covered a concentration range from 10 to max. 1000 µM Fe^{III} considering the applied $[Fe^{II}]_0$. By means of a mass balance the Fe^{III}-concentration at a certain time (t) was converted to the corresponding Fe^{II}-concentration (equation 3.XIV) (Figure 3.8).

$$[Fe^{II}]_t = [Fe^{II}]_0 - [Fe^{III}]_t \qquad (3.XIV)$$

Finally, the natural logarithm of $[Fe^{II}]_t$ over $[Fe^{II}]_0$ was calculated to plot $-\ln\frac{[Fe^{II}]_t}{[Fe^{II}]_0}$ vs. time (Figure 3.9). From this plot, observed pseudo first order rate constants were derived from the slope of a linear regression analysis of the first 15 milliseconds. These observed pseudo first order rate constants were plotted against the corresponding [H_2O_2] to investigate whether there is kinetic evidence for the existence of the postulated $Fe(H_2O_2)^{2+}$.

$k_{3.2}$ was derived from these data by fitting with an exponential function (equation 3.XV). Thereby $k_{3.2}$ can be derived by extrapolation to infinite [H_2O_2].[7]

$$k' = k_{3.2} + A \times e^{\frac{[H_2O_2]}{B}} \qquad (3.XV)$$

with A and B being fitting parameters.[7]

However, those data, which do not exhibit clear plateaus within the investigated range of $[H_2O_2]$, *k'* measured at high $[H_2O_2]$ are not exactly depicted by the function leading to values for $k_{3.2}$, which reveal large statistical errors since the error is leveraged by the strong extrapolation to infinite $[H_2O_2]$. Unfortunately, it was not possible to determine *k'* at higher $[H_2O_2]$, due to the strong background absorbance of H_2O_2, which largely interfered with Fe^{III} absorbance.

Instead, $k_{3.2}$ was derived from these data by linear regression analysis of *k'* vs. $[H_2O_2]$ in the plateau with a slope of 0. The plateau was defined as the range starting from the highest $[H_2O_2]$ until no overlap of determined standard errors could be observed between *k'* at a certain $[H_2O_2]$ and *k'* at the next lower $[H_2O_2]$. The respective y-intercept equals $k_{3.2}$ (Table 3.1). Corresponding errors correspond to the 95% confidence interval.

However, both methods are approximations not matching the real value of $k_{3.2}$ in case of *k'* not exhibiting a clear plateau at highest $[H_2O_2]$ investigated.

Besides $k_{3.2}$, obtained data also allow determination of second order rate constants (k_{2nd}). Those can be determined from the slope of a linear regression analysis of *k'* vs. $[H_2O_2]$ prior to the plateau and give information about the overall kinetics of the Fe^{III}-formation. Considering the assumption that Fe^{III} is just formed due to the reaction of Fe^{II} and H_2O_2, this rate constant equals k_{2nd} of the Fenton reaction.

3.3.3 Determination of $^{\bullet}OH$-yields by DMSO assay

Experimental setup

The utilised IC-system was composed of a Metrohm 883 Basic IC plus, a Metrohm 863 Compact IC Autosampler, and a Metrohm IC conductivity detector. As column a Metrosep A

Supp 4 (250/4.0) was used with particles having a diameter of 9 µm. A bicarbonate/carbonate buffer (0.34 mM/0.36 mM) was used as eluent. The flow was set to 1.0 mL min^{-1}.

Experimental conditions

For •OH-quantification $[Fe^{II}]_0$ was set to 100 µM. Selected $[H_2O_2]$ were 0.01, 0.05, 0.1, and 0.25 M corresponding to a maximum H_2O_2-excess of 2500 times $[Fe^{II}]_0$. Besides Fe^{II} and H_2O_2 samples contained DMSO as radical scavenger, which was used to quantify generated •OH by determining the oxidation products MSIA and MSOA. The [DMSO] required to achieve a > 99% scavenging of •OH was calculated for each $[H_2O_2]$ with equation IX. Required concentrations ranged from 0.017 to 0.11 M.

Water, H_2O_2, and DMSO solutions were adjusted to the desired pH by addition of H_2SO_4 and mixed before starting the reaction by the addition of Fe^{II} solution, which was adjusted to the same pH. After 10 s of vigorous mixing an aliquot was taken and mixed with 1 mM NaOH to precipitate generated Fe^{III}. Each sample was prepared directly before the IC-measurement.

In order to investigate the contribution of the Fenton-like reaction (reaction 1.12) to the overall •OH-yield within the reaction time of 10 s, all experiments were repeated starting with Fe^{III} as Fe-source.

Data evaluation

Detected peaks of MSIA and MSOA were quantified using calibrations ranging from 0.5 to 50 µM of the corresponding compounds. Calculated concentrations of MSIA and MSOA in the samples were summed up. The •OH-yields correspond to 92% of the combined MSIA and MSOA yields (for details see Veltwisch, *et al.* (1980)[8]).

3.4 RESULTS AND DISCUSSIONS

Influence of $[Fe^{II}]_0$

Pseudo first order rate constants of Fe^{III}-formation in the Fenton reaction were measured at increasing values of $[H_2O_2]$ in order to investigate whether there is any kinetic indication for the existence of an intermediate formed during the reaction of Fe^{II} with H_2O_2.

All experiments showed fast formation of Fe^{III}. Hence, the above made assumption that the term $k_{3.1}[H_2O_2]$ is much larger compared to $k_{-3.1}$ is legitimated, as according to the steady state approximation Fe^{III}-formation would have been markedly suppressed in case of $k_{-3.1}$ being much larger than $k_{3.1}[H_2O_2]$.[9]

Figure 3.1 illustrates the development of *k'* at increasing values of $[H_2O_2]$ for four different $[Fe^{II}]_0$. Regardless of the applied $[Fe^{II}]_0$ *k'* increases up to $[H_2O_2]$ = 0.6 M at 50 µM Fe^{II}, 0.675 M at 135 µM Fe^{II}, 0.9 M at 300 µM Fe^{II}, and 1 M at 500 µM Fe^{II}. With further increasing $[H_2O_2]$ *k'* becomes independent of $[H_2O_2]$ and stagnates within the range of the 95% confidence intervals (error bars) at about 50 s^{-1} (Table 3.1). According to assumptions made as basis of these experiments the results indicate the formation of an intermediate in the reaction of Fe^{II} with H_2O_2 its decay rate would be responsible for the plateau in *k'* with increasing $[H_2O_2]$. Hence, the value of *k'* reached at the plateau is interpreted as $k_{3.2}$ and provides information concerning the stability of the intermediate. The data show that the intermediate does not reveal any $[Fe^{II}]_0$-dependent stability. According to von Sonntag (2008) it is assumed that this intermediate is $FeOOH^+$ ($Fe(H_2O_2)^{2+}$).[5, 10] The measurement uncertainty increases at high $[H_2O_2]$ due to spectral interferences with the peroxide at the selected wavelength. These interferences could not be avoided as detection of Fe^{III} is only possible at 300 nm. Additionally, there is a higher measurement uncertainty for smaller $[Fe^{II}]_0$ due to limited sensitivity.

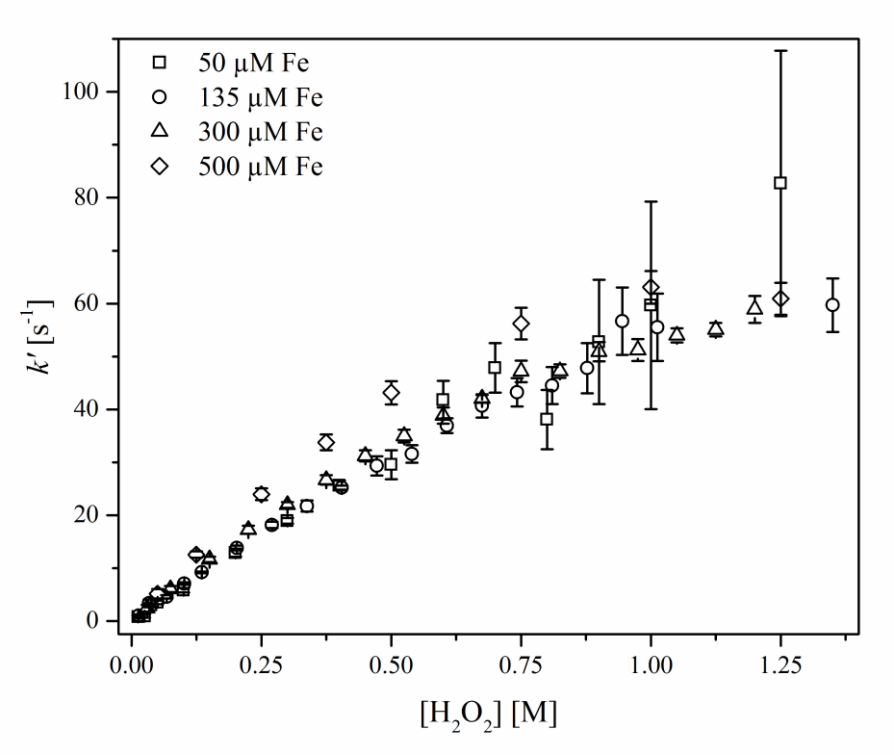

Figure 3.1: Observed pseudo first order reaction rate constants of the Fenton reaction at increasing values of $[H_2O_2]_0$ measured for different $[Fe^{II}]_0$ at pH 3 and T = 20 °C. $[Fe^{II}]_0$ = 50 µM (squares), 135 µM (circles), 300 µM (triangles), and 500 µM (diamonds). The error bars indicate the 95% confidence interval of the applied regression analysis.

The presented data also allow the determination of second order reaction rate constants (k_{2nd}) of the Fenton reaction (i.e., H_2O_2 plus Fe^{2+}). They are derived from a linear regression analysis of *k'*-data until the plateau is reached (see Table 3.1). Values determined for k_{2nd} varied from 63 ± 2 to 80 ± 5 M^{-1} s^{-1} over the range of $[Fe^{II}]_0$ investigated. Obtained values for k_{2nd} are confirmed by literature. Published values for the Fenton system in the presence of SO_4^{2-} range from 63 M^{-1} s^{-1} to 89 M^{-1} s^{-1}. [11-13] Hence, our experimental approach seems suitable to observe effects on Fenton kinetics.

Table 3.1: First order rate constants for the decay of $Fe(H_2O_2)^{2+}$ ($k_{3.2}$) and second order rate constants (k_{2nd}) for the Fenton reaction determined for various $[Fe^{II}]_0$ in absence (−) and presence (+) of DMSO at various pHs and T = 20 °C. Uncertainties of $k_{3.2}$ and k_{2nd} represent the 95% confidence interval of the y-intercept and the slope of the linear regressions used to derive $k_{3.2}$ and k_{2nd} respectively.

$[Fe^{II}]_0$ [µM]	pH	*DMSO*	$k_{3.2}$ [s^{-1}]	k_{2nd} [M^{-1} s^{1}]
50	3	−	44 ± 2	63 ± 2
50	3	+	51 ± 4	55 ± 2
135	3	−	45 ± 2	62 ± 1
135	3	+	52 ± 1	55 ± 1
300	1	−	60 ± 1	74 ± 2
300	2	−	70 ± 4	81 ± 2
300	3	−	51 ± 1	67 ± 4
300	3	+	54 ± 2	56 ± 1
300	4	−	53 ± 4	77 ± 6
500	3	−	62 ± 1	80 ± 5
500	3	+	n.a.	n.a.

Influence of an $^{\bullet}OH$-scavenger

In the Fenton chain reaction Fe^{II} can be oxidised by several reactions involving different oxidants (reactions 1.8, 1.10, and 1.13). With the applied method it cannot be differentiated by which pathway the detected Fe^{III} was formed. Therefore, reactions yielding Fe^{III} other than oxidation of Fe^{II} by H_2O_2 (reaction 1.8) must be excluded.

Fe^{III} can also be formed in reactions of $^{\bullet}OH$ (reaction 1.10) and $HO_2^{\bullet}$ (reaction 1.13) with Fe^{II}. These oxidants are formed in reactions 1.8, 1.9, 1.11, and 1.12. The influence of reaction 1.12

on $HO_2^{\bullet}$-formation can be neglected as this reaction is several orders of magnitude slower than reaction 1.8 and is therefore not likely to be relevant in the investigated timeframe (15 ms). However, $^{\bullet}OH$-based reactions (reactions 1.9 and 1.10) must be prevented. This is possible by means of an $^{\bullet}OH$-scavenger. Therefore, DMSO was used that reacts with $^{\bullet}OH$ with a rate of 7×10^9 M^{-1} s^{-1}.[6] By scavenging of $^{\bullet}OH$, reaction 1.9 will be suppressed, which is an important source of $HO_2^{\bullet}$. Hence, reactions 1.11 and 1.13 are also suppressed by addition of DMSO and Fe^{III}-formation is largely controlled by reaction 1.8.

In Figure 3.2 *k'* is presented at increasing values of $[H_2O_2]$ for four different $[Fe^{II}]_0$ in the presence of the $^{\bullet}OH$-scavenger DMSO. Even in presence of DMSO, *k'* increases up to $[H_2O_2]$ ~ 0.75 M regardless of $[Fe^{II}]_0$ except for 500 µM Fe^{II}. For this $[Fe^{II}]$ *k'* increases over the entire $[H_2O_2]$-range. With further increasing $[H_2O_2]$ the formation of a plateau in *k'* is not as pronounced as in absence of the scavenger due to higher scattering of the data. This might result from additional spectral interferences caused by DMSO even if spectra were corrected for background absorption of H_2O_2 and DMSO before further calculations. Representative blank spectra of 1.05 M H_2O_2 in absence and presence of DMSO (0.4 M) are shown in Figure 3.10.

Table 3.1 compiles decay rates calculated for different $[Fe^{II}]_0$ in absence and presence of DMSO. $k_{3.2}$ determined in presence of DMSO ranged from 51 ± 4 s^{-1} at 50 µM Fe^{II} to 54 ± 2 s^{-1} at 300 µM Fe^{II}. For 500 µM Fe^{II} no plateau could be observed and hence, no $k_{3.2}$ could be derived. Considering a 2-tailed t-test there is no significant difference between $k_{3.2}$ determined in absence or presence of DMSO. Consequently, it can be concluded that $^{\bullet}OH$ is neither responsible for the plateau in *k'* nor does it influence the stability of $Fe(H_2O_2)^{2+}$. This was expected as in absence of DMSO $^{\bullet}OH$ are to a large extend scavenged by surplus H_2O_2 (reaction 1.9).

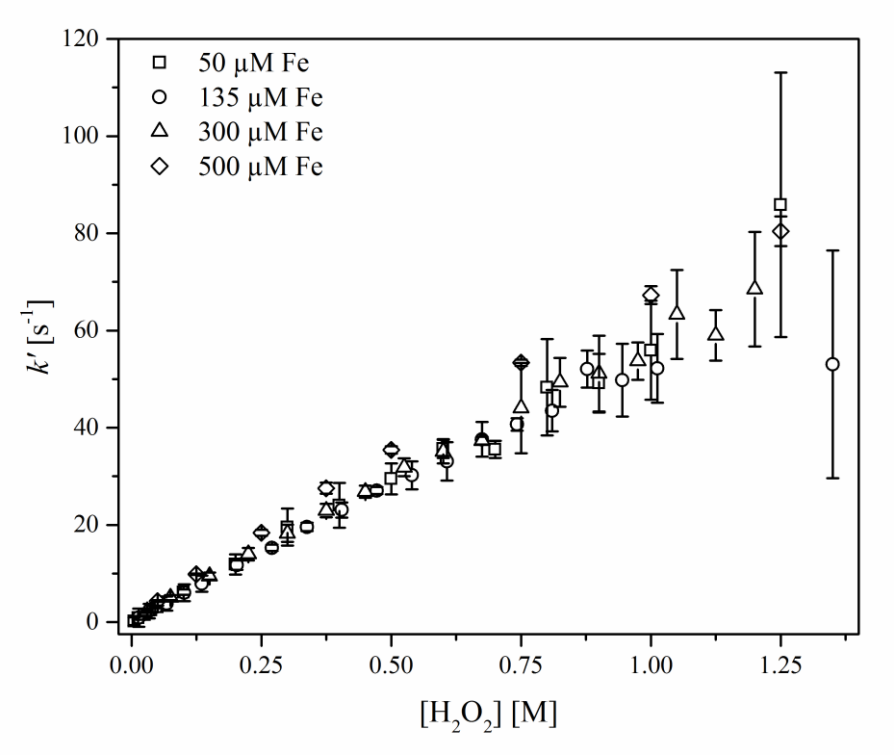

Figure 3.2: Observed pseudo first order reaction rate constants of the Fenton reaction at increasing values of $[H_2O_2]_0$ measured for different $[Fe^{II}]_0$ in presence of DMSO as ˙OH-scavenger at pH 3 and T = 20 °C. $[Fe^{II}]_0$ = 50 µM (squares), 135 µM (circles), 300 µM (triangles), and 500 µM (diamonds). The error bars indicate the standard deviation of three independent measurements.

k_{2nd} calculated from these data are only slightly smaller in presence of DMSO than in its absence (see Table 3.1). Since reaction 1.10 cannot be relevant anymore in the presence of DMSO Fe^{III}-formation via this reaction can be neglected. As the difference of the two systems (presence and absence of DMSO) is very small ˙OH may not be important for reactions with Fe^{II} in both systems. With increasing $[H_2O_2]$ reaction 1.10 is suppressed by reaction 1.9 even if reaction 1.9 is one order of magnitude slower. Hence, in absence of DMSO most ˙OH react with H_2O_2 to form HO_2˙, which could react with both, Fe^{II} and Fe^{III} according to reactions 1.13 and 1.14, with reaction 1.13 being dominant due to the higher rate constant. By blocking reaction 1.9 the presence of DMSO will also indirectly prevent Fe^{III}-formation via reaction 1.13 resulting in an overall reduced reaction rate for Fe^{III}-formation.

Influence of pH

As mentioned above, pH influences the Fenton reaction but only little is known about underlying mechanisms. Therefore, it was examined whether the pH influences formation and stability of $Fe(H_2O_2)^{2+}$. Due to limited solubility of Fe^{III} at pH > 4 (solubility product (K_{sp}) ($Fe(OH)_3$) = 2.79×10^{-39})[14] experiments were carried out at pH 1 – 4.

Figure 3.3 illustrates the effect of pH on *k'* at increasing values of $[H_2O_2]$. Data obtained at pH 1 and 2 differ from those obtained at pH 3 and 4. Regardless of the pH, *k'* rises linearly with increasing $[H_2O_2]$ and plateaus at high peroxide concentrations. For pH 1 and 2 growing *k'* is detected until $[H_2O_2]$ = 1 M, whereas for pH 3 and 4 the plateau in *k'* starts at $[H_2O_2]$ = 0.75 M.

Indeed, *k'* stagnates at high surplus of $[H_2O_2]$ for all investigated pH values leading to the conclusion that the intermediate $Fe(H_2O_2)^{2+}$ is formed regardless of the pH. According to a 2-tailed t-test (p = 0.05) significant differences were detected between $k_{3,2}$-values determined at pH 1 – 4 in every combination except for pH 3 and 4. Hence, $k_{3,2}$ determined at pH 1 and 2 tend to be higher compared to those determined at pH 3 and 4 (Table 3.1). As the value of *k'* at the plateau is interpreted as the decay rate of $Fe(H_2O_2)^{2+}$, a smaller *k'* indicates that this complex is more stable. Hence, with increasing pH, $Fe(H_2O_2)^{2+}$ becomes more stable.

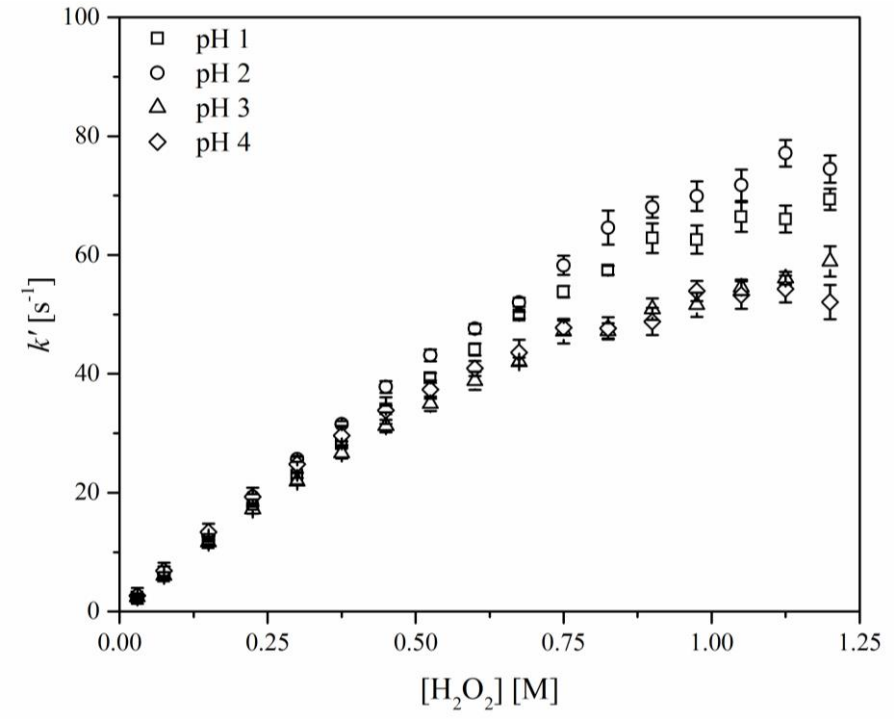

Figure 3.3: Observed pseudo first order reaction rate constants of the Fenton reaction at increasing values of $[H_2O_2]_0$ measured for different pHs at T = 20 °C and $[Fe^{II}]_0$ = 300 µM. pH 1 (squares), pH 2 (circles), pH 3 (triangles), and pH 4 (diamonds). The error bars indicate the standard deviation of three independent measurements.

As expected k_{2nd} of the reaction Fe^{II} with H_2O_2 determined for the investigated pH values are not influenced by the pH. Calculated values are in the range between 67 and 81 M^{-1} s^{-1} (Table 3.1). Despite significant differences (statistical testing was performed by means of a 2-tailed t-test (p = 0.05)) between k_{2nd} determined at various pHs the absence of any pH-dependent trend indicates that the pH does not systematically influence k_{2nd} in the observed pH-range. Rather, these differences show up due to measurement and experimental uncertainties. The overall reaction rate of the Fenton reaction is controlled by Fe^{II}-speciation as $Fe(OH)^+$ and $Fe(OH)_2^0$ are much more reactive towards H_2O_2 than Fe^{2+}.[15-17] However, Fe^{2+} is the only Fe^{II}-species present at pH 1 – 4 explaining that no effect on k_{2nd} could be observed.[18] No effect of pH (pH 1 – 3) was also observed by Bataineh, *et al.* (2012)[3], even if the absolute value for k_{2nd}

determined by them is not comparable as they conducted their experiments in non-coordinating media and it is already known that SO_4^{2-} accelerates the Fenton reaction.[3, 12, 19]

Determination of ˙OH-yields by DMSO assay

Different decay routes of the $Fe(H_2O_2)^{2+}$-complex may either result in ˙OH or other reactive species depending on the prevailing pH.[5] This was investigated by quantification of the ˙OH-yield using DMSO as radical scavenger (see chapter 3.3.3).

Relative ˙OH-yields referred to $[Fe^{II}]_0$ of 100 µM were determined for different $[H_2O_2]$ at pH 1 – 4 (Figure 3.11). ˙OH-yields tend to increase with the applied H_2O_2-dosage. Furthermore, ˙OH-yields exceeded 100% per added Fe^{II}-dose at $[H_2O_2] \geq 0.05$ M. This indicates an increasing impact of the Fenton-like reaction, recycling Fe^{III} to Fe^{II} (reaction 1.12) that again feeds the Fenton reaction (reaction 1.8) and thus, increases the overall ˙OH-yields.

In order to quantify the impact of the Fenton-like induced Fe-recycling on the overall ˙OH-yield experiments were repeated using Fe^{III} instead of Fe^{II} as primary Fe-source (Figure 3.12). As expected, ˙OH-yields increased with $[H_2O_2]$ as an increasing $[H_2O_2]$ accelerates the reaction between Fe^{III} and H_2O_2.

This surplus in ˙OH-yield from the Fe^{III}-induced Fenton-cycle can be taken into account by subtracting the ˙OH-yield of the Fenton-like experiments from the overall ˙OH-yield shown in Figure 3.11. Corrected ˙OH-yields are shown in Figure 3.4. ˙OH-yields were determined at pH 1 – 4 at different $[H_2O_2]$. The majority of yields does not differ significantly from 100% regarding $[Fe^{II}]_0$ of 100 µM considering depicted standard errors but show random variations. The yields that deviate from 100% can be considered as outlier since yields show no clear trend with $[H_2O_2]$ or pH. Depicted errors consist of standard deviations of three replicate experiments for each pH, $[H_2O_2]$, and Fe oxidation state. The errors also include error propagation as shown

•OH-yields were determined by a combination of two independent measurements (i.e. Fe^{II}/H_2O_2 and Fe^{III}/H_2O_2-system). The fact that sample preparation and subsequent measurement requires an exact schedule also contributes to standard errors. Deviations of a few (milli)-seconds in the performance of the schedule can cause noticeable effects on determined •OH-yields. This can explain the variation of •OH-yields per $[Fe^{II}]_0$ around 100%. Hence, it can be concluded that the pH does not systematically affect formation of reactive species in the Fenton reaction between pH 1 and 4.

This result that •OH is the only active oxidant generated in Fenton chemistry at acidic pH is confirmed by Bataineh, *et al.* (2012)[3]. Also Walling's work on ionic strength effects in the Fenton reaction yielded •OH as sole oxidant at acidic pH. Their conclusion was based on the observation that changes of the ionic strength did not affect the reaction of Fe^{II} and H_2O_2 with methanol.[20-21] A substantial formation of Fe^{IV} would result in a •OH-yield below 100% since the formation of •OH by reactions of Fe^{IV} can be ruled out. Reaction 3.4 only becomes dominant when Fe^{II} and H_2O_2 are applied in nanomolar or even smaller concentrations. In this case, the resulting [•OH] would not be detectable. In case of larger concentrations of Fe^{II} or H_2O_2 reactions 3.5 or 3.6 would become dominant not leading to •OH.

$FeO^{2+} + H_2O \rightarrow Fe^{III} + OH^- + {}^{\bullet}OH$ $\quad k = 1.3 \times 10^{-2}\ s^{-1}$ (3.4)[22]

$FeO^{2+} + Fe^{II} + 2\ H^+ \rightarrow 2\ Fe^{III} + H_2O$ $\quad k = 1.4 \times 10^{5}\ M^{-1}\ s^{-1}$ (3.5)[22]

$FeO^{2+} + H_2O_2 \rightarrow Fe^{III} + HO_2^{\bullet} + OH^-$ $\quad k = 1.0 \times 10^{4}\ M^{-1}\ s^{-1}$ (3.6)[22]

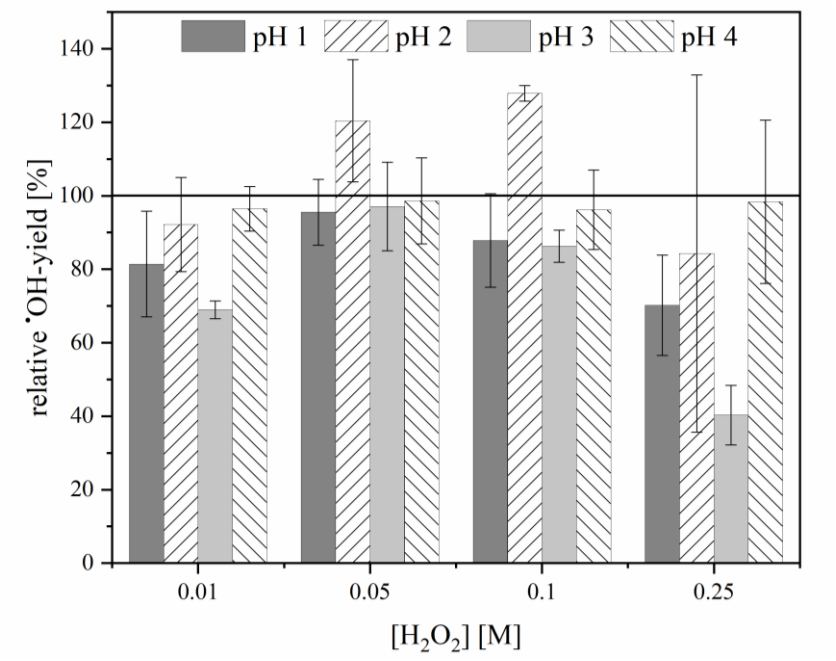

Figure 3.4: Relative •OH-yields referred to $[Fe^{II}]_0$ determined for the reaction of 100 µM Fe^{II} and various concentrations of H_2O_2 corrected for •OH-yields determined for the reaction of 100 µM Fe^{III} and same concentrations of H_2O_2 at pH 1 – 4. Error bars indicate the standard deviation of three independent measurements.

As there is no considerable difference in the •OH-yields in dependence on pH the increased stability of $Fe(H_2O_2)^{2+}$ at pH 3 and 4 compared to pH 1 and 2 could not be explained by a mechanistic changeover from •OH- to Fe^{IV}-generation. Possibly, speciation of formed Fe^{III} plays a role in this context, as at pH 1 and 2 Fe^{3+} is the dominant species whereas $Fe(OH)^{2+}$ and $Fe(OH)_2^{+}$ are prevalent species at pH 3 and 4, respectively.[23] Another possible explanation is based on an expected speciation of $Fe(H_2O_2)^{2+}$ that might be in a pH-dependent equilibrium with $Fe(HO_2)^{+}$ ($pK_a \approx 3$).[10] Since stability of the complex was higher at pH > 3 $FeOOH^{+}$ seems to be more stable than $Fe(H_2O_2)^{2+}$.

The present paper provides the first kinetic indication for the existence of an intermediate Fe^{II}-H_2O_2-complex formed in the Fenton reaction.[5] Hence, widely accepted literature suggesting that the reaction between Fe^{II} and H_2O_2 occurs via an inner sphere electron transfer based on kinetic modelling data[24-27] is consistent with the experimental data reported here. Furthermore,

it could be shown that kinetics of the Fenton reaction can be accelerated by increasing [H_2O_2] up to 1 M to a maximum of 60 – 70 s^{-1}. At this reaction kinetics Fe^{II} will be consumed very rapidly (90% of iron degrades within < 1 s, without considering Fenton-like reaction). These fast reaction kinetics can be used in case very small reaction times are provided in a full scale application of the Fenton reaction. However, with regard to pollutant degradation $^{\bullet}OH$-scavenging by H_2O_2 must be taken into account at high [H_2O_2], which will largely decrease the efficiency of pollutant degradation. Furthermore, the study revealed that the decay of the intermediate Fe^{II}-H_2O_2-complex exclusively yields $^{\bullet}OH$ at pH 1 – 4. The formation of Fe^{IV} as a reactive species, which could also be used for pollutant degradation seems to be of minor importance. This shows that efficient Fenton remediation as part of industrial wastewater treatment is possible between pH 1 and 4.

For on-site application of Fenton's reagent even feasibility at circumneutral pH is a topic of interest. Several researchers proposed a mechanistic changeover from $^{\bullet}OH$-formation at acidic to Fe^{IV}-formation at neutral pH.[1, 3] In parallel, even other factors like e.g. presence of complexing agents influence oxidant formation in Fenton chemistry. $^{\bullet}OH$ as well as Fe^{IV} are discussed as reactive species in this context. Hence, a systematic investigation of pH-dependent effects of complexing agents on the Fenton mechanism, i.e. existence of $Fe(H_2O_2)^{2+}$ as intermediate and type of oxidant, is required. To evaluate economic feasibility of Fenton remediation in terms of wastewater treatment the nature of the generated reactive species is a topic of interest, especially, as Fe^{IV} appears to be a more selective oxidant compared to $^{\bullet}OH$. This can largely affect the efficiency of pollutant degradation as well as formation of transformation products and by-products.

3.5 SUPPORTING INFORMATION

3.5.1 SCHEMATIC SETUP OF THE APPLIED STOPPED-FLOW SYSTEM

Figure 3.5 illustrates a schematic drawing of the applied stopped-flow system. Two 10-mL syringes are connected with a mixing chamber via capillaries. From this mixing chamber the reaction mixture flows into a cuvette with dimensions of 1 × 1 × 10 mm. A waste container is connected to the cuvette to collect outflowing samples.

Two optical fibres are connected to the cuvette. One connecting the light source with the cuvette and the other connecting the cuvette with the diode array detector (DAD).

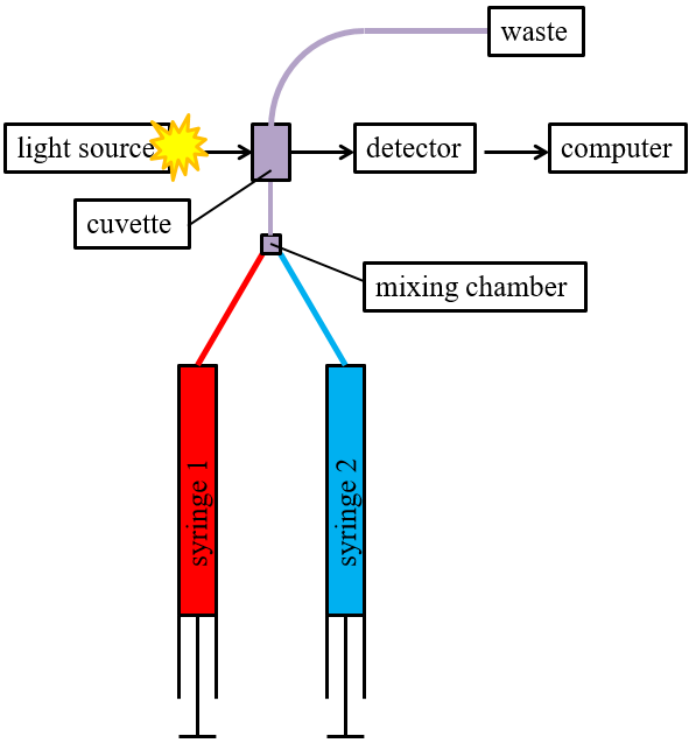

Figure 3.5: Schematic setup of the stopped-flow system.

3.5.2 WORKFLOW FROM KINETIC RAW DATA TO PSEUDO FIRST ORDER RATE CONSTANTS

Figure 3.6 shows exemplary raw data (absorbance at 300 nm vs. time) obtained for kinetic stopped-flow experiments.

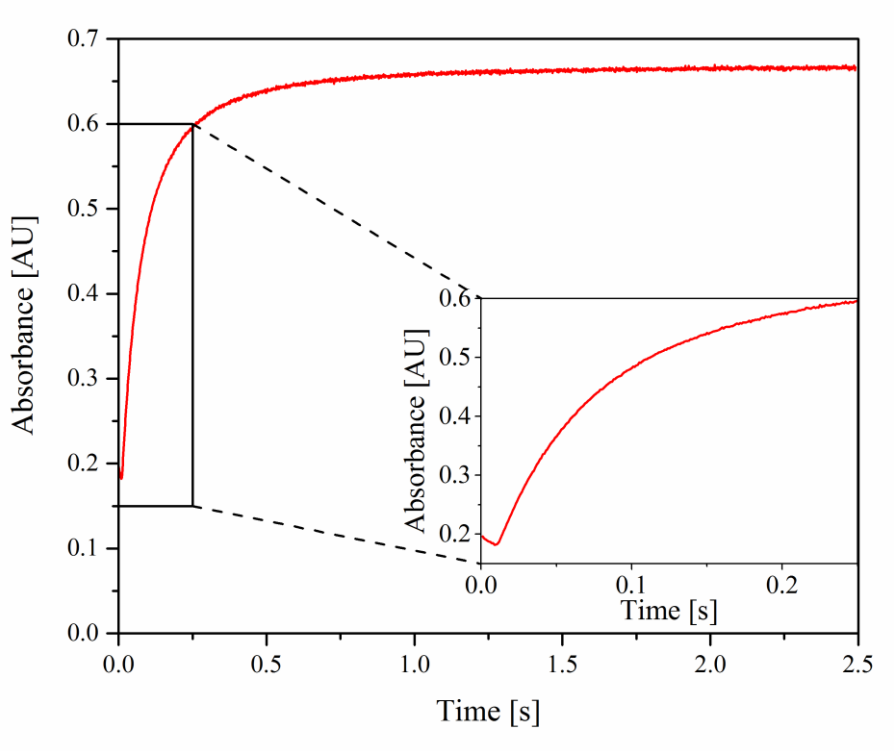

Figure 3.6: Representative spectrum of upcoming absorbance measured at 300 nm over time for a sample containing 300 µM Fe^{II} and 0.15 M H_2O_2 at pH 3; insert: magnification of the first 0.25 seconds.

Data exhibit a period of 11 ms of random variation at an almost constant absorbance level (absolute values depend on applied reactant concentrations) until an increase in the measured absorbance is detected. This results from the setup of the stopped-flow system (Figure 3.5). The total volume of capillaries, mixing chamber and the cuvette is 134.2 µL. With an injection volume of 100 µL per syringe the whole path is flushed until the whole system contains the intended reaction mixture. Recording of data starts before the flushing process has finished

resulting in the 11 ms period of almost constant data, which is therefore cut off prior to the data evaluation.

Figure 3.7 depicts the same data as shown in Figure 3.6 after conversion of measured absorbance to the corresponding $[Fe^{III}]_t$ using a calibration curve recorded prior to Fenton experiments.

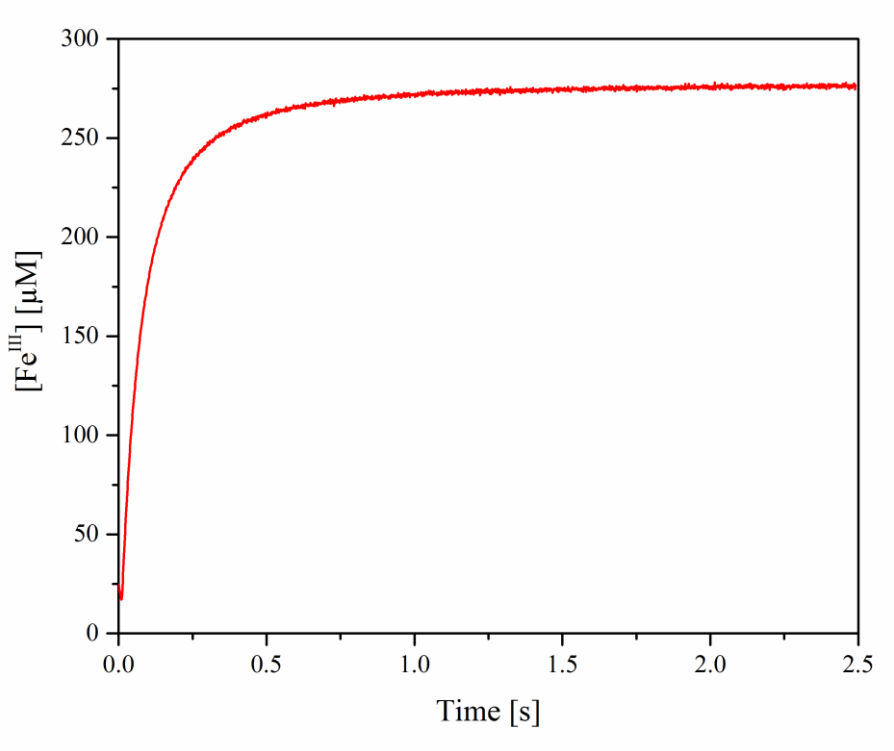

Figure 3.7: Representative Fe^{III}-formation over time for a sample containing 300 µM Fe^{II} and 0.15 M H_2O_2 at pH 3.

This $[Fe^{III}]_t$ is then converted to the corresponding $[Fe^{II}]_t$ by means of a mass balance considering the applied $[Fe^{II}]_0$ as Fe^{III} can just result from the oxidation of added Fe^{II}. Respective data are presented in Figure 3.8.

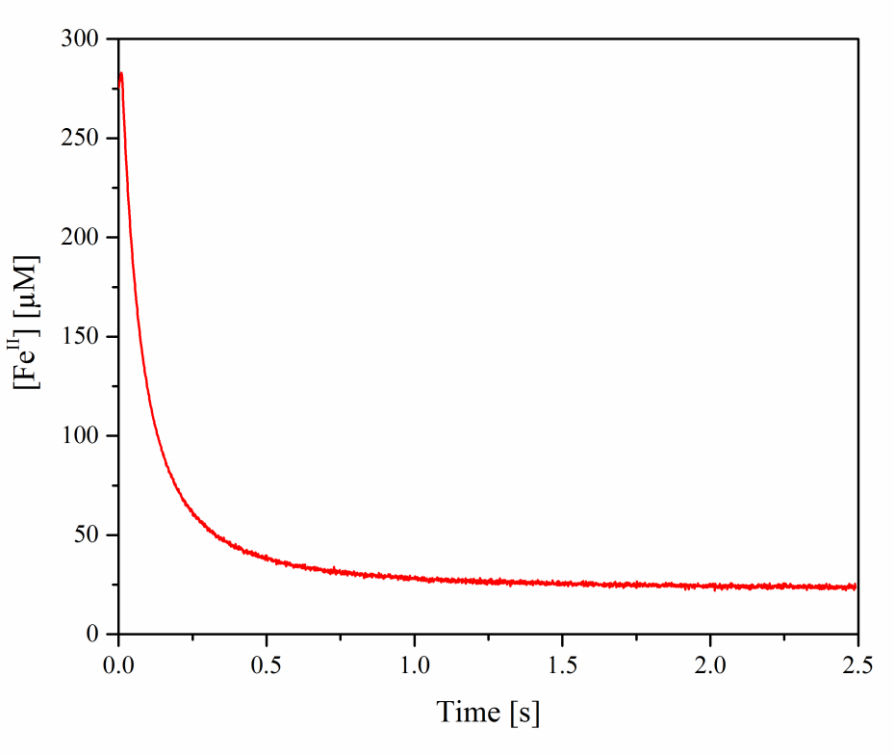

Figure 3.8: Representative decreasing [Fe^{II}] ([Fe^{II}]$_0$ = 300 µM) over time after addition of 0.15 M H_2O_2 at pH 3.

Figure 3.9 shows the final plot of $-\ln\frac{[Fe^{II}]_t}{[Fe^{II}]_0}$ vs. time, which is used to derive intended pseudo first order rate constants by linear fitting of data of the first 15 ms (i.e. 12 – 26 ms without correction). The time of 15 ms was chosen for the fit as with increasing [H_2O_2] data more and more deviated from the expected linear relationship between $-\ln\frac{[Fe^{II}]_t}{[Fe^{II}]_0}$ and time (Figure 3.8). This deviation can be explained by the increasing influence of reaction 6 with increasing [H_2O_2]. Data of the first 15 ms showed the required linear correlation for all applied [H_2O_2] and hence, could yield pseudo first order rate constants for the very beginning of the reaction.

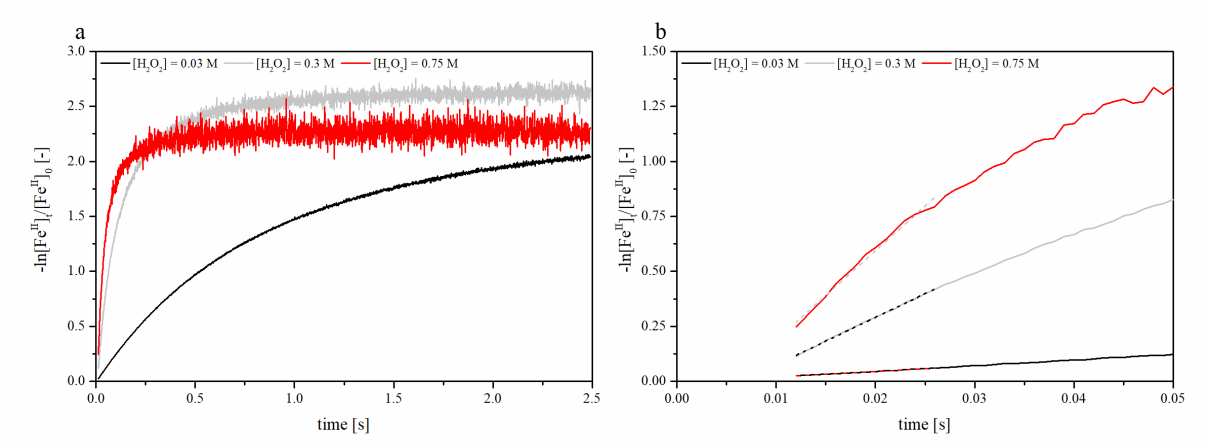

Figure 3.9: a) Representative graphic of -ln([Fe^{II}]$_t$/[Fe^{II}]$_0$) vs. time measured for samples containing 300 µM Fe^{II} and 0.03 (black), 0.3 (grey), and 0.75 M (red) H_2O_2, respectively. Figure b) is a magnification of the first 0.05 s to illustrate the linearity of data in the first 15 ms which are used for the determination of k'.

3.5.3 Representative background spectra of H_2O_2 in absence and presence of DMSO

Figure 3.10 shows the absorbance at 300 nm measured for 1.05 M H_2O_2 in absence and presence of 0.4 M DMSO. Absorbance measured in presence of DMSO is higher than in its absence. The higher background absorbance results in a higher total absorbance measured for Fenton samples (Fe^{II} + H_2O_2 + DMSO) and consequently in data with higher noise. Hence, pseudo first order rate constants determined from these data are more uncertain.

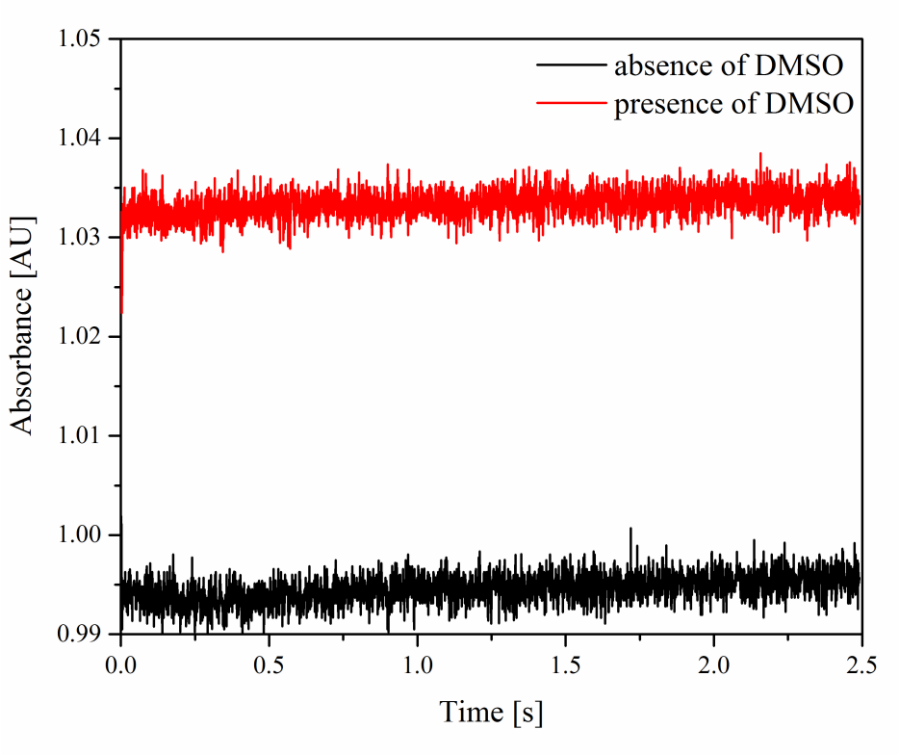

Figure 3.10: Representative background spectra of 1.05 M H_2O_2 in absence (black) and presence (red) of 0.4 M DMSO.

3.5.4 •OH-YIELDS DETERMINED IN THE FENTON AND FENTON-LIKE SYSTEM AT PH 1 – 4

Figure 3.11 shows relative •OH-yields referred to $[Fe^{II}]_0$ of 100 µM determined for different $[H_2O_2]$ at pH 1 – 4.

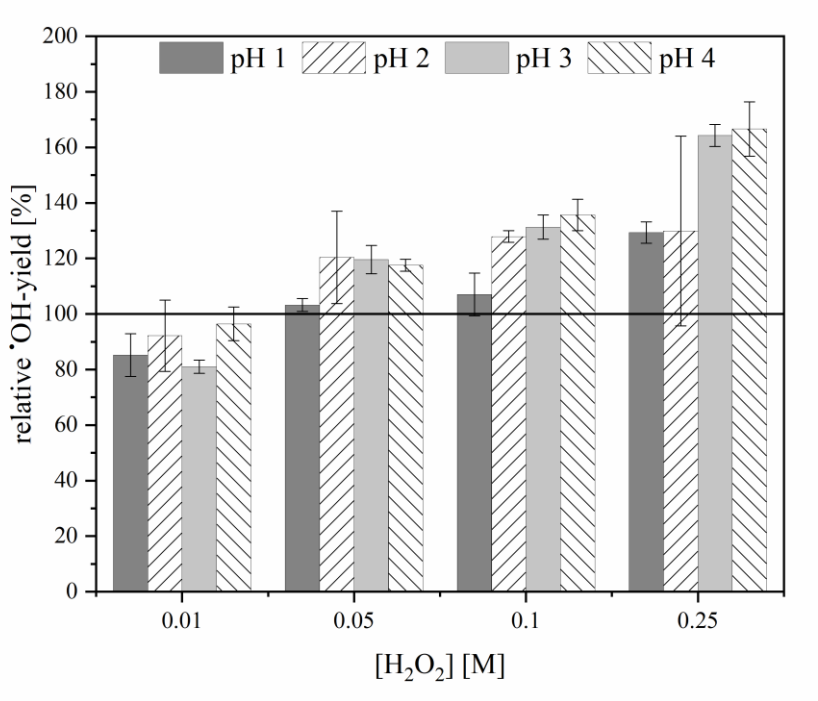

Figure 3.11: Relative •OH-yields referred to $[Fe^{II}]_0$ determined for the reaction of 100 µM Fe^{II} and various concentrations of H_2O_2 at pH 1 – 4. Error bars indicate the standard deviation of three independent measurements.

Figure 3.12 illustrates relative •OH-yields of the Fenton-like reaction determined at same $[H_2O_2]$ and pH as in Fe^{II} based experiments.

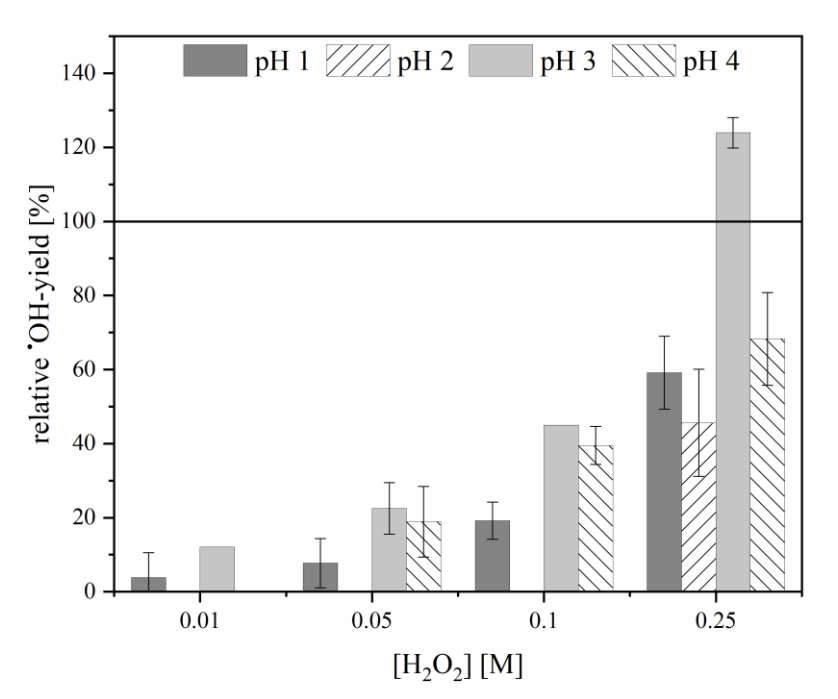

Figure 3.12: Relative •OH-yields referred to $[Fe^{II}]_0$ determined for the reaction of 100 µM Fe^{III} and various concentrations of H_2O_2 at pH 1 – 4. Error bars indicate the standard deviation of three independent measurements.

3.6 REFERENCES

1. Hug, S. J.; Leupin, O., Iron-catalyzed oxidation of arsenic(III) by oxygen and by hydrogen peroxide: pH-dependent formation of oxidants in the Fenton reaction. *Environ. Sci. Technol.* **2003,** *37* (12), 2734-2742.

2. Katsoyiannis, I. A.; Ruettimann, T.; Hug, S. J., pH dependence of Fenton reagent generation and As(III) oxidation and removal by corrosion of zero valent iron in aerated water. *Environ. Sci. Technol.* **2008,** *42* (19), 7424-7430.

3. Bataineh, H.; Pestovsky, O.; Bakac, A., pH-induced mechanistic changeover from hydroxyl radicals to iron(IV) in the Fenton reaction. *Chem. Sci.* **2012,** *3* (5), 1594-1599.

4. Lee, H.; Lee, H. J.; Sedlak, D. L.; Lee, C., pH-Dependent reactivity of oxidants formed by iron and copper-catalyzed decomposition of hydrogen peroxide. *Chemosphere* **2013,** *92* (6), 652-658.

5. von Sonntag, C., Advanced oxidation processes: Mechanistic aspects. *Water Sci. Technol.* **2008,** *58* (5), 1015-1021.

6. Buxton, G. V.; Greenstock, C. L.; Helman, W. P.; Ross, A. B., Critical review of rate constants for reactions of hydrated electrons, hydrogen atoms and hydroxyl radicals (•OH/•O⁻) in aqueous solution. *J. Phys. Chem. Ref. Data* **1988,** *17* (2), 513-886.

7. El Seoud, O. A.; Baader, W. J.; Bastos, E. L., Practical Chemical Kinetics in Solution. In *Encyclopedia of Physical Organic Chemistry*, 1 ed.; Wang, Z.; Wille, U.; Juaristi, E., Eds. John Wiley & Sins, Inc.: Hoboken, **2017**.

8. Veltwisch, D.; Janata, E.; Asmus, K. D., Primary processes in the reaction of •OH-radicals with sulphoxides. *J. Chem. Soc. Perkin Trans. 2* **1980,** (1), 146-153.

9. Connors, K. A., *Chemical Kinetics - The study of Reaction Rates in Solution*. VCH Publishers, Inc.: New York, **1990**.

10. Rachmilovich-Calis, S.; Masarwa, A.; Meyerstein, N.; Meyerstein, D.; van Eldik, R., New mechanistic aspects of the Fenton reaction. *Chem. Eur. J.* **2009,** *15* (33), 8303-8309.

11. Rigg, T.; Taylor, W.; Weiss, J., The rate constant of the reaction between hydrogen peroxide and ferrous ions. *J. Chem. Phys.* **1954,** *22* (4), 575-577.

12. Truong, G. L.; de Laat, J.; Legube, B., Effects of chloride and sulfate on the rate of oxidation of ferrous ion by H_2O_2. *Water Res.* **2004,** *38* (9), 2383-2393.

13. Wells, C. F.; Salam, M. A., Complex formation between iron(II) and inorganic anions. Part II. The effect of oxyanions on the reaction of iron(II) with hydrogen peroxide. *J. Chem. Soc. A* **1968**, 308-315.

14. Vanysek, P., Electrochemical series. In *CRC Handbook of Chemistry and Physics*, 90th (internet version) ed.; Lide, D. R.; Hynes, W. M. M., Eds. CRC Press/Taylor and Francis: Boca Raton, FL, **2010**.

15. Wells, C. F.; Salam, M. A., The effect of pH on the kinetics of the reaction of iron(II) with hydrogen peroxide in perchlorate media. *J. Chem. Soc. A* **1968**, 24-29.

16. Millero, F. J.; Sotolongo, S., The oxidation of Fe(II) with H_2O_2 in seawater. *Geochim. Cosmochim. Acta* **1989,** *53* (8), 1867-1873.

17. González-Davila, M.; Santana-Casiano, J. M.; Millero, F. J., Oxidation of iron (II) nanomolar with H_2O_2 in seawater. *Geochim. Cosmochim. Acta* **2005,** *69* (1), 83-93.

18. Fischbacher, A.; Von Sonntag, C.; Schmidt, T. C., Hydroxyl radical yields in the Fenton process under various pH, ligand concentrations and hydrogen peroxide/Fe(II) ratios. *Chemosphere* **2017,** *182*, 738-744.

19. Hardwick, T. J., The rate constant of the reaction between ferrous ions and hydrogen peroxide in acid solution. *Canadian Journal of Chemistry-Revue Canadienne De Chimie* **1957,** *35* (5), 428-436.

20. Walling, C., Intermediates in the reactions of Fenton type reagents. *Acc. Chem. Res.* **1998,** *31* (4), 155-157.

21. Walling, C.; El-Taliawi, G. M.; Johnson, R. A., Fenton's Reagent. IV. Structure and Reactivity Relations in the Reactions of Hydroxyl Radicals and the Redox Reactions of Radicals. *J. Am. Chem. Soc.* **1974,** *96* (1), 133-139.

22. Løgager, T.; Holcman, J.; Sehested, K.; Pedersen, T., Oxidation of ferrous ions by ozone in acidic solutions. *Inorg. Chem.* **1992,** *31* (17), 3523-3529.

23. Stefánsson, A., Iron(III) hydrolysis and solubility at 25°C. *Environ. Sci. Technol.* **2007,** *41* (17), 6117-6123.

24. Goldstein, S.; Meyerstein, D.; Czapski, G., The Fenton reagents. *Free Radical Biol. Med.* **1993,** *15* (4), 435-445.

25. Bossmann, S. H.; Oliveros, E.; Göb, S.; Siegwart, S.; Dahlen, E. P.; Payawan Jr, L.; Straub, M.; Wörner, M.; Braun, A. M., New evidence against hydroxyl radicals as reactive intermediates in the thermal and photochemically enhanced Fenton reactions. *J. Phys. Chem. A* **1998,** *102* (28), 5542-5550.

26. Gallard, H.; de Laat, J.; Legube, B., Effect of pH on the oxidation rate of organic compounds by Fe^{II}/H_2O_2. Mechanisms and simulation. *New J. Chem.* **1998,** *22* (3), 263-268.

27. Buda, F.; Ensing, B.; Gribnau, M. C. M.; Baerends, E. J., DFT study of the active intermediate in the Fenton reaction. *Chem. Eur. J.* **2001,** *7* (13), 2775-2783.

Chapter 4 -

INFLUENCE OF ORGANIC CHELATING AGENTS ON THE FENTON REACTION – REACTION KINETICS AND ˙OH-YIELDS

Submitted for publication in *Chemosphere*

4.1 ABSTRACT

Effects of organic chelates on kinetics and generation of reactive species by the Fenton reaction (ferrous iron + hydrogen peroxide) are subject of controversial discussions and strongly depend on experimental conditions.

The present study systematically investigates pH-dependent kinetics of Fenton reactions in presence of diethylenetriaminepentaacetic acid (DTPA), ethylenediaminetetraacetic acid (EDTA), *N*-hydroxyethylenediaminetriaacetic acid (HEDTA), and nitrilotriacetic acid (NTA) with special interest in the existence of an intermediate iron-peroxo-complex.

Results indicate the existence of this intermediate regardless of pH and applied type of ligand (L). For each ligand it was found that the reaction rate constant for the decay of an intermediary formed Fe^{II}-L(H_2O_2)-complex increases with increasing pH. This indicates that Fe^{II}-L(H_2O_2) forfeits stability with increasing pH. Regardless of the applied pH Fe^{II}-L(H_2O_2) decay rate follows the order: NTA < HEDTA < DTPA < EDTA. Derived second order reaction rate constants for the ligand-assisted Fenton reaction changed in their order with increasing pH indicating pH-dependent changes in their oxidation/reduction potential.

Additionally, pH-dependent hydroxyl radical yields were determined. It was found that 100% hydroxyl radicals are generated with respect to applied iron concentrations regardless of pH and ligand. Thus, considerable formation of more selective tetravalent iron as reactive species can be ruled out.

4.2 INTRODUCTION

The reaction of ferrous iron (Fe^{II}) with hydrogen peroxide (H_2O_2) is known as Fenton reaction. As described above the "classical Fenton mechanism" comprises reactions 1.8 – 1.15.[1-2] This mechanism includes catalytic cycling between Fe^{II} and ferric iron (Fe^{III}), which enables continuous production of highly reactive hydroxyl radicals (•OH) until H_2O_2 is fully consumed.[1-2]

Reaction 1.8 is accelerated with increasing pH. This can be attributed to the formation of Fe^{II}-hydroxide species. $Fe(H_2O)_4(OH)_2$, for example, is about ten times more reactive towards H_2O_2 than $Fe(H_2O)_6^{2+}$.[3] However, at pH values > 3, Fe^{III} precipitates, which suppresses the Fenton-like reaction (reaction 1.12) and results in undesired sludge formation and thus, terminates catalytic recycling of Fe^{III} into Fe^{II}. This outweighs the benefits of an accelerated reaction 1.8. One possibility to keep Fe^{III} dissolved at pH > 3 is the addition of ligands, which form soluble complexes with Fe^{III}. In general ligand-assisted Fenton reactions can be formulated as follows:

$$Fe^{II}\text{-}L + H_2O_2 \rightarrow Fe^{III}\text{-}L + OH^- + {}^{\bullet}OH \qquad (4.1)$$

However, literature indicates that ligands affect kinds and yields of reactive species generated in the Fenton reaction. However, the controversies mentioned in chapter 1.4.4 point out that effects of ligands in Fenton chemistry are not sufficiently understood yet. Ligand effects in Fenton chemistry will be relevant in terms of remediation of contaminated sites or wastewater treatment. Hence, it is important to investigate ligand effects for improving process control in the Fenton reaction and thus, economic feasibility and assessment of transformation or by-products.

The present study investigates the pH-dependent influence of different organic chelates (DTPA, EDTA, HEDTA, and NTA) on the Fenton reaction. Mechanistic aspects such as formation of

an intermediate iron-peroxo-complex, which would indicate the reaction occurring via an inner sphere electron transfer, are addressed as well as reaction kinetics and the yield of generated reactive species. Obtained results are discussed with respect to their relevance in practical applications.

4.3 MATERIALS AND METHODS

4.3.3 CHEMICALS

Ammonium iron(II) sulfate hexahydrate ($(NH_4)_2Fe(SO_4)_2 \times 6\ H_2O$) (99%) (Sigma Aldrich, Germany), ammonium iron(III) sulfate dodecahydrate ($(NH_4)Fe(SO_4)_2 \times 12\ H_2O$) (≥ 98.5%) (Carl Roth, Germany), hydrogen peroxide (H_2O_2) (30%) (AppliChem, Germany), sulfuric acid (H_2SO_4) (> 95%) (Fischer Chemicals, Switzerland), sodium hydroxide solution (NaOH) (1 M) (Bernd Kraft, Germany), dimethyl sulfoxide (DMSO) (Merck, Germany), sodium methane sulfinate ($NaCH_3O_2S$, MSIA) (95%) (Alfa Aesar, Germany), methane sulfonic acid (CH_4O_3S, MSOA) (≥ 99.9%) (Merck, Germany), diethylenetriaminepentaacetic acid (≥ 99.0%) (Fluka, Germany), ethylenediaminetetraacetic acid disodium salt dihydrate (≥ 99.0%) (Merck, Germany), *N*-(2-hydroxyethyl)-ethylenediamine-*N*,*N*,*N'*-triacetic acid trisodium salt (≥ 99.0%) (Fluka, Germany), and nitrilotriacetic acid (≥ 99.0%) (Sigma-Aldrich, Germany) were used as received without further purification. Disodium carbonate (Na_2CO_3) (≥ 99.5%) (Carl Roth, Germany) and sodium bicarbonate ($NaHCO_3$) (99.7%) (Riedel de Haën, Germany) were dried at 80 °C overnight before use. Once dried, the two salts were stored in a desiccator. Solutions of $(NH_4)_2Fe(SO_4)_2 \times 6\ H_2O$, $(NH_4)Fe(SO_4)_2 \times 12\ H_2O$ and DMSO were prepared by dissolution of an appropriate amount in ultrapure water (PURELAB ultra, ELGA, Germany) pH-adjusted with H_2SO_4 or NaOH to the respective pH. Stock solutions of MSIA and MSOA were prepared

by dissolution of an appropriate amount or volume, respectively, in ultrapure water. A bicarbonate/carbonate buffer stock solution was prepared by dissolution of appropriate amounts of dried salts in ultrapure water and was used to prepare bicarbonate/carbonate buffer as eluent for IC-measurements.

4.3.2 KINETIC EXPERIMENTS

Experimental setup

Kinetic Fenton experiments were performed with a stopped-flow system (SFM-20, Biologic, France) using a diode array detector (DAD) (TIDAS S 300K, j & m Analytics AG, Germany). The system worked with two 10-mL syringes, one of them containing Fe^{II}-solution and the other containing H_2O_2 and the respective ligand solution.

100 µL out of each syringe were injected per measurement applying a flow rate of 3.5 mL min^{-1} per syringe. After being rapidly mixed in a mixing chamber, injected solutions reached the measurement cell – a 10-µL quartz cuvette; path length: 10 mm. Spectroscopic data were recorded every 0.4 ms for 1 s.

A schematic figure of the stopped-flow setup is shown in Figure 3.5.[4]

Experimental conditions

Observed pseudo first order reaction rate constants of Fe^{III}-formation from the reaction of Fe^{II}-chelates with a surplus of H_2O_2 were determined spectrophotometrically. Spectra ranging from λ = 190 – 700 nm were recorded (for an example spectrum see Figure 4.5). The absorbance detected at λ = 300 nm was utilised to observe Fe^{III}-formation. Indeed, different iron complexes show different molar absorptivities, even depending on the protonation level for each ligand.

However, as calibration was conducted separately for each ligand at respective pH values, these differences can be neglected.

For these experiments $[Fe^{II}]_0$ was chosen to be 100 µM, $[H_2O_2]$ ranged from 0.001 to 0.25 M and respective ligand concentrations equalled the fivefold $[Fe^{II}]_0$. Investigated pH values ranged from 2 to 6 in presence of DTPA, HEDTA, and NTA, respectively, and from 2.5 to 6 in presence of EDTA due to limited solubility of EDTA at lower pH. As experiments were conducted without buffer changes of pH during the reaction must be taken into account. However, preliminary experiments had shown that changes of pH are not relevant in the observed time frame (data not shown).

All experiments were performed as triplicates at room temperature (~ 20 °C).

Data evaluation

All calculations and regression analyses described were performed with OriginPro 2015G.

It is assumed that reactions formulated for formation and pH-dependent decay of the intermediate iron-peroxo-complex are true even in presence of organic chelates. Consequently, in presence of ligands (L) these equations are formulated as follows (reactions 4.2 – 4.4):

$$Fe^{II}\text{-}L + H_2O_2 \rightleftharpoons Fe^{II}\text{-}L(H_2O_2) \quad (4.2)$$

$$Fe^{II}\text{-}L(H_2O_2) \rightarrow Fe^{III}\text{-}L + OH^- + {}^{\bullet}OH \quad (4.3)$$

$$Fe^{II}\text{-}L(H_2O_2) \rightarrow Fe^{IV}O\text{-}L + H_2O \quad (4.4)$$

Depending on pH and type of ligand the intermediate iron-peroxo-ligand-complex (Fe^{II}-$L(H_2O_2)$) will reveal a certain charge, which is not indicated due to its high variability. Additionally, the oxidation state of iron is of much more interest than the net-charge of the complex.

For data evaluation the measured absorbance at 300 nm was corrected for by blank subtraction. Samples containing equal H_2O_2 and ligand concentrations compared to the respective Fenton experiment served as blanks. Corrected absorbance was then converted to the corresponding [Fe^{III}] via calibration with $(NH_4)Fe(SO_4)_2 \times 12\ H_2O$ complexed by the respective ligand at the same wavelength. Calibration was performed every laboratory day at the different pH values and ligand conditions as applied in the kinetic experiments. The ligand concentration was in excess over all [Fe^{III}]. The varying [Fe^{III}]/[ligand]-ratio did not influence the measured absorbance at 300 nm (data not shown). Calibration standards were prepared from 10 to 250 µM Fe^{III}. It was assumed that the maximum [Fe^{III}] ([Fe^{III}]$_{max}$) did not exceed the applied [Fe^{II}]$_0$.

The ratio of [Fe^{III}] at a certain time (t) ([Fe^{III}]$_t$) to [Fe^{III}]$_{max}$ was calculated and plotted vs. time. From this plot, observed pseudo first order reaction rate constants for Fe^{III}-formation ($k_{4.1}'$) were derived from an exponential fit function (equation 4.I) applied for data obtained in the first 60 ms. This method enables derivation of k_1' in case of very fast reactions, for which the method to derive $k_{4.1}'$ from a linear fit of the plot ln(c/c$_0$) vs. time fails (for further information and explanations see chapter 4.5.3). Assuming that in the observed time span Fe^{III} is only generated by the reaction of Fe^{II} with H_2O_2, $k_{4.1}'$ can be also denoted as observed pseudo first order reaction rate constant of the Fenton reaction.

$$\frac{[Fe^{III}]_t}{[\mathrm{Fe^{III}}]_{\max}} = \mathrm{N} \cdot \left(1 - \mathrm{e}^{-k_{4.1}'(\mathrm{t}-0.0064)}\right) \qquad (4.\mathrm{I})$$

with N being a factor, which was introduced in the equations due to a random error occurring in the maximum value. The value of 0.0064, which is subtracted from the time (t) results from the dead time of the system, in which no data can be recorded.

These $k_{4.1}'$ were plotted vs. corresponding [H_2O_2] in order to derive the first order reaction rate constant for the decay of Fe^{II}-L(H_2O_2) (reaction 4.2) ($k_{4.2}$) as well as second order reaction rate constants ($k_{4.1}^{2nd}$) of ligand-assisted Fenton reaction (reaction 4.1) (see Figure 4.8).

4.3.3 DETERMINATION OF •OH-YIELDS BY ION CHROMATOGRAPHY

Experimental setup

The IC-system, which was used to quantify MSIA and MSOA, was composed of a Metrohm 883 Basic IC plus, a Metrohm 863 Compact IC Autosampler, and a conductivity detector coupled with chemical suppression. As column a Metrosep A Supp 4 (250/4.0) was used with particles having a diameter of 9 µm. A bicarbonate/carbonate buffer (0.34 mM/0.36 mM) was used as eluent. The flow was set to 1.0 mL min^{-1}.

Experimental conditions

Concentrations of Fe^{II} and ligand were chosen as for kinetic measurements. Regarding [H_2O_2] and pH a smaller set of conditions was applied compared to the kinetic studies due to high experimental effort. Selected [H_2O_2] were 0.01, 0.05, 0.1, and 0.25 M. For investigation of the pH effect pH values ranging from 2 to 6 were adjusted.

These samples also contained DMSO as radical scavenger, which was used to quantify generated •OH by means of its oxidation products MSIA and MSOA.[5] [DMSO] required to achieve a ≥ 99 % scavenging of •OH was calculated for each [H_2O_2] and type of ligand by means of a competition kinetic (equation 4.II). Required concentrations ranged from 0.015 to 0.175 M.

$$f(^{\bullet}OH + DMSO) = \frac{[DMSO]\times k(^{\bullet}OH+DMSO)}{[DMSO]\times k(^{\bullet}OH+DMSO)+[Fe^{II}]\times k(^{\bullet}OH+Fe^{II})+[H_2O_2]\times k(^{\bullet}OH+H_2O_2)+[ligand]\times k(^{\bullet}OH+ligand)} \quad (4.II)$$

With f(•OH + DMSO) being the fraction of •OH reacting with DMSO. For calculations, the following rate constants were used.[6]

$k(\bullet OH + Fe^{II}) = 3 \times 10^8\ M^{-1}\ s^{-1}$

$k(\bullet OH + H_2O_2) = 2.7 \times 10^7\ M^{-1}\ s^{-1}$

$k(\bullet OH + DMSO) = 7 \times 10^9\ M^{-1}\ s^{-1}$

$k(\bullet OH + DTPA) = 2.3 \times 10^9\ M^{-1}\ s^{-1}$

$k(\bullet OH + EDTA) = 2 \times 10^9\ M^{-1}\ s^{-1}$

$k(\bullet OH + HEDTA) = 1.1 \times 10^{10}\ M^{-1}\ s^{-1}$

$k(\bullet OH + NTA) = 2.5 \times 10^9\ M^{-1}\ s^{-1}$

Note that the above values do not include corresponding metal complexes, which may reveal different reaction rate constants. However, reaction rates of metal chelates are smaller or at most similar compared to those of free ligands (e.g. $k(\bullet OH + Fe^{III}\text{-DTPA})$[7] $= 1.5 \times 10^9\ M^{-1}\ s^{-1}$, $k(\bullet OH + Fe^{III}\text{-EDTA})$[8] $= 5.0 \times 10^8\ M^{-1}\ s^{-1}$, $k(\bullet OH + Fe^{III}\text{-NTA})$[9] $= 1.1 \times 10^8\ M^{-1}\ s^{-1}$).

In analogy to experiments described elsewhere, water, H_2O_2, DMSO and the respective ligand solution were adjusted to the desired pH by addition of H_2SO_4 and NaOH, respectively, and mixed before starting the reaction by adding Fe^{II}-solution of the same pH.[4] After 10 s of vigorous mixing an aliquot of the sample (1.2 mL) was taken and mixed with 7.8 mL 1 mM NaOH straight prior to IC-measurement.

In order to investigate the contribution of the Fenton-like reaction to the overall •OH-yield within the reaction time of 10 s, all experiments were repeated starting with Fe^{III} as Fe source. For these experiments Fe^{III}-solution contained the respective ligand to avoid precipitation of Fe^{III} prior to the reaction, especially at pH > 3.

Experiments were carried out as triplicates and performed at room temperature (~ 20 °C).

Data evaluation

Detected peaks of MSIA and MSOA were quantified using calibrations ranging from 0.5 to 20 µM of the corresponding compounds. Calculated concentrations of MSIA and MSOA in the samples were summed up considering error propagation. The •OH-yields correspond to 92% of the sum of MSIA and MSOA yields (for details see Veltwisch, *et al.* (1980)[5]). To determine •OH-yields of exclusively the Fenton reaction (without Fenton-like reaction) •OH-yields obtained from Fe^{III}-based experiments were subtracted from those obtained from Fe^{II}-based experiments. Error propagation was taken into account.

4.4 RESULTS AND DISCUSSION

4.4.1 KINETIC EXPERIMENTS

Observed pseudo first order reaction rate constants of Fe^{III}-formation in ligand-assisted Fenton reactions were measured at increasing values of $[H_2O_2]$ to investigate formation and lifetime of the intermediate iron-peroxo-complex in presence of organic chelates as done in a previous study in absence of such ligands.[4] Investigated chelates differ in size, number of Lewis base groups potentially participating in Fe-complexation, and the ratio of amino groups to carboxylic groups. The complex formation constants of these complexing agents increase with the number of their Lewis base groups (see Table 1.1).

Figure 4.1 shows the observed pseudo first order reaction rate constants of Fe^{III}-formation in ligand-assisted Fenton reactions ($k_{4.1}'$) at increasing $[H_2O_2]$ in presence of EDTA at pH 2.5 to

6. Regardless of pH, $k_{4.1}'$ first increases with increasing $[H_2O_2]$ and tends to reach a plateau at very high $[H_2O_2]$.

As described in our preceding work, in case of an iron-peroxo-complex generated as intermediate in the reaction of Fe^{II} with H_2O_2 $k_{4.1}'$ will become independent of $[H_2O_2]$ in case of high $[H_2O_2]$ (equation (4.III)).[4]

$$k_{4.1}' = \frac{k_{4.3}k_{4.2}[H_2O_2]}{k_{4.2}[H_2O_2]} \approx k_{4.3} \qquad (4.III)$$

with k_x being the reaction rate constant of a certain reaction x. Hence, $k_{4.1}'$ at high $[H_2O_2]$ equals the first order reaction rate constant for the decay of Fe^{II}-L(H_2O_2) ($k_{4.3}$) (reaction 4.3). The value of $k_{4.1}'$ reached in the plateau, i.e. $k_{4.3}$, increases with increasing pH, indicating that the intermediate Fe^{II}-L(H_2O_2) forfeits stability with increasing pH. At pH 5 and 6 $k_{4.1}'$ could not be determined at $[H_2O_2] \geq 0.2$ M as the reaction was too fast.

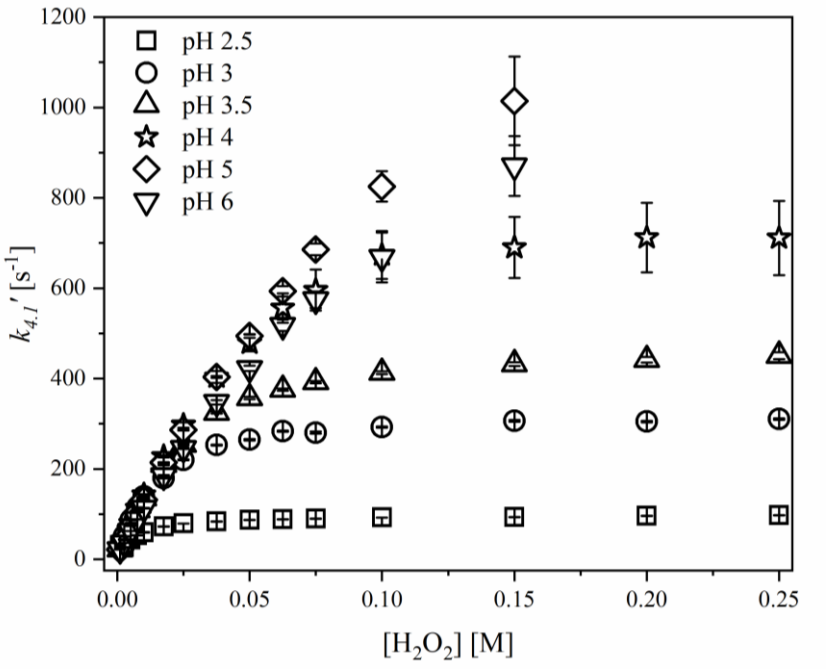

Figure 4.1: pH-dependent observed pseudo first order reaction rate constants of Fe^{III}-formation in EDTA-assisted Fenton reactions determined at $[H_2O_2]$ = 0.001 – 0.25 M. Depicted error bars indicate the 95% confidence interval of the applied regression analyses.

Similar figures were obtained for experiments carried out in presence of DTPA or HEDTA (Figure 4.9, Figure 4.10). Corresponding second order reaction rate constants ($k_{4.1}^{2nd}$) for all investigated ligands are compiled in Table 4.1. Note that second order reaction rate constants ($k_{4.1}^{2nd}$) were derived from Fe^{III} induced absorbance measurements. Hence, derived constants must be ascribed to reaction 4.1.

Table 4.1: Second order rate constants of ligand-assisted Fenton reactions (L-Fe^{II} + H_2O_2) at various pH values. [L]:[Fe^{II}] = 5:1. Statistical errors of $k_{4.1}^{2nd}$ represent the 95% confidence interval of the slope of the linear regression used to derive $k_{4.1}^{2nd}$.

pH	$k_{4.1}^{2nd}$×10^{-3} [M^{-1} s^{-1}]	$k_{4.1}^{2nd}$×10^{-3} [M^{-1} s^{-1}]	$k_{4.1}^{2nd}$×10^{-3} [M^{-1} s^{-1}]	$k_{4.1}^{2nd}$×10^{-3} [M^{-1} s^{-1}]
	DTPA	**EDTA**	**HEDTA**	**NTA**
2	0.4 ± 0.04	cannot be determined [a]	0.3 ± 0.03	0.1 ± 0.03
2.5	0.9 ± 0.2	4.3 ± 0.5	0.9 ± 0.1	n. d.
2.75	3.2 ± 0.3	8.3 ± 0.8	2.0 ± 0.2	n. d.
3	3.9 ± 0.7	13.8 ± 0. 9	3.12 ± 0.6	1.4 ± 0.2
3.25	6.3 ± 1.0	14.0 ± 0.7	3.63 ± 0.7	n. d.
3.5	14.5 ± 2.0	13.2 ± 0.6	6.23 ± 1.1	n. d.
3.75	14.6 ± 1.6	14.1 ± 0.3	6.86 ± 1.1	n. d.
4	17.4 ± 1.4	13.7 ± 0.4	10.9 ± 1.6	1.6 ± 0.2
4.5	17.8 ± 0.7	n. d.	13.5 ± 1.6	n. d.
5	17.7 ± 0.9	12.4 ± 0.2	19.1 ± 2.2	1.9 ± 0.2
6	15.9 ± 0.7	10.3 ± 0.1	21.9 ± 2.3	1.9 ± 0.2

[a] in presence of EDTA $k_{4.1}^{2nd}$ could not be determined at pH 2 due to limited solubility of EDTA at low pH, n. d.: not determined

In case of Fe complexed by DTPA $k_{4.1}^{2nd}$ increased from (0.4 ± 0.04) × 10^3 M^{-1} s^{-1} at pH 2 to (17.8 ± 0.7) × 10^3 M^{-1} s^{-1} at pH 4.5. Considering the statistical errors rate constants determined at pH ≥ 3.5 are almost constant. A similar trend was observed when rate constants were determined in presence of EDTA or NTA. In case of EDTA $k_{4.1}^{2nd}$ is almost constant at pH ≥ 3, in case of HEDTA and NTA $k_{4.1}^{2nd}$ tends to stagnate at pH ≥ 5.

Previously published data are available for the investigated ligands at circumneutral pH (7.0 – 7.4). Unfortunately, it was not possible to derive reaction rate constants at pH > 6 with the described experimental setup as initial reaction kinetics were too fast. Published values determined for $k_{4.1}^{2nd}$ in presence of DTPA range from 0.51 × 10^3 M^{-1} s^{-1} to 2.7 × 10^3 M^{-1} s^{-1}.[10-13] In presence of EDTA $k_{4.1}^{2nd}$ was determined to be about 7 × 10^3 M^{-1} s^{-1}.[10-11, 13] In case of HEDTA-assisted Fenton reactions values for $k_{4.1}^{2nd}$ between 10 × 10^3 M^{-1} s^{-1} and 42 × 10^3 M^{-1} s^{-1} were determined.[11, 13] In presence of NTA $k_{4.1}^{2nd}$ was determined to be 9.7 × 10^3 M^{-1} s^{-1}. These data are comparable to ours even if pH-conditions do not coincide, but as mentioned above for the investigated chelates almost no changes in determined $k_{4.1}^{2nd}$ could be detected at pH ≥ 5.

Oxidation-reduction potentials (E) of chelated Fe^{III}/Fe^{II} pairs are considerably lower compared to the $Fe^{III}(H_2O)_6/Fe^{II}(H_2O)_6$ pair.[14] That is why determined second order reaction rate constants are much higher in presence of such ligands compared to the $Fe(H_2O)_6$-complex.[15] At pH 2 for selected iron chelates E decreases in the order NTA > DTPA > CDTA > EDTA.[14] Hence, at that pH Fe^{II}-EDTA is the strongest reducing agent and reaction kinetics is expected to be fastest in the EDTA-assisted Fenton reaction. Even though at pH 2 $k_{4.1}^{2nd}$ could not be measured in presence of EDTA for reasons mentioned above this hypothesis is corroborated by data determined at pH 2.5 (EDTA showed fastest $k_{4.1}^{2nd}$). Overall, the ligand-assisted Fenton reactions under study corroborate the trend of $k_{4.1}^{2nd}$ vs. E. However, no E(Fe^{III}-HEDTA/Fe^{II}-

HEDTA) is available, but from the kinetic data one can deduce that it might be between E(Fe^{III}-NTA/Fe^{II}-NTA) and E(Fe^{III}-DTPA/Fe^{II}-DTPA) at pH 2.

At higher pH values the order of $k_{4.1}{}^{2nd}$ changes for the different iron chelates investigated. Between pH 2.5 and 3.25 $k_1{}^{2nd}$ determined in presence of EDTA is fastest while between pH 3.25 and 4.5 the DTPA-assisted Fenton reaction revealed the highest reactivity. However, at pH > 4.5 the Fenton reaction is fastest in presence of HEDTA. This observation indicates that E of different iron chelates is influenced by pH possibly due to changes in the ligand's electronic structure caused by pH-dependent speciation.

Figure 4.2 correlates first order reaction rates for the decay of the intermediate Fe^{II}-L(H_2O_2) (i.e., $k_{4.3}$) in presence of DTPA, EDTA, or HEDTA, respectively, with the ratio of nitrogen to oxygen based functional groups (N/O-ratio) of the respective ligand at various pH values. It can be derived from the figure that $k_{4.3}$ increases with pH and decreases with the N/O-ratio of the ligands. This corroborates the findings of Welch, *et al.* (2002)[16] that oxygen rich chelates stabilise Fe^{III} and thus, promote oxidation of Fe^{II} whereas nitrogen rich chelates stabilise Fe^{II} and thus, hamper its oxidation. As the actual oxidation step occurs during the decay of the intermediate complex, it is reasonable that ligands with a higher proportion of O-based functional groups accelerate $k_{4.3}$.

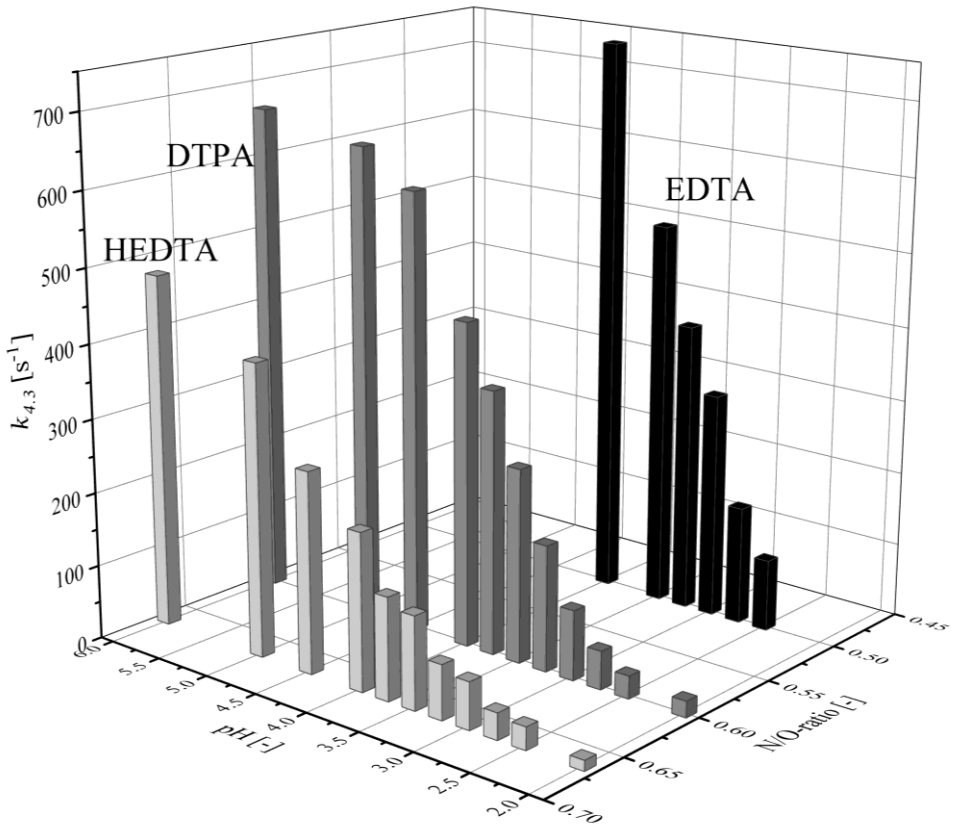

Figure 4.2: First order reaction rate constants for the decay of the intermediate Fe^{II}-L(H_2O_2)-complexes in dependence on pH and N/O-ratio of the respective ligand.

Kinetic data obtained in presence of NTA did not match the trend of other chelates investigated. An increase in [H_2O_2] did not result in a distinct plateau of determined $k_{4.1}'$ (Figure 4.3). Hence, no first order rate constants for the decay of the intermediate Fe-NTA(H_2O_2) -complex could be derived from these data. However, there is no linear increase on $k_{4.1}'$ over the entire [H_2O_2]-range. Instead data tend to form a plateau at high [H_2O_2] indicating $k_{4.1}'$ becoming independent from [H_2O_2] at even higher [H_2O_2]. Unfortunately, it was not possible to investigate higher [H_2O_2] due to high background absorbance caused by high [H_2O_2]. Possibly, denticity of ligands is responsible for differences between NTA and the other ligands. Assuming relevance of all available functional groups 5, 6, or 8 coordination sites at the iron centre will be covered by the ligand in case of HEDTA, EDTA, and DTPA, respectively, whereas only four coordination sites of the iron will be occupied by NTA. In case of EDTA, a seventh coordination

site is known to be occupied by an additional H_2O- or OH^--ligand. In case of tetra-dentate NTA, several complex structures are discussed, as for example those involving aqua or hydroxyl ligands or complexes composed of one Fe-ion and two NTA-molecules.[17-20]

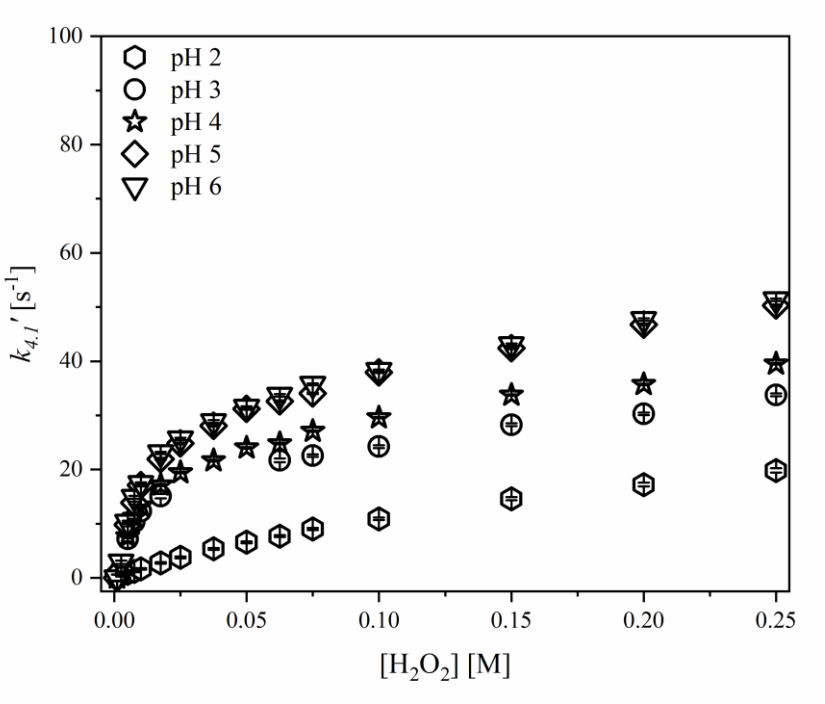

Figure 4.3: pH-dependent observed pseudo first order rate constants of Fe^{III}-formation in NTA-assisted Fenton reactions determined at [H_2O_2] = 0.001 – 0.25 M. Depicted error bars indicate the 95% confidence interval of the applied regression analyses.

4.4.2 DETERMINATION OF •OH-YIELDS

Variations in the decay route of the Fe^{II}-L(H_2O_2)-complex might influence the type of generated reactive species. As in literature reactive species involved in ligand-assisted Fenton reactions are a subject of controversial discussions we systematically investigated pH-dependent •OH-yields in presence of DTPA, EDTA, HEDTA, or NTA using DMSO as radical scavenger.

Relative •OH-yields referred to $[Fe^{II}]_0$ of 100 µM were determined for different [H_2O_2] at pH 2 – 6 except for EDTA-based experiments (Figure 4.11). Regardless of the applied ligand, •OH-

yields increased with increasing [H_2O_2] without significant difference between investigated pH-values. Furthermore, •OH-yields exceeded 100 % at [H_2O_2] ≥ 0.05 M (in case of DTPA assisted reactions at [H_2O_2] ≥ 0.01 M). This can be explained by an increasing effect of the Fenton-like reaction (reaction 1.12). Recycling Fe^{III} to Fe^{II} re-feeds the Fenton reaction (reaction 1.8) and hence, increases overall •OH-yields.

Analogous experiments were performed using Fe^{III} instead of Fe^{II} as primary Fe-source in order to evaluate the effect of the Fenton-like reaction on overall •OH-yields. As expected, increasing [H_2O_2] caused increasing •OH-yields as reaction 1.12 is accelerated by increasing [H_2O_2] (Figure 4.12).

The contribution of reaction 1.12 on the overall •OH-yields was assessed by subtracting •OH-yields of the Fe^{III}-based experiments from overall •OH-yields. Corresponding data for [H_2O_2] = 0.1 M are shown in Figure 4.4 (•OH-yields determined at further [H_2O_2] are compiled in Figure 4.13). 2-Tailed t-tests (p = 0.05) yielded significant differences for •OH-yields at most pH-values and [H_2O_2] within each ligand as well as between different ligands. However, no trend could be observed in •OH-yields with regard to pH, [H_2O_2] or type of ligand. Considering depicted standard deviations •OH-yields can be assumed to be around 100% with respect to $[Fe^{II}]_0$. This indicates that •OH is the only relevant oxidant generated in ligand-assisted Fenton reactions at all investigated experimental conditions. Dominant or even exclusive formation of Fe^{IV} as proposed in some previous studies would result in •OH-yields substantially below 100% referred to $[Fe^{II}]_0$ as Fe^{IV} is not expected to react with DMSO forming MSIA and MSOA. Instead dimethyl sulfone is built in the reaction of DMSO with Fe^{IV} as shown by Pestovsky, *et al.* (2005)[21]. Although •OH could also be generated by Fe^{IV} via reaction 1.19, this reaction can hardly compete with reaction 1.20 and 1.21. Indeed, reaction 1.19 may only become important in presence of nM or even smaller concentrations of Fe^{II} and H_2O_2. Otherwise, either reaction 1.20 or 1.21 prevails not yielding any •OH.[4, 22]

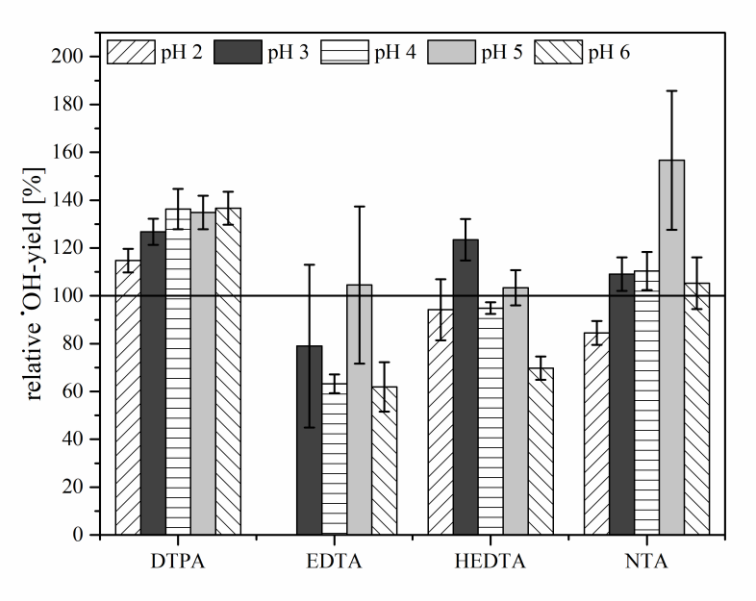

Figure 4.4: Relative ˙OH-yields referred to $[Fe^{II}]_0$ of 100 µM determined at $[H_2O_2]$ = 0.1 M at pH 2 – 6 in presence of DTPA, EDTA, HEDTA, or NTA. ˙OH-yields were calculated by subtracting ˙OH-yields determined in experiments using Fe^{III} as primary iron source from those determined in experiments using Fe^{II} as primary iron source to correct overall yields for the contribution of the Fenton-like reaction. Error bars indicate standard deviations of three independent measurements including error propagation.

That ˙OH are the only oxidant generated in ligand-assisted Fenton reactions is also reported in literature at least for circumneutral pH.[10, 13, 23-25] In parallel, other studies suggested formation of Fe^{IV} as reactive species in Fenton chemistry depending on the type of ligand,[12, 15, 26] which could not be confirmed by our results. Possibly, this inconsistency results from differences in experimental procedures and reaction conditions and hence, underlines that literature lacks systematic investigations of pH effects on oxidant formation in ligand-assisted Fenton reactions involving different organic chelates.

For all ligands of interest a decreased stability of the intermediate Fe^{II}-L(H_2O_2)-complex was observed with increasing pH. As different oxidants are discussed as reactive species in Fenton chemistry it seemed possible that differences in kinetics might result in different decay routes

of the detected intermediate. However, the ~ 100% •OH-yields determined regardless of ligand, pH and [H_2O_2] indicate that the decreased stability of Fe^{II}-L(H_2O_2) cannot be related with a mechanistic changeover from •OH- to Fe^{IV}-formation with increasing pH. Thus, it is more likely that the decreased stability of the intermediate Fe^{II}-L(H_2O_2)-complex can be ascribed to the pH-dependent speciation of the iron-complexes. It is conceivable that this speciation might change the electron density distribution in the Fe^{II}-L(H_2O_2)-complex, which in turn affects the stability of that complex.

Based on depicted data, the present paper provides kinetic indication for the formation of an intermediate Fe^{II}-L(H_2O_2)-complex in ligand-assisted Fenton reactions. The existence of an iron-peroxo-complex generated as intermediate in the Fenton reaction was already indicated earlier in absence of organic chelates.[4] Hence, results of this study show that the reaction mechanism, i.e. formation of an intermediate Fe-L(H_2O_2)-complex via an inner sphere electron transfer from the H_2O_2-ligand to the Fe-centre[27] remains unaffected by such ligands. Indeed, it was shown that primary reactions of the Fenton process are accelerated with increasing pH but the final oxidant, •OH, is generated regardless of applied conditions.

This may allow to use the Fenton reaction for remediation or as part of industrial wastewater treatment in presence of chelating agents at pH 2 – 6. The fact that a ~ 100% conversion of Fe^{II} into •OH occurred regardless of pH and type of ligand indicates that very recalcitrant pollutants can also be degraded by the energy efficient Fenton process in other fields than industrial wastewater treatment.[28] Formation of Fe^{IV} as a rather mild oxidant would largely limit the range of pollutants which could be degraded. Furthermore, real water matrix constituents may serve as complexing agents in a similar manner as the compounds under study.

A matter of further research is the investigation of the degradation of certain target compounds in a real water matrix at pH 4 to 6 to examine the Fenton performance at real conditions.

4.5 SUPPORTING INFORMATION

4.5.1 REPRESENTATIVE SPECTRUM RECORDED TO DETERMINE Fe^{III}-CONCENTRATIONS

Figure 4.5 shows a representative spectrum of Fe^{III} complexed by DTPA. Absorbance detected at λ = 300 nm was used to observe Fe^{III}-formation.

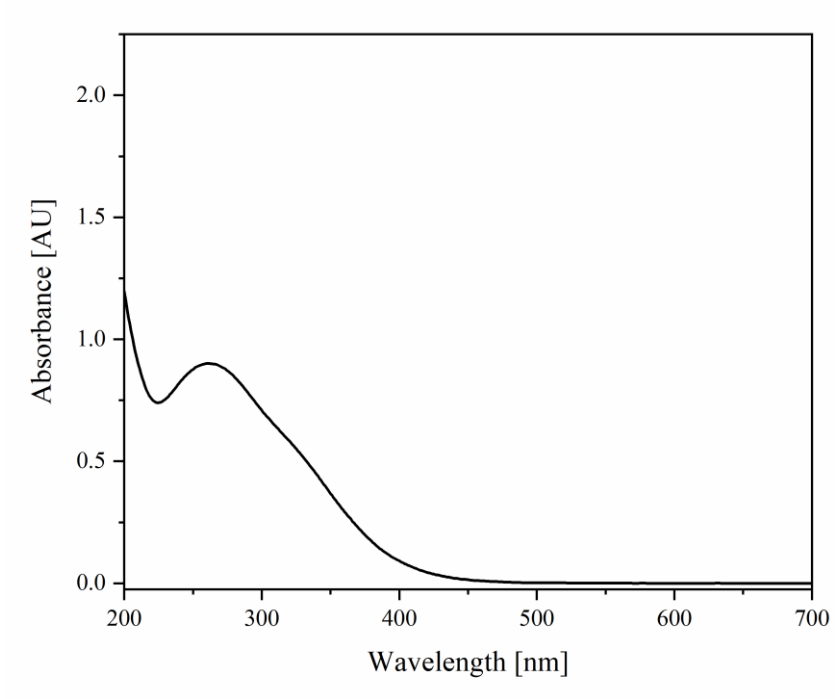

Figure 4.5: Representative spectrum of Fe^{III} complexed by DTPA.

4.5.2 VALIDATION OF THE EXPONENTIAL FIT-FUNCTION FOR THE DETERMINATION OF PSEUDO FIRST ORDER REACTION RATE CONSTANTS

Figure 4.6 shows representative time-dependent spectroscopic data of ligand-assisted Fenton reaction analysed according to the method described elsewhere.[4] A linear fit applied for data recorded within the first 15 ms strongly deviates from real data. Hence, it can be deduced that this approach is not suitable to yield reliable observed pseudo first order reaction rate constants ($k_{4.1}$').

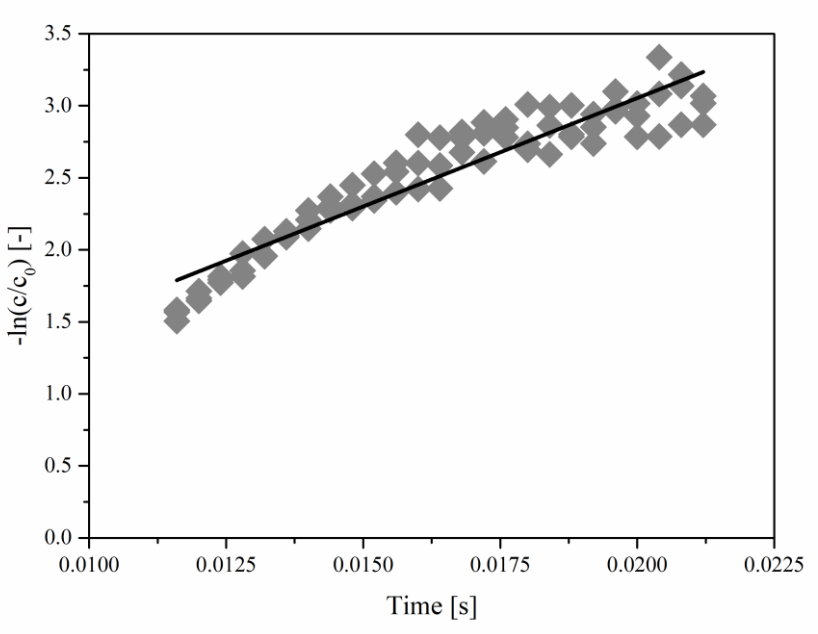

Figure 4.6: Representative plot of ln(c/c$_0$) vs. time with a linear fit applied to derive observed pseudo first order reaction rate constants.

Therefore, an exponential fit function was develop based on the 2nd order rate law.

$$\frac{[Fe^{III}]}{[Fe^{III}]_{max}} = N \cdot \left(1 - e^{-k_{4.1}'(t-0.0064)}\right) \qquad (4.I)$$

The factor N was introduced due to slight variations occurring in the maximum value effectively making equation (4.I) a double exponential fit. It equals the simplest form of multi-exponential fits, which are often used in literature and by computer programs[29-30] but is reduced to only one

exponential fit parameter. The value of 0.0064, which is subtracted from the time (t) results from the dead time of the system in which no data can be recorded.

The new function was validated by comparing resulting $k_{4.1}$'-values with those obtained from the classical linear approach. It can be derived from Figure 4.7 that for experiments, in which a $Fe^{II} \rightarrow Fe^{III}$ turnover within the dead time of ≤ 50 µM was detected, almost equal data are obtained regardless of the applied fit function. In case of $Fe^{II} \rightarrow Fe^{III}$ turnover within the dead time of > 50 µM, the difference in $k_{4.1}$' becomes larger with increasing initial turnover. This difference results from the fact that reliable linear fitting of $ln\frac{[Fe^{II}]}{[Fe^{II}]_0}$ vs. time is not possible anymore in such cases. In turn it can be derived from this figure that the exponential fit is suitable to determine $k_{4.1}$'.

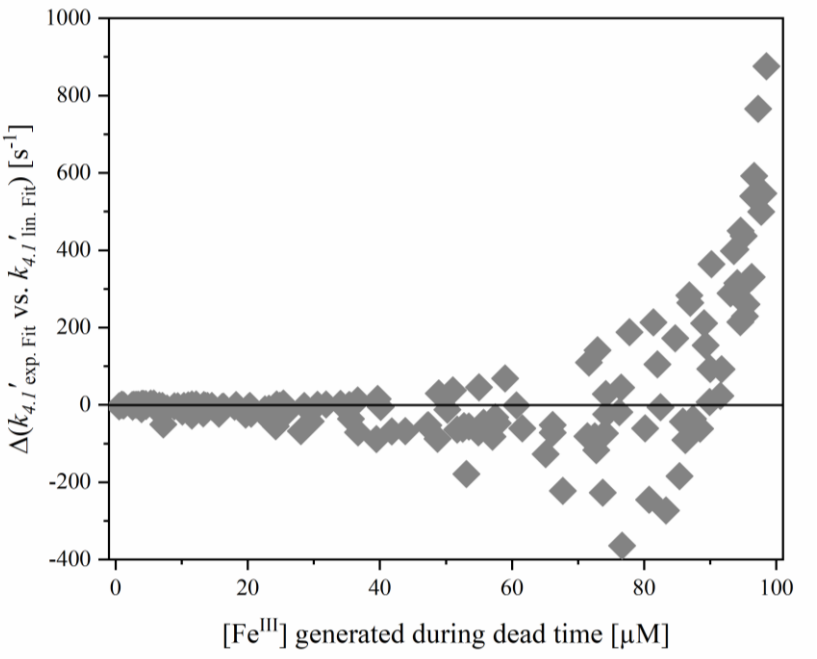

Figure 4.7: Difference between observed pseudo first order reaction rate constants of the Fenton reaction derived by linear fitting of ln($[Fe^{II}]/[Fe^{II}]_0$) vs. time and exponential fitting of $[Fe^{III}]/[Fe^{III}]_{max}$ vs. time.

4.5.3 DERIVATION OF $k_{4.1}^{2ND}$ AND $k_{4.3}$ FROM PLOTS OF $k_{4.1}'$ VS. $[H_2O_2]$

Second order reaction rate constants of the Fenton reaction ($k_{4.1}^{2nd}$) can be derived from plots of $k_{4.1}'$ vs. $[H_2O_2]$ by linear regression analysis of those data revealing a linear relationship of $k_{4.1}'$ at increasing values of $[H_2O_2]$ (cf. red data points in Figure 4.8). The slope of the linear regression line corresponds $k_{4.1}^{2nd}$.

First order reaction rate constants for the decay of intermediate Fe^{II}-L(H_2O_2)-complexes can be derived from same plots by exponential fitting of all data with a semi empirical exponential function (4.IV) of the type

$$k'_{4.1} = k_{4.3} + A_1 \times e^{\frac{[H_2O_2]}{B_1}} + A_2 \times e^{\frac{[H_2O_2]}{B_2}} \qquad (4.IV)$$

with A_x and B_x being fitting parameters (cf. dashed line in Figure 4.8).[31] The function has been developed in analogy to Wiegand, *et al.* (2018)[32]. However, the equation mentioned in the literature has been extended by the term $A_2 \times e^{\frac{[H_2O_2]}{B_2}}$. By that means the semi empirical function agrees very well with our measured data allowing to determine the plateau kinetics ($k_{4.3}$). As described earlier, $k_{4.3}$ can be derived by extrapolation to infinite $[H_2O_2]$.[32]

For those data, which do not exhibit a distinct plateau within the investigated range of $[H_2O_2]$ (especially at higher pH-values), $k_{4.1}'$ measured at high $[H_2O_2]$ are not exactly depicted by the function leading to an underestimation of $k_{4.3}$. That is why those values for $k_{4.3}$ are not presented, even if data of $k_{4.1}'$ vs. $[H_2O_2]$ are available for respective pH-values.

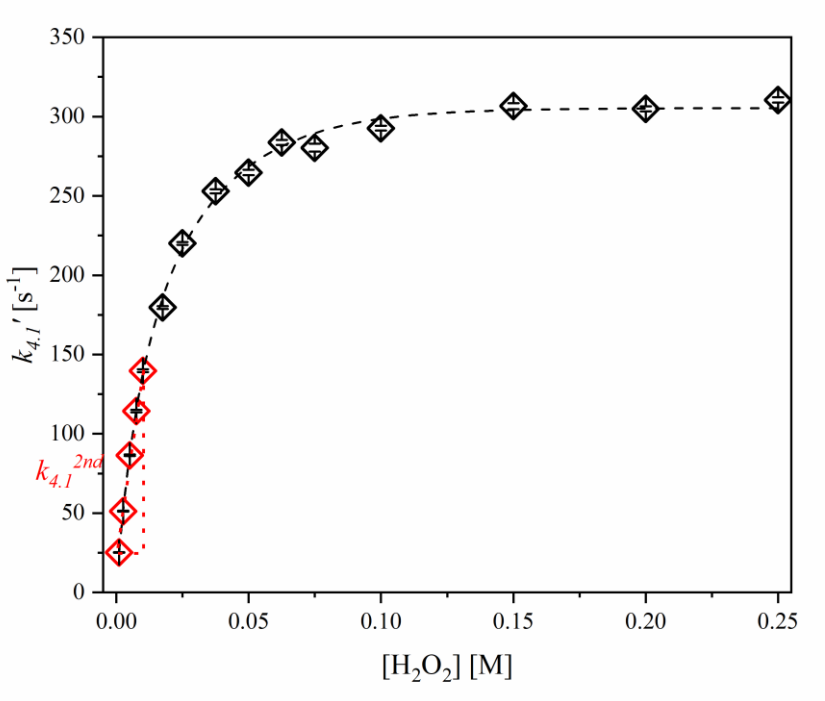

Figure 4.8: Representative plot of observed pseudo first order reaction rate constants of the Fenton reaction at increasing values of [H_2O_2] showing derivation of $k_{4.1}^{2nd}$ and $k_{4.1}$'.

4.5.4 INFLUENCE OF DTPA AND HEDTA ON FENTON KINETICS

Figure 4.9 and Figure 4.10 illustrate the pH-dependent effect of an increasing H_2O_2-concentration on $k_{4.1}$' of DTPA and HEDTA-assisted Fenton reactions. The trend in $k_{4.1}$' observed with increasing [H_2O_2] in presence of DTPA and HEDTA equals the one described for EDTA-assisted Fenton reactions in the main paper. Hence, there is kinetic indication for the existence of an intermediate Fe^{II}-L(H_2O_2)-complex even in presence of DTPA or HEDTA, respectively.

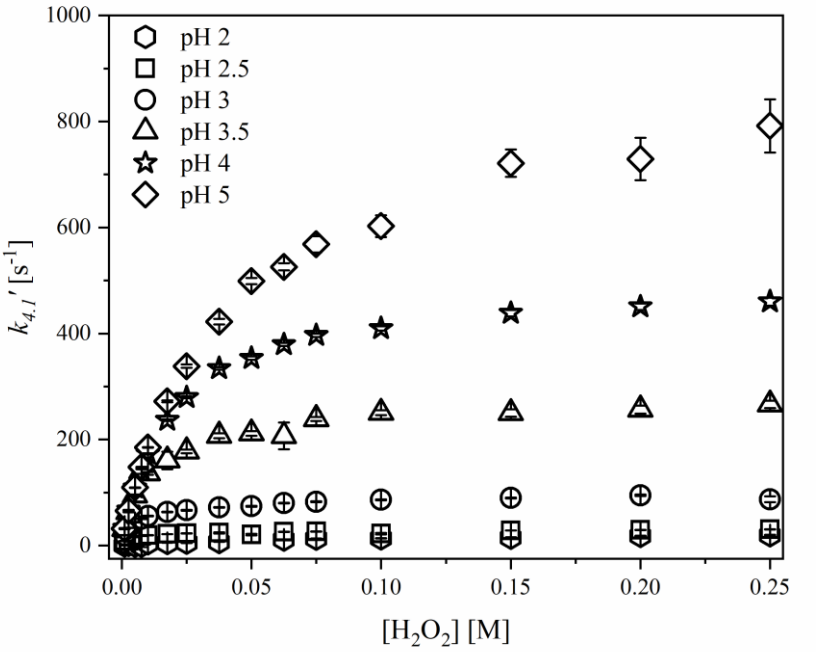

Figure 4.9: pH-dependent observed pseudo first order rate constants of Fe^{III}-formation in DTPA-assisted Fenton reactions determined at [H_2O_2] = 0.001 – 0.25 M. Depicted error bars indicate the 95% confidence interval of the applied regression analyses.

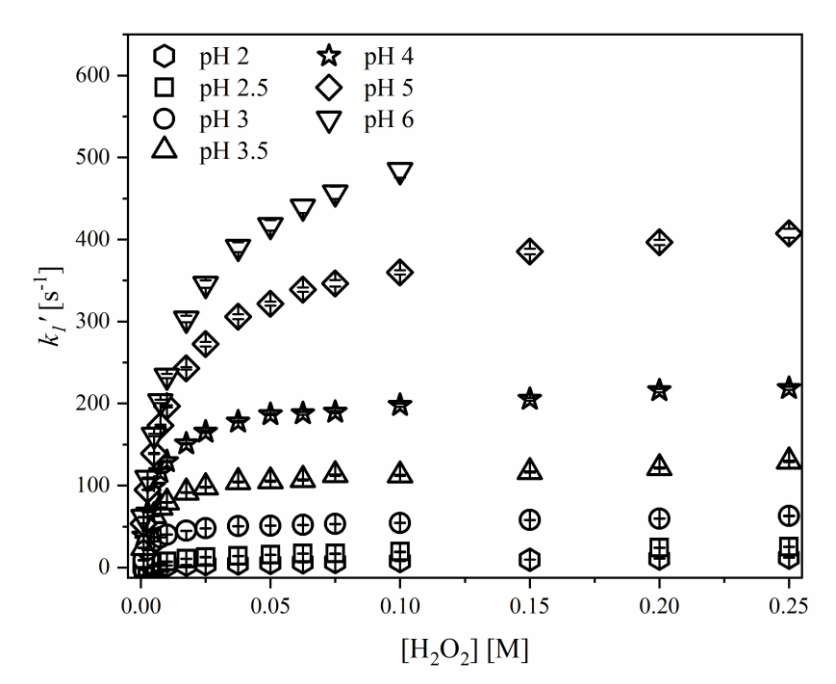

Figure 4.10: pH-dependent observed pseudo first order rate constants of Fe^{III}-formation in HEDTA-assisted Fenton reactions determined at [H_2O_2] = 0.001 – 0.25 M. Depicted error bars indicate the 95% confidence interval of the applied regression analyses.

4.5.5 INFLUENCE OF ORGANIC CHELATES ON ˙OH YIELD IN LIGAND-ASSISTED FENTON REACTIONS

Figure 4.11 shows relative ˙OH-yields referred to $[Fe^{II}]_0$ of 100 µM determined for different $[H_2O_2]$ in presence of DTPA (a), EDTA (b), HEDTA (c), and NTA (d).

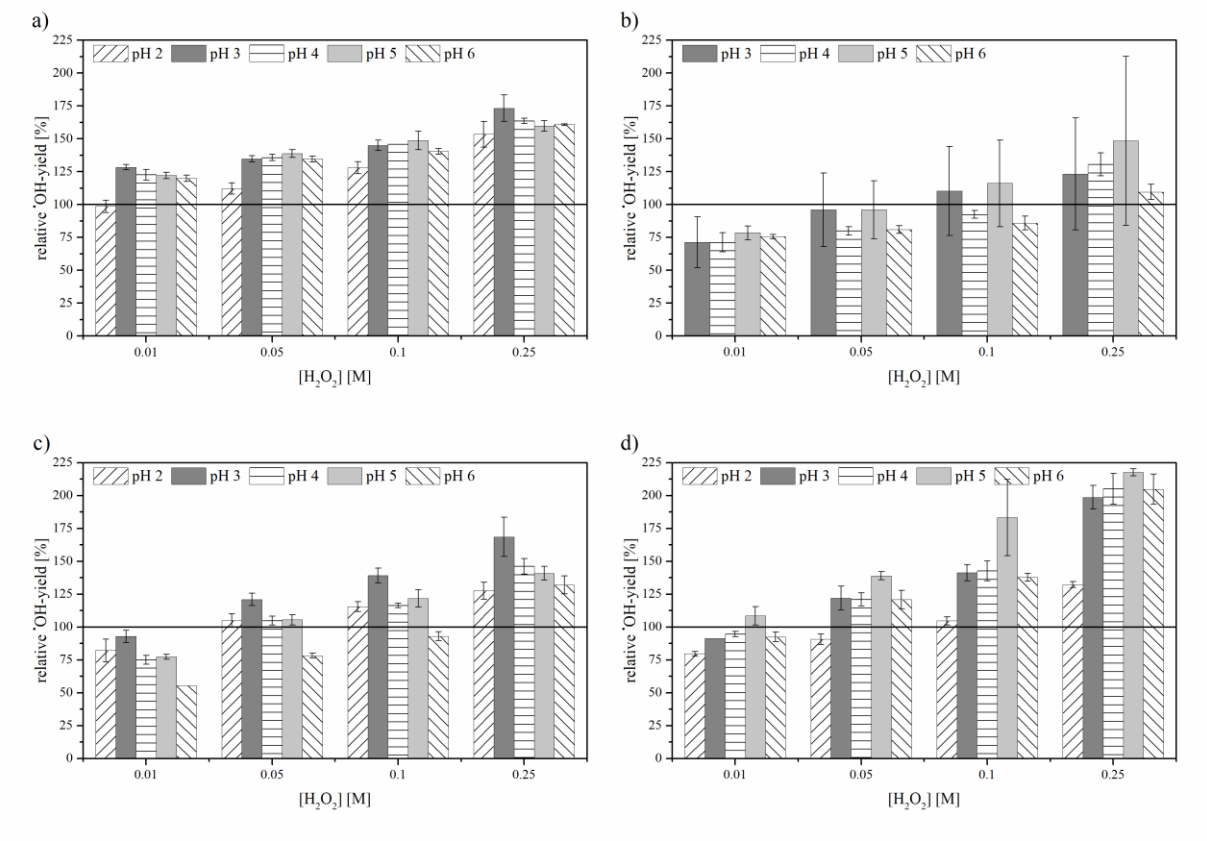

Figure 4.11: Relative ˙OH-yields referred to $[Fe^{II}]_0$ determined for the reaction of 100 µM Fe^{II} with 0.01 – 0.25 M H_2O_2 at various pH in presence of a) DTPA, b) EDTA, c) HEDTA, and d) NTA. Error bars indicate the standard deviation of three independent measurements.

4.5.6 INFLUENCE OF ORGANIC CHELATES ON ˙OH-YIELDS IN LIGAND ASSISTED FENTON-LIKE REACTIONS

Figure 4.12 shows relative ˙OH-yields referred to $[Fe^{II}]_0$ of 100 µM of the Fenton-like reaction determined at same $[H_2O_2]$ and pH as in Fe^{II} based experiments.

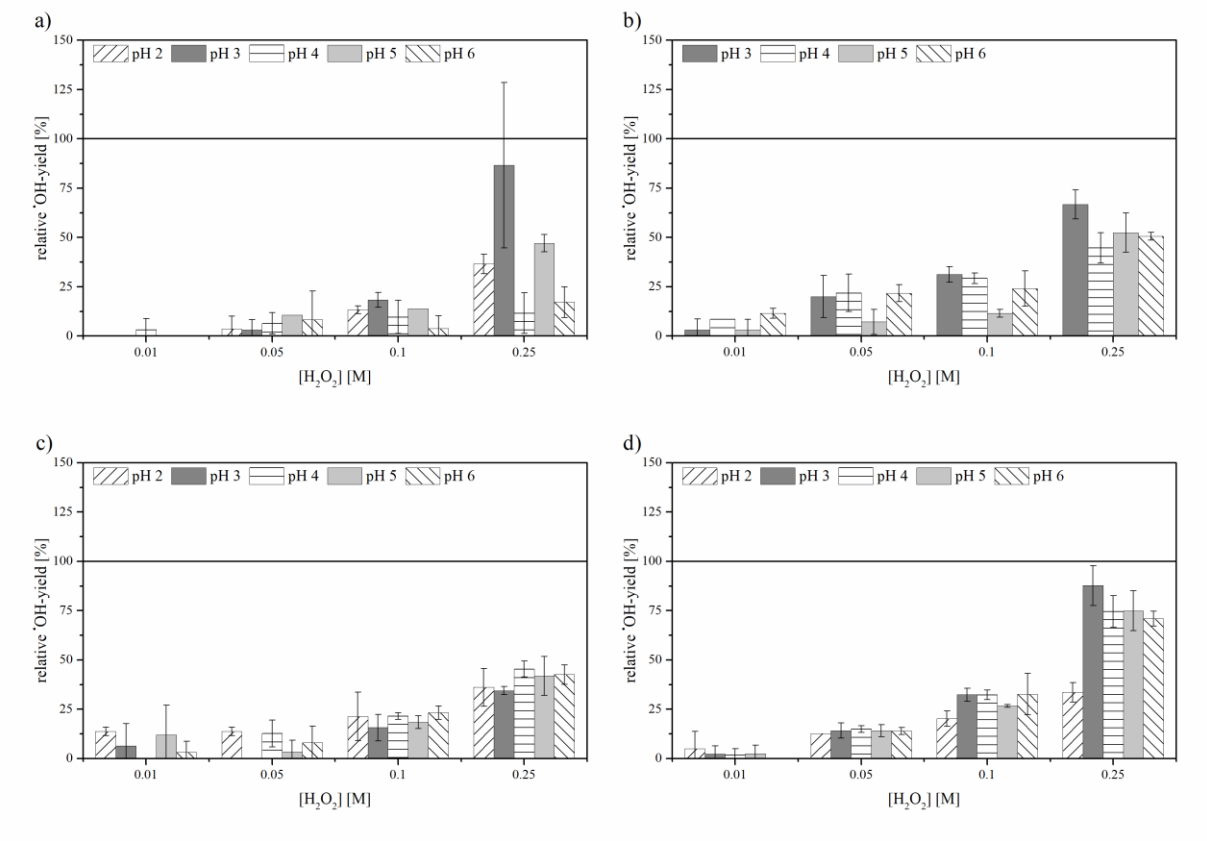

Figure 4.12: Relative ˙OH-yields referred to $[Fe^{III}]_0$ determined for the reaction of 100 µM Fe^{III} with 0.01 – 0.25 M H_2O_2 at various pH-values in presence of a) DTPA, b) EDTA, c) HEDTA, and d) NTA. Error bars indicate the standard deviation of three independent measurements.

4.5.7 INFLUENCE OF ORGANIC CHELATES ON ˙OH-YIELDS IN LIGAND ASSISTED FENTON REACTIONS CORRECTED FOR THE CONTRIBUTION OF FENTON-LIKE REACTION BASED ˙OH-YIELDS.

Figure 4.13 shows relative ˙OH-yields referred to $[Fe^{II}]_0$ of 100 µM of the Fenton reaction corrected for the contribution of Fenton-like reaction based ˙OH-yields by subtracting the latter from those obtained in Fe^{II}-based experiments.

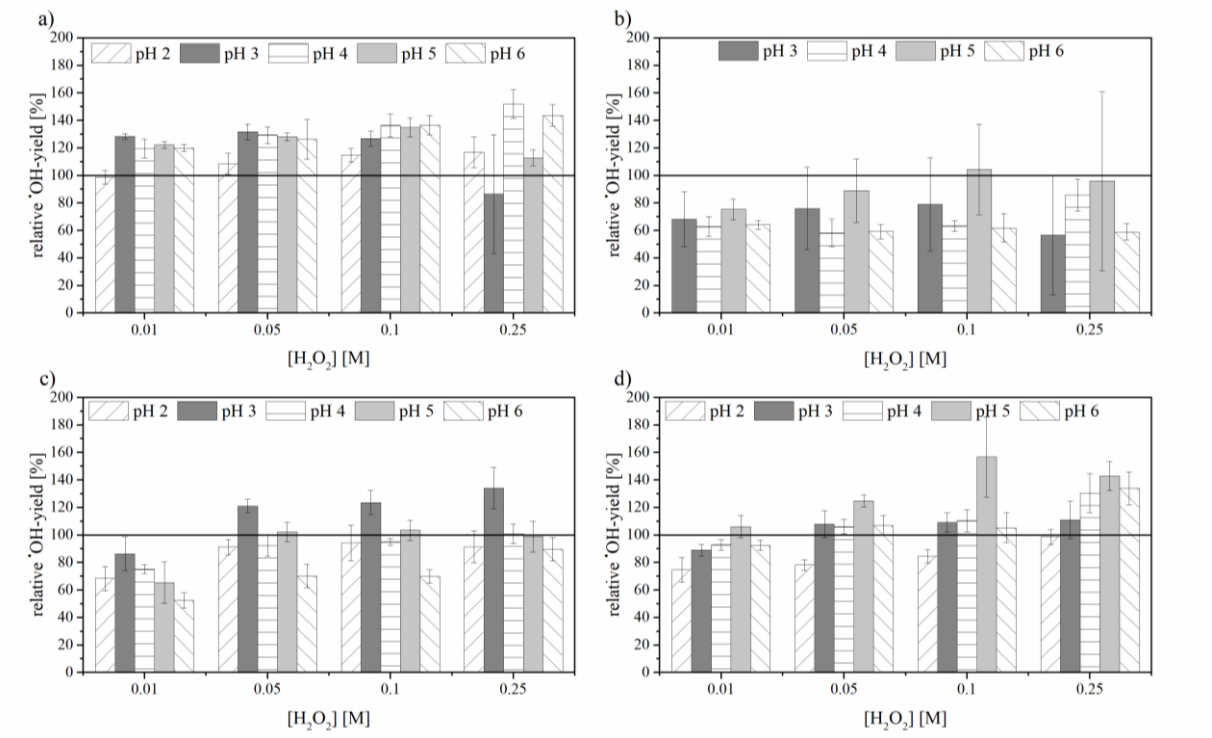

Figure 4.13: Relative ˙OH-yields referred to $[Fe^{II}]_0$ of 100 µM determined at various $[H_2O_2]$ at pH 2 – 6 in presence of a) DTPA, b) EDTA, c) HEDTA, d) NTA. ˙OH-yields were calculated by subtracting ˙OH-yields determined in experiments using Fe^{III} as primary iron source from those determined in experiments using Fe^{II} as primary iron source to correct overall yields for the contribution of the Fenton-like reaction. Error bars indicate standard deviation of three independent measurements including error propagation.

4.6 REFERENCES

1. Barb, W. G.; Baxendale, J. H.; George, P.; Hargrave, K. R., Reactions of ferrous and ferric ions with hydrogen peroxide. Part I. - The ferrous ion reaction. *Trans. Faraday Soc.* **1951,** *47*, 462-500.

2. Barb, W. G.; Baxendale, J. H.; George, P.; Hargrave, K. R., Reactions of ferrous and ferric ions with hydrogen peroxide. Part II. - The ferric ion reaction. *Trans. Faraday Soc.* **1951,** *47*, 591-616.

3. Wells, C. F.; Salam, M. A., The effect of pH on the kinetics of the reaction of iron(II) with hydrogen peroxide in perchlorate media. *J. Chem. Soc. A* **1968**, 24-29.

4. Wiegand, H. L.; Orths, C. T.; Kerpen, K.; Lutze, H. V.; Schmidt, T. C., Investigation of the iron-peroxo-complex in the Fenton reaction: Kinetic indication, decay kinetics and hydroxyl radical yields. *Environ. Sci. Technol.* **2017,** *51* (24), 14321-14329.

5. Veltwisch, D.; Janata, E.; Asmus, K. D., Primary processes in the reaction of •OH-radicals with sulphoxides. *J. Chem. Soc. Perkin Trans. 2* **1980,** (1), 146-153.

6. Buxton, G. V.; Greenstock, C. L.; Helman, W. P.; Ross, A. B., Critical review of rate constants for reactions of hydrated electrons, hydrogen atoms and hydroxyl radicals (•OH/•O⁻) in aqueous solution. *J. Phys. Chem. Ref. Data* **1988,** *17* (2), 513-886.

7. Stemmler, K.; Glod, G.; Von Gunten, U., Oxidation of metal-diethylenetriamine-pentaacetate (DTPA) - Complexes during drinking water ozonation. *Water Res.* **2001,** *35* (8), 1877-1886.

8. von Gunten, U., Ozonation of drinking water: Part I. Oxidation kinetics and product formation. *Water Res.* **2003,** *37* (7), 1443-1467.

9. Sharma, B. K.; Sahul, K., 60Co y-radiolysis of iron(III)nitrolotriacetate in aqueous solutions. *Radiat. Phys. Chem.* **1982,** *20* (5-6), 341-346.

10. Sutton, H. C.; Winterbourn, C. C., Chelated iron-catalyzed •OH formation from paraquat radicals and H_2O_2: Mechanism of formate oxidation. *Arch. Biochem. Biophys.* **1984,** *235* (1), 106-115.

11. Rush, J. D.; Koppenol, W. H., The reaction between ferrous polyaminocarboxylate complexes and hydrogen peroxide: An investigation of the reaction intermediates by stopped flow spectrophotometry. *J. Inorg. Biochem.* **1987,** *29* (3), 199-215.

12. Rahhal, S.; Richter, H. W., Reduction of hydrogen peroxide by the ferrous iron chelate of diethylenediamine-N,N,N',N'',N''-pentaacetate. *J. Am. Chem. Soc.* **1988,** *110* (10), 3126-3133.

13. Croft, S.; Gilbert, B. C.; Lindsay Smith, J. R.; Whitwood, A. C., An E.S.R. investigation of the reactive intermediate generated in the reaction between Fe^{II} and H_2O_2 in aqueous solution. Direct evidence for the formation of the hydroxyl radical. *Free Radical Res.* **1992,** *17* (1), 21-39.

14. Bottari, E.; Anderegg, G., Komplexone XLII. Die Untersuchung der 1:1:-Komplexe von einigen drei-und vierwertigen Metall-Ionen mit Polyaminocarboxylaten mittels Redoxmessungen. *Helv. Chim. Acta* **1967,** *50* (8), 2349-2356.

15. Rahhal, S.; Richter, H. W., Reaction of hydrogen peroxide with low molecular weight iron complexes. *International Journal of Radiation Applications and Instrumentation. Part* **1988,** *32* (1), 129-135.

16. Welch, K. D.; Davis, T. Z.; Aust, S. D., Iron autoxidation and free radical generation: Effects of buffers, ligands, and chelators. *Arch. Biochem. Biophys.* **2002,** *397* (2), 360-369.

17. Schwarzenbach, G.; Heller, J., Komplexone XXI. Die Eisenkomplexe der Nitrilo-triessigsäure. *Helv. Chim. Acta* **1951,** *34* (6), 1889-1900.

18. Schwarzenbach, G.; Heller, J., Komplexone XVIII. Die Eisen(II)- und Eisen(III)-komplexe der Äthylendiamin-tetraessigsäure und ihr Redoxgleichgewicht. *Helv. Chim. Acta* **1951,** *34* (2), 576-591.

19. Krishnamurthy, M.; Morris, K. B., Studies on iron(III) nitrilo triacetates. *J. Inorg. Nucl. Chem.* **1972,** *34* (2), 719-724.

20. Mizuta, T.; Yamamoto, T.; Miyoshi, K.; Kushi, Y., The ligand field stabilization effect on the metal-ligand bond distances in octahedral metal complexes with EDTA-type ligands. Redetermination of the molecular structure of (ethylenediaminetriacetatoacetic acid)-(aqua)iron(III), [Fe(HEDTA)(H_2O)]. *Inorg. Chim. Acta* **1990,** *175* (1), 121-126.

21. Pestovsky, O.; Stoian, S.; Bominaar, E. L.; Shan, X.; Münck, E.; Que Jr, L.; Bakac, A., Aqueous FeIV=O: Spectroscopic identification and oxo-group exchange. *Angewandte Chemie - International Edition* **2005,** *44* (42), 6871-6874.

22. Løgager, T.; Holcman, J.; Sehested, K.; Pedersen, T., Oxidation of ferrous ions by ozone in acidic solutions. *Inorg. Chem.* **1992,** *31* (17), 3523-3529.

23. Cohen, G.; Sinet, P. M., The Fenton reaction between ferrous-diethylenetriaminepentaacetic acid and hydrogen peroxide. *FEBS Lett.* **1982,** *138* (2), 258-260.

24. Sutton, H. C., Efficiency of chelated iron compounds as catalysts for the Haber-Weiss reaction. *J. Free Radic. Biol. Med.* **1985,** *1* (3), 195-202.

25. Šnyrychová, I.; Pospíšil, P.; Nauš, J., The effect of metal chelators on the production of hydroxyl radicals in thylakoids. *Photosynth. Res.* **2006,** *88* (3), 323-329.

26. Rush, J. D.; Koppenol, W. H., Reactions of Fe^{II}NTA and Fe^{II}EDDA with hydrogen peroxide. *J. Am. Chem. Soc.* **1988,** *110* (15), 4957-4963.

27. Goldstein, S.; Meyerstein, D.; Czapski, G., The Fenton reagents. *Free Radical Biol. Med.* **1993,** *15* (4), 435-445.

28. Pignatello, J. J.; Oliveros, E.; MacKay, A., Advanced oxidation processes for organic contaminant destruction based on the Fenton reaction and related chemistry. *Crit. Rev. Environ. Sci. Technol.* **2006,** *36* (1), 1-84.

29. Rachmilovich-Calis, S.; Masarwa, A.; Meyerstein, N.; Meyerstein, D.; van Eldik, R., New mechanistic aspects of the Fenton reaction. *Chem. Eur. J.* **2009,** *15* (33), 8303-8309.

30. Enderlein, J.; Erdmann, R., Fast fitting of multi-exponential decay curves. *Optics Communications* **1997,** *134* (1-6), 371-378.

31. El Seoud, O. A.; Baader, W. J.; Bastos, E. L., Practical Chemical Kinetics in Solution. In *Encyclopedia of Physical Organic Chemistry*, 1 ed.; Wang, Z.; Wille, U.; Juaristi, E., Eds. John Wiley & Sins, Inc.: Hoboken, **2017**.

32. Wiegand, H. L.; Kerpen, K.; Lutze, H. V.; Schmidt, T. C., Response to Comment on "Investigation of the Iron-Peroxo Complex in the Fenton Reaction: Kinetic Indication, Decay Kinetics, and Hydroxyl Radical Yields". *Environ. Sci. Technol.* **2018,** *52* (7), 4483-4484.

Chapter 5 -

INVESTIGATION OF FACTORS INFLUENCING FENTON-BASED DEGRADATION OF BISPHENOL S

Submitted for publication in *Chemical Engineering Journal*

5.1 ABSTRACT

Due to numerous adverse health effects of bisphenol A (BPA) it is progressively substituted by its structural analogue bisphenol S (BPS) and hence, release of the latter to the environment increases. However, knowledge on toxicological effects as well as on degradability of BPS is scarce. Degradation of BPA by means of Fenton reaction has already been successfully applied.

Thus, the present study investigates Fenton based degradation of BPS including BPS degradation rates at different reaction parameters (i.e. reactant concentrations, pH, and presence of hydroxyl radical scavenging matrix constituents).

It was found that degradation of BPS can be accelerated by varying reactant concentrations (i.e., ferrous iron and hydrogen peroxide). The optimal pH for BPS degradation was pH 3. However, surprisingly even at pH 7 complete degradation of BPS could be achieved even if it is slower than at pH 3. At pH < 3 BPS degradation was shown to be restricted by insufficient Fe^{II} recycling. In presence of hydroxyl radical scavenging matrix components such as organic matter BPS degradation is decelerated. Comparison of degradation of BPS and *para*-chlorobenzoic acid in presence of tertiary butanol indicates that hydroxyl radicals might be the main oxidant involved in BPS degradation at all investigated pH values.

5.2 INTRODUCTION

Bisphenols (BPs) such as bisphenol A (BPA) or bisphenol S (BPS) are monomers frequently used to produce, e.g., (thermal) paper products or polymer products (polycarbonate plastics, epoxy phenolic resins), which are used as food packaging materials.[1-2] As there is increasing evidence for endocrine and toxic effects related to BPA, the European Union has proposed to ban the use of BPA in thermal paper products from 2020.[3] That is why its application in commercial products is progressively replaced by its structural analogue BPS. Thus, increasing environmental concentrations of BPS are expected to occur in the future.

Indeed, BPS exhibits lower toxicity on *Daphnia magna* (48 h EC_{50}-values of BPS are higher by a factor of five compared to BPA)[4] but in comparison to the diverse investigations regarding the toxicity of BPA, effects of BPS are less understood.[5] Rochester and Bolden (2015)[6] conducted a literature research investigating adverse health effects of BPS. They found that BPS has similar endocrine disrupting effects as BPA.[6] However, in order to completely estimate environmental and/or health effects of BPS, also factors such as biodegradability and bioaccumulation must be taken into account.

A recent study shows that BPS can nowadays be ubiquitously found in the environment worldwide. BPS concentrations found in various environmental samples, such as sediment, sludge, indoor dust and air, consumer products, and human urine are lower compared to BPA. However, BPS concentrations found in the aquatic environment are comparable or even equal to those of BPA.[5] A study concerning the occurrence of different BPs in 76 U.S. sewage sludge samples found BPS to be the second most abundant BP analogue after BPA.[7] For BPA similar concentrations were found in German sewage sludge samples.[8-9] Furthermore, Danzl, *et al.* (2009)[10] and Ike, *et al.* (2006)[11] investigated biodegradability of BPA and BPS in seawater and river water, respectively. They found that BPS is, other than BPA, not sensitive towards

biodegradation and hence, might accumulate in the aquatic environment. Thus, the replacement of BPA by BPS results in higher requirements in terms of water treatment.

As mentioned above, advanced oxidation processes (AOPs) produce hydroxyl radicals (•OH) in sufficient quantities to affect water purification.[12] The highly reactive •OH can degrade complex organic molecules in smaller, biodegradable structures. One of these AOPs is the so-called Fenton reaction, which is typically conducted at acidic conditions.[13] Among other AOPs, Fenton or modified Fenton reactions (photo-, sono-, or ligand-assisted Fenton) have already successfully been applied to degrade BPA,[14-18] whereas to our knowledge nothing is known about Fenton based degradation of BPS. Studies focusing on oxidative BPS degradation by means of UV + H_2O_2, UV + O_3, or O_3 + H_2O_2 have already shown that •OH based processes are suitable to degrade BPS in aqueous solutions.[18-19] However, investigations regarding BPS degradation are scarce.

Due to the diverse advantages of Fenton chemistry compared to other AOPs, it seems to be a promising tool in this respect.[20-22] Thus, the presented study aims to investigate BPS degradation by means of the Fenton reaction including variation of factors influencing degradation efficiency such as initial iron concentration, molar ratio of Fe^{II} and H_2O_2, pH, as well as matrix components.

5.3 MATERIALS AND METHODS

5.3.1 CHEMICALS

4,4'-Sulfonyldiphenol (BPS) (98%) (Sigma-Aldrich, Germany), 4,4'-dimethylmethane-diphenol (BPA) (> 99%) (Aldrich Chemistry, Germany), *para*-chlorobenzoic acid (*p*CBA)

(99%) (Sigma-Aldrich, Germany), ammonium iron(II) sulfate hexahydrate ($(NH_4)_2Fe(SO_4)_2 \times 6\ H_2O$) (99%) (Sigma-Aldrich, Germany), hydrogen peroxide (H_2O_2) (30%) (AppliChem, Germany), sulfuric acid (H_2SO_4) (> 95%) (Fischer Chemicals, Switzerland), sodium hydroxide solution (NaOH) (1 M) (Bernd Kraft, Germany) dimethyl sulfoxide (DMSO) (≥ 99.9%) (Merck, Germany), tertiary butanol (*t*-BuOH) (100%) (Merck, Germany), Suwannee river natural organic matter (SR NOM) (RO isolation) (International Humic Substances Society, USA), sodium chloride (NaCl) (p.a.) (Bernd Kraft, Germany), uridine (≥ 99%) (Sigma Life Science, Germany), hydrogen chloride (HCl) (~ 37%) (Fisher Chemicals, United Kingdom), and methanol (MeOH) (100%) (VWR, Germany) were used as received without further purification.

5.3.2 Determination of the first order reaction rate constant for the reaction of BPS with •OH

The first order reaction rate constant for the reaction of BPS with •OH (k(BPS + •OH)) was determined by means of competition kinetics in a merry-go-round photo-reactor (H. & Th. Schneider Glasapparatebau (DEMA); Germany). For irradiation a low pressure mercury lamp (λ = 254 nm; 185 nm band suppressed) with a nominal power of 15 W was used (Peschl Ultraviolett; Germany). A fluid-circulation (Ministat 125; Huber, Germany) filled with ultrapure water was used to keep the temperature within the reactor constant at 25 ± 0.2 °C. Before and after determination of k(BPS + •OH) the average fluence rate of the system was determined by uridine actinometry according to von Sonntag and Schuchmann (1992)[23] to be 7.7×10^{-2} mEinstein m^{-2} s^{-1}.

For determination of k(BPS + •OH) 70 mL of an aqueous mixture of BPS and BPA (10 µM each) and 1 mM H_2O_2 were filled in quartz glass tubes located circularly around the UV lamp. Aliquots of the mixture were withdrawn in certain time intervals. BPS and BPA were quantified

in these samples by means of HPLC-UV measurements with an external calibration. The HPLC method is described in chapter 5.5.1.

From these data, k(BPS + •OH) was derived from a plot of ln[BPA]/[BPA]$_0$ vs. ln[BPS]/[BPS]$_0$ by multiplication of the slope with the known reaction rate constant for the reaction of BPA with •OH (1.7×10^{10} M^{-1} s^{-1})[24] to be 1.2×10^{10} M^{-1} s^{-1} at pH ≤ 4.

5.3.3 BATCH EXPERIMENTS FOR BPS DEGRADATION

Degradation of BPS was studied in batch experiments (total volume of 30 mL) at various conditions. All solutions were prepared in ultrapure water adjusted to a certain pH either with H_2SO_4 or NaOH. For each experiment, ultrapure water of a certain pH, 10 µM BPS, the required amount of H_2O_2 and in respective experiments the required amount of a *t*-BuOH or SR NOM (and chloride) as •OH-scavenging matrix components were put in a reaction vessel and stirred at 215 rpm. Before the reaction was started by adding the required amount of Fe^{II}, an aliquot of the mixture was taken as reference sample and put in a DMSO containing HPLC vial. DMSO was used to stop BPS degradation immediately after sampling. The amount of DMSO required to scavenge ≥ 99.9% of all •OH generated was calculated by means of equation 5.I. During the reaction, aliquots of the reaction mixture were taken and handled as the reference sample. Experiments were conducted at room temperature (~ 20 °C) as triplicates.

$$f(x + {}^{\bullet}OH) = \frac{k(x+{}^{\bullet}OH)\times[x]}{k(x+{}^{\bullet}OH)\times[x]+k(y+{}^{\bullet}OH)\times[y]+k(z+{}^{\bullet}OH)\times[z]} \qquad (5.I)$$

f represents the fraction of a certain compound x reacting with •OH, k is the reaction rate of relevant compounds (x, y, z, …) with •OH (for relevant rate constants see Table 5.2). In those experiments in which no •OH-scavenging matrix components were added, x = DMSO, y = BPS, and z = H_2O_2. Concentrations are indicated by squared brackets. In the denominator the

equation can be extended according to the compounds involved in the reaction (e.g. $^{\bullet}OH$-scavenging matrix components).

5.3.4 BPS ANALYSIS

Either an Agilent 1100 Series HPLC (Agilent 1100 Series, G1311 Quatpump coupled to a Agilent 1100 Series G1314A VWD detector) (Agilent, Germany) or a Shimadzu HPLC-DAD system (LC-10AT pump coupled to a SPD-M10A detector) (Shimadzu, Germany) both equipped with a high pressure pump and a 5 µm EVO C18 100 Å (50 × 2.1 mm) column (Phenomenex, Germany) was used for BPS quantification. An isocratic mixture of 70% ultrapure water (pH 2 adjusted with HCl) and 30% MeOH was used as eluent. The flow rate was set to 0.5 mL min^{-1}. The injection volume was 50 µL. As detection wavelength 258 nm was chosen.

5.3.5 DATA ANALYSIS

Peak areas resulting from HPLC measurements were transformed in BPS concentrations by means of an external calibration (0.05 – 10.5 µM) considering dilution of the taken sample by DMSO in the HPLC vial. Sample concentrations were then divided by the concentration of the reference sample and these ratios were plotted against the experiment time. First order reaction rate constants for the initial degradation of BPS were determined by fitting data of the initial degradation phase (15 s) with an exponential function of the type

$$\frac{[BPS]}{[BPS]_0} = e^{-k_{BPS}t}$$

with t being the time and k_{BPS} the first order reaction rate constant for the initial degradation of BPS.

5.4 RESULTS AND DISCUSSION

5.4.1 EFFECT OF Fe^{II}-CONCENTRATION ON BPS DEGRADATION

BPS degradation was studied applying three different initial Fe^{II}-concentrations ($[Fe^{II}]_0$) (50 µM, 100 µM, and 200 µM). All $[Fe^{II}]_0$ experiments were conducted at pH 3 and H_2O_2 was dosed in 25-fold excess per $[Fe^{II}]_0$.

The results show that BPS degradation is accelerated at increasing $[Fe^{II}]_0$ (Figure 5.6a). Whereas BPS could not be detected anymore after about 90 s when 50 µM Fe^{II} were used, degradation was already completed after 15 s in case of $[Fe^{II}]_0$ = 200 µM. That is also indicated by corresponding observed reaction rate constants (k_{BPS}), which increase with increasing $[Fe^{II}]_0$ and the decreasing fraction of BPS remaining after 15 s of degradation, which is caused by the accelerated kinetic. Both are shown in Figure 5.6b.

In case of a constant excess of H_2O_2 over Fe^{II} the accelerating effect of an increased $[Fe^{II}]_0$ can be explained by an increased amount of $^{\bullet}OH$ as it was shown earlier that the $^{\bullet}OH$-yield is about 100% per $[Fe^{II}]_0$.[25] However, it must be taken into account that at least Fenton based degradation at pH > 3 $[Fe^{II}]_0$ finally results in the formation of undesired insoluble Fe^{III}-sludge. Hence, one must find a compromise between fast degradation and the generated amount of Fe^{III}-sludge. Furthermore, it has to be considered that at very high concentrations Fe^{II} can also scavenge $^{\bullet}OH$.

5.4.2 EFFECT OF H_2O_2-CONCENTRATION ON BPS DEGRADATION

Applying a constant $[Fe^{II}]_0$ of 50 µM at pH 3 the influence of the H_2O_2-concentration ($[H_2O_2]$) (0.025 – 10 mM) was investigated. These concentrations correspond to $[H_2O_2]/[Fe^{II}]_0$-ratios ranging from 0.5 to 200.

Figure 5.1 depicts reaction rate constants for the initial BPS degradation and the residual fraction of BPS after 15 s at increasing $[H_2O_2]/[Fe^{II}]_0$-ratios. It can be derived from the figure that optimum conditions for BPS degradation with respect to both, k_{BPS} and remaining BPS are in the range of $[H_2O_2]/[Fe^{II}]_0$ = 25 – 100. At smaller $[H_2O_2]/[Fe^{II}]_0$ degradation is decelerated but respective degradation curves, which are shown in Figure 5.7, indicate that complete degradation of 10 µM BPS can still be achieved within 3 minutes at $[H_2O_2]/[Fe^{II}]_0$ = 5 – 10. Even longer degradation times will be required to achieve complete degradation at $[H_2O_2]/[Fe^{II}]_0$ = 0.5 – 1. In case of $[H_2O_2]/[Fe^{II}]_0$ = 200 degradation efficiency again decreases and it can be deduced from the corresponding degradation curve that even in case of longer degradation times no complete degradation will be achieved. That might possibly result from $^{\bullet}OH$-scavenging effects of H_2O_2 as the fraction of $^{\bullet}OH$, which is available for the reaction with BPS, is only ~ 30% at such conditions compared to ~ 85% at $[H_2O_2]/[Fe^{II}]_0$ = 5. Hence, increasing the $[H_2O_2]$ in order to accelerate degradation of contaminants is limited.

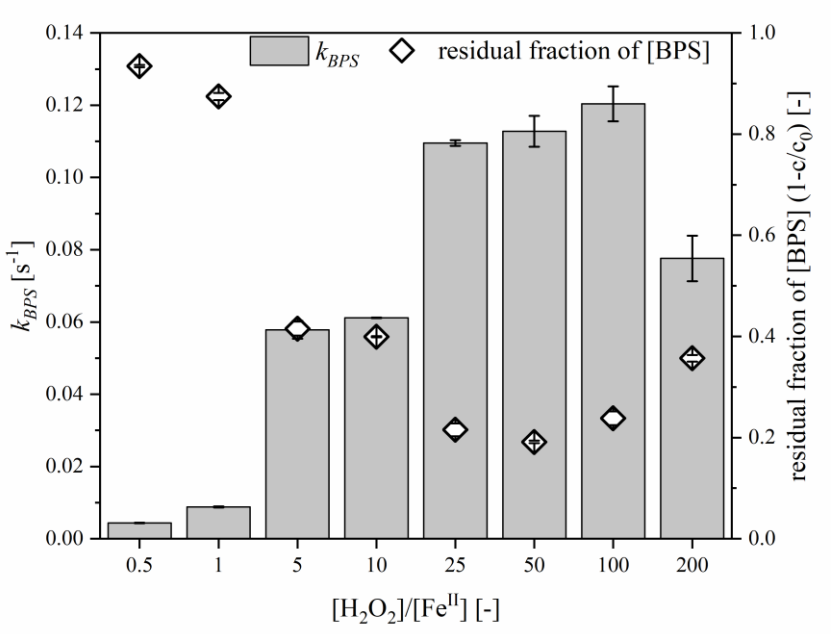

Figure 5.1: First order reaction rate constants for initial BPS degradation (15 s reaction time) and residual fractions of BPS after 15 s of reaction at different $[H_2O_2]/[Fe^{II}]_0$-ratios. $[Fe^{II}]_0$ = 50 µM, pH = 3, room temperature. Error bars indicate standard deviations of triplicates.

5.4.3 EFFECT OF PH ON BPS DEGRADATION

The influence of the pH on Fenton based BPS degradation was studied using a $[H_2O_2]/[Fe^{II}]_0$-ratio of 25 ($[Fe^{II}]_0$ = 50 µM). Figure 5.2 illustrates the effect of the pH on reaction rate constants for degradation of BPS as well as on the BPS fraction remaining after 15 s of degradation. The results show that optimum degradation is achieved at pH 3, indicated by the highest k_{BPS} and the smallest residual fraction of BPS. This result is confirmed by several researchers who all published optimum conditions for Fenton based degradation of contaminants to be at pH 3.[20] At smaller as well as at higher pH values degradation of BPS was slowed down. However, it can be derived from respective degradation curves (Figure 5.8) that BPS degradation levels off after about 90 s at pH 1 and 2 at $[BPS]/[BPS]_0$ = 0.3 and 0.1, respectively, and no further degradation occurs until 180 s, whereas complete degradation of 10 µM BPS is obtained at pH 3 – 7 in the same time scale.

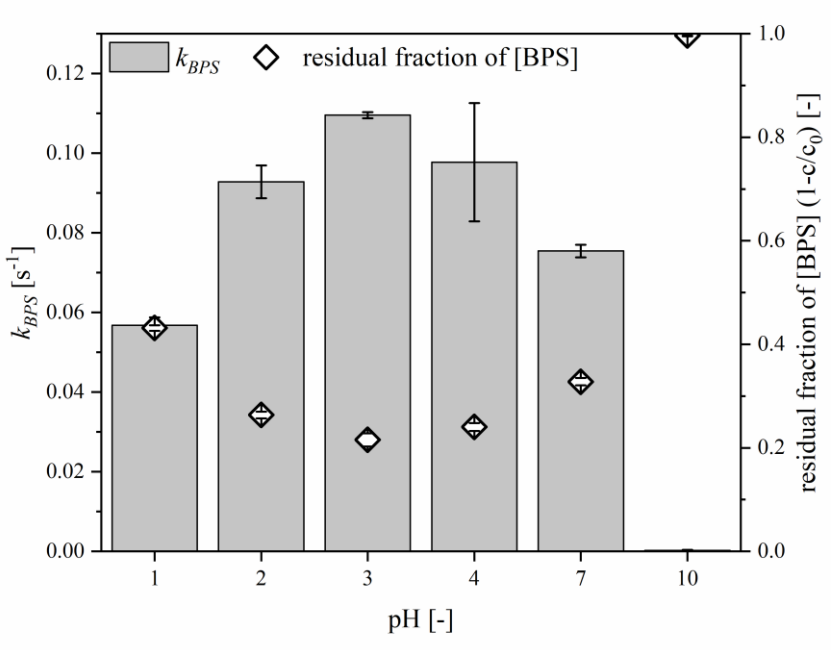

Figure 5.2: First order reaction rate constants for initial BPS degradation (15 s reaction time) and residual fractions of BPS after 15 s of degradation at various pH values. $[H_2O_2]/[Fe^{II}]_0$ = 25, $[Fe^{II}]$ = 50 µM, pH = 3, room temperature. Error bars indicate standard deviations of triplicates.

In order to explain incomplete degradation of BPS at pH 1 and 2, respective experiments were repeated but with addition of another 50 µM Fe^{II} after 90 s (Figure 5.9). These results indicate that incomplete BPS degradation at pH 1 and 2 can be ascribed to deficient Fe^{II} possibly due to insufficient Fe^{II} re-cycling as degradation was re-started by the addition of further Fe^{II}. As the Fenton-like reaction (reaction 1.12), which is responsible for re-formation of Fe^{II} from generated Fe^{III}, reveals a pH dependent equilibrium it was assumed that this reaction might be responsible for the observed phenomenon. However, experiments on Fenton-like induced BPS degradation (experimental details can be found in chapter 5.5.5) disprove this assumption as no degradation of BPS was observed regardless of the pH (pH 1 – 3) within 3 min (data not shown). Note that the Fenton-like reaction is about three orders of magnitude slower compared to the Fenton reaction so that pH dependent differences might occur when experiments will be conducted for more than 3 min.

On the other hand, participation of reactions 1.9 and 1.14 might be responsible for insufficient Fe^{II} re-cycling as the reaction rate constant of reaction 1.14 strongly depends on the pH.[26] Due to formation of H^+ in reaction 1.14, the reaction is decelerated at low pH. Sehested, *et al.* (1969)[26] determined the reaction rate constant of reaction 1.14 to be 2.1×10^5 M^{-1} s^{-1} at pH 1.5 and 1×10^6 M^{-1} s^{-1} at pH 2.7.

Even though it was frequently reported in literature that the Fenton reaction is limited at neutral pH due to the low solubility of Fe^{III} complete BPS degradation was observed at pH 7. As it was shown at pH 1 and 2 that 10 µM BPS cannot be fully degraded without Fe^{II} re-cycling the same is assumed to be true at pH 7. Hence, it is proposed that the chosen reaction conditions contribute to reactions of Fe^{III} in the Fenton process occurring faster than its precipitation. However, it must be taken into account that Fe^{II} autoxidation is largely accelerated with

increasing pH.[27] Hence, Fe^{II} stock solutions must be prepared immediately prior to the experiment. Otherwise, Fe^{III} would be dosed instead of Fe^{II}.

At pH 10, Fe^{II} autoxidation (reaction 1.14←) is so fast that even if stock solutions are prepared immediately prior to the experiment, Fe^{III} is dosed instead of Fe^{II}, which will precipitate at that pH.[27] Hence, no BPS degradation by the Fenton reaction could be investigated at pH 10.

5.4.4 Effect of •OH-scavenging matrix components on BPS degradation

With respect to real applications of Fenton chemistry in terms of water purification a compromise must be found between short hydraulic residence times and low chemical demand. As common hydraulic residence times for oxidative wastewater treatment can be up to 30 minutes and experiments described above indicate that even with equal concentrations of H_2O_2 and Fe^{II} might be achieved within less than 30 minutes, the influence of •OH-scavenging matrix components on BPS degradation by means of Fenton chemistry was examined using a $[H_2O_2]/[Fe^{II}]_0$-ratio of 1 ($[Fe^{II}]_0$ = 50 µM) at pH 3 and 7. As •OH-scavenging matrix constituents *t*-BuOH and SR NOM were chosen. BPS degradation was followed at increasing concentrations of the respective scavenger, which were dosed to scavenge 25, 50, 75, or 90% of generated •OH by *t*-BuOH and 25 or 75% by SR NOM (for calculations equation 5.I was used). Furthermore, experiments were conducted examining the effect of 10 mM NaCl in combination with SR NOM.

Figure 5.3 shows BPS degradation curves obtained in presence of *t*-BuOH (a/b) or SR NOM (c/d) at pH 3 (a/c) and 7 (b/d). It can be derived from the figure that regardless of pH BPS degradation is inhibited with increasing fraction of •OH scavenged by *t*-BuOH. However, the extent of inhibition differs with pH. At pH 3 scavenging of 90% •OH resulted in a remaining

fraction of BPS of 90% (900 s reaction time); without *t*-BuOH no BPS is left after 900 s. In contrast, at pH 7 residual BPS increases from ~ 20% without scavenger to ~ 85% when 90% of generated $^{\bullet}OH$ are scavenged by *t*-BuOH.

This effect might result from the reaction of $^{\bullet}OH$ with *t*-BuOH. In presence of oxygen $HO_2^{\bullet}/O_2^{\bullet -}$ can be formed ($pK_a = 4.5$).[28] Both of these radicals are capable of reacting with Fe^{III} and thus, regenerating Fe^{II}. However, it must be taken into account that the reaction of Fe^{III} with $O_2^{\bullet -}$ (i.e. at pH > 4.5) is about two orders of magnitude faster than its reaction with $HO_2^{\bullet}$ (i.e. at pH < 4.5).[29] Hence, at pH 7 the $^{\bullet}OH$-scavenging effect of *t*-BuOH could be compensated to some extent by the more effective regeneration of Fe^{II}.

Additionally, the main oxidant may be different at the two pH values. At pH 3 $^{\bullet}OH$ may be formed while at pH 7 Fe^{IV} could be formed instead (cf. Hug and Leupin (2003)[30] and Bataineh, *et al.* (2012)[31]). Due to the fact that *t*-BuOH is a good $^{\bullet}OH$- but weak Fe^{IV}-scavenger[20] no effect of increasing [*t*-BuOH] would have been expected in case of exclusive Fe^{IV}-formation at pH 7. Hence, the weaker scavenging by *t*-BuOH at pH 7 compared to pH 3, cannot be explained by formation of Fe^{IV}.

This was further examined by experiments with *p*CBA as model compound instead of BPS. *p*CBA is known to react fast with $^{\bullet}OH$ but barely with the more selective oxidant ozone.[32] As Fe^{IV} is supposed to be even more selective than ozone,[33] no degradation of *p*CBA should be observed in case of Fe^{IV} being the major reactive species. However, effects caused by $^{\bullet}OH$-scavenging due to *t*-BuOH on BPS- and *p*CBA-degradation are similar for both pH values under study (compare Figure 5.3a and Figure 5.3b and Figure 5.10). Thus, it is concluded that

formation of Fe^{IV} is indeed unlikely to occur at investigated experimental conditions, even at elevated pH (i.e., pH 7).

As shown in Figure 5.3c and d, the scavenging effect of SR NOM is slightly stronger at pH 7 compared to pH 3. At pH 3 addition of SR NOM in a concentration leading to scavenging of 75% ˙OH resulted in a 55% remaining fraction of BPS after a reaction time of 900 s; without SR NOM no BPS is left after 900 s. In contrast, at pH 7 residual BPS increases from ~ 20% to 85% in case of 75% of generated ˙OH being scavenged.

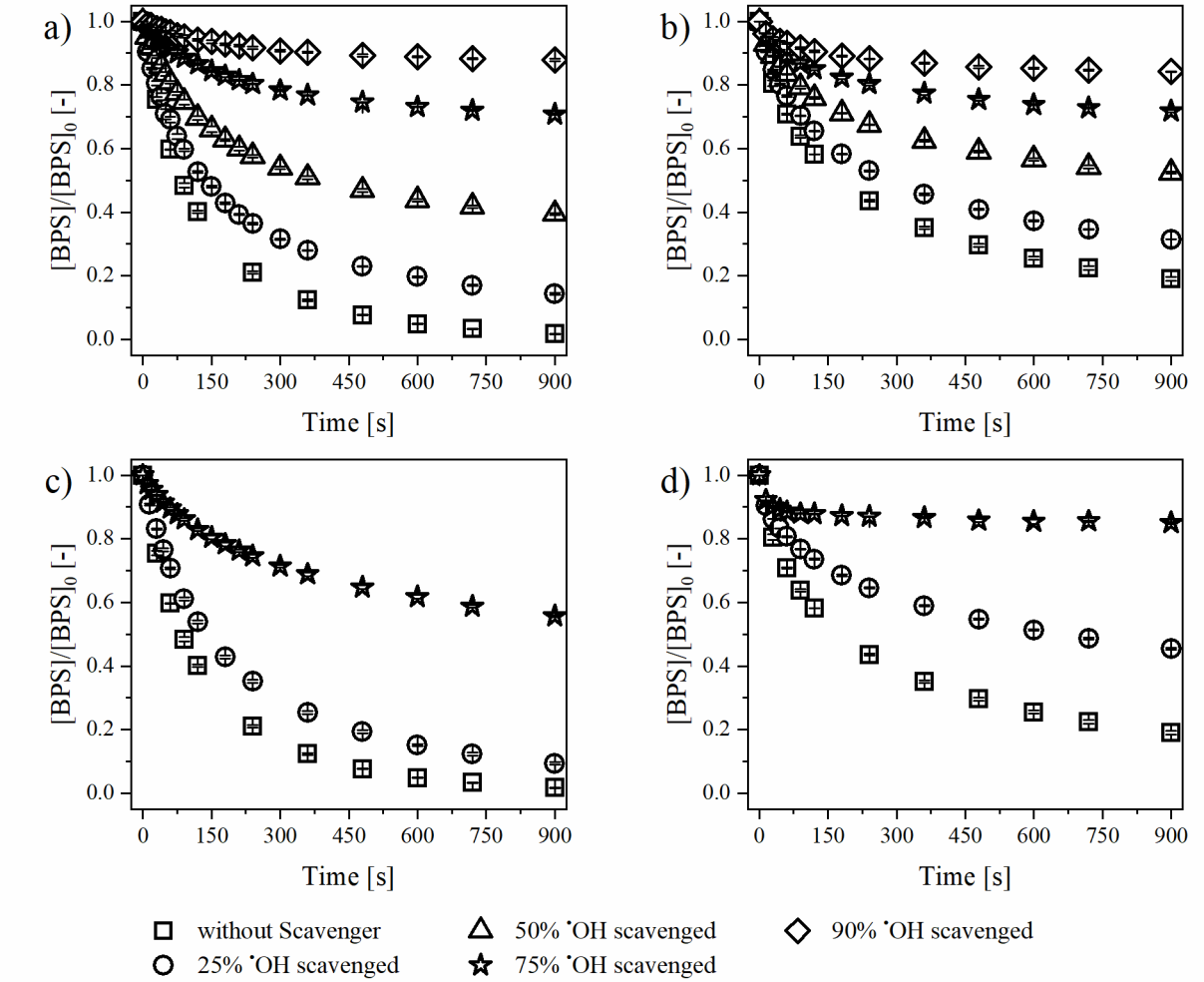

Figure 5.3: BPS degradation measured in presence of various concentrations of t-BuOH (a/b) or SR NOM (c/d) at pH 3 (a/c) and 7 (b/d). $[H_2O_2]/[Fe^{II}]$ = 1, $[Fe^{II}]_0$ = 50 µM, room temperature. Error bars indicate standard deviations of triplicates.

In comparison to the results obtained in presence of *t*-BuOH it can be concluded that not only $^{\bullet}OH$-scavenging effects are caused by SR NOM as otherwise no differences should have been observed in the extent of inhibition of BPS degradation. As published earlier, dissolved iron species can be complexed by SR NOM[34] and thus, Fenton reaction is accelerated. That might explain why inhibition of BPS degradation at pH 3 is stronger in presence of *t*-BuOH than in presence of SR NOM.

At pH 7 inhibition of BPS degradation by NOM is less pronounced. This can be explained by different reaction kinetics of NOM of $^{\bullet}OH$ at pH 3 and 7. It is likely that NOM reacts faster with $^{\bullet}OH$ at pH 7 than at pH 3 since dissociation of e.g. phenolic groups activates reactive sites of NOM. This effect is less pronounced in case of *t*-BuOH (higher pK_a).

The combined effect of 10 mM chloride (Cl^-) and SR NOM at pH 3 and 7 is shown in Figure 5.4. It can be derived from the figure that BPS degradation is further hampered at pH 3 (Figure 5.4a) due to the presence of Cl^-, whereas no Cl^- related effect can be observed at pH 7 (Figure 5.4b). This phenomenon can be explained by a pH-dependent sequence of reactions (reaction 5.1 – 5.2).

$$Cl^- + {}^{\bullet}OH \rightleftharpoons HOCl^{\bullet-} \qquad (5.1)^{35}$$

$$k_{\rightarrow} = 4.3 \times 10^9\ M^{-1}\ s^{-1}$$

$$k_{\leftarrow} = 6 \times 10^9\ s^{-1}$$

$$HOCl^{\bullet-} + H^+ \rightleftharpoons Cl^{\bullet} + H_2O \qquad (5.2)^{35}$$

$$k_{\rightarrow} = 2 \times 10^{10}\ M^{-1}\ s^{-1}$$

$$k_{\leftarrow} = 1.6 \times 10^5\ s^{-1}$$

Due to the fast back reaction of reaction 5.1, steady state concentrations of $HOCl^{\bullet-}$ are small. Furthermore, the equilibrium of reaction 5.2 strongly depends on pH leading to a reaction rate

constant of 10^3 M^{-1} s^{-1} at pH 7 for the oxidation of chloride by $^{\bullet}OH$ to chlorine radicals ($Cl^{\bullet}$). As H^+ is directly involved in the reaction, this reaction rate constant increases by a factor of 10 per pH unit decrease (i.e. increase of $[H^+]$ by a factor of 10).[35] Hence, at pH 3 the fraction of $^{\bullet}OH$ available for the reaction with BPS is reduced from about 66% without chloride to about 43% in presence of chloride, whereas at pH 7 addition of chloride does not affect the fraction of $^{\bullet}OH$ available for BPS degradation. Thus, at pH 3 chloride lowers oxidation efficiency about 30% more than at pH 7.

Generated $Cl^{\bullet}$ can further react with Cl^- to form $Cl_2^{\bullet-}$ (reaction 5.3).[36-37] Whereas $Cl^{\bullet}$ shows reaction rate constants of the same order of magnitude as $^{\bullet}OH$ for reactions with organic compounds, $Cl_2^{\bullet-}$ is less reactive.[38] Typically $Cl^{\bullet}$ and $Cl_2^{\bullet-}$ oxidation reactions occur *via* electron transfer reactions, H-abstraction or addition to unsaturated C-C bonds.[38] Grebel, *et al.* (2010)[38] expected formation of reactive halogen species caused by halide induced scavenging of $^{\bullet}OH$ to result in greater selectivity with increasing preference for attack at electron-rich centres.[38] For electron-poor contaminants treatment efficiency of AOPs may be drastically reduced in presence of halides, whereas degradation of electron-rich compounds will mainly remain unaffected.[38]

$$Cl^{\bullet} + Cl^- \rightarrow Cl_2^{\bullet-} \qquad (5.3)$$

These results are promising with respect to application of the Fenton reaction for wastewater treatment. Indeed, at circumneutral pH Fenton chemistry is restricted due to limited solubility of Fe^{III}. On the other hand, presence of chloride does hardly affect the oxidation of pollutants at pH 7 while at pH 3 chloride strongly mitigates the oxidation strength. Consequently, at the investigated chloride concentration, efficiency of BPS degradation is the same at pH 3 and pH 7.

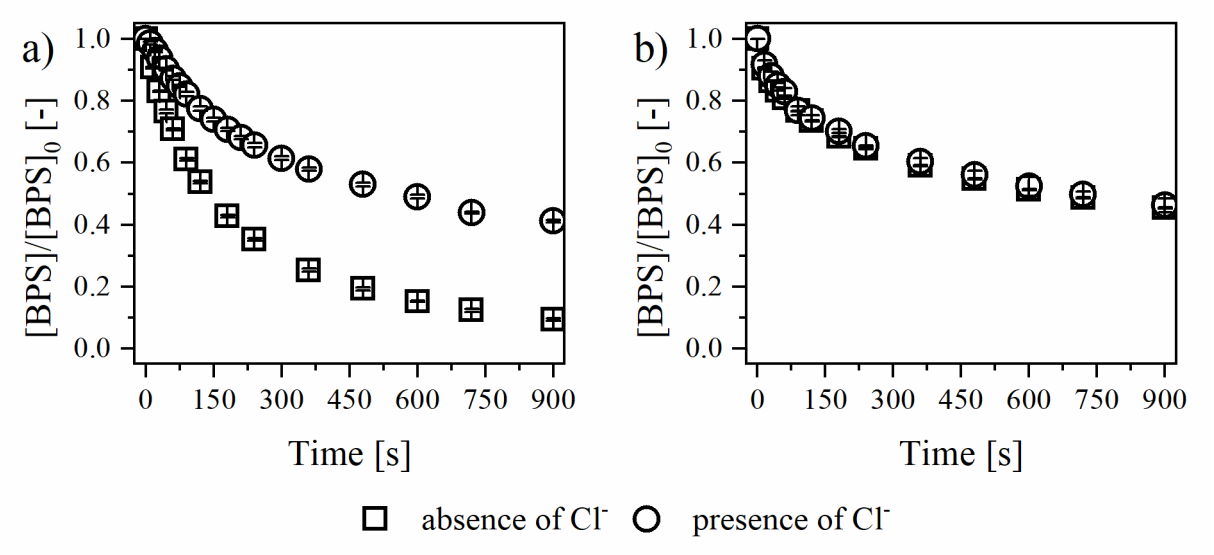

Figure 5.4: BPS degradation recorded at constant $[H_2O_2]/[Fe^{III}]_0$-ratio of 1 ($Fe^{II}]_0$ = 50 µM) in presence of SR NOM scavenging 25% of generated $^{\bullet}OH$ and absence or presence of 10 mM NaCl at pH 3 (a) and 7 (b), room temperature. Error bars indicate standard deviations of triplicates.

When experiments were conducted in treated wastewater of a municipal wastewater treatment plant, hardly any BPS was degraded (~ 7%) (Figure 5.11). pH, chloride and dissolved organic carbon (DOC) content were determined in the treated wastewater to be 7.6, 12.5 mM and 0.33 mM, respectively. As it was shown that chloride does not affect degradation of BPS at circumneutral pH, chloride cannot be responsible for the poor degradation. Also the DOC content, which is markedly lower compared to the DOC content applied in NOM experiments, is unlikely to be responsible for the observed effects. Indeed, at pH 7.6 Fe^{II} autoxidation is faster compared to pH 7.[27] However, this effect might not completely explain that almost no BPS degradation took place. A further factor, which must be considered, is the carbonate content of the wastewater. It is known that in presence of carbonate Fe^{II} autoxidation is drastically accelerated.[39] It is assumed that this carbonate induced Fe^{II} autoxidation outcompetes Fenton chemistry and thus, is mainly responsible for deficient BPS degradation. Furthermore, structural characteristics of the DOC present are unknown and might differ from SR NOM.

Thus, it is possible that DOC in treated wastewater contains structural elements, which are more reactive than those of SR NOM and compete with BPS to be degraded by •OH.

The present paper provides first investigations on degradation of BPS by means of Fenton chemistry. It was shown that kinetics of BPS degradation depends on applied reactant concentrations and can to some extent be accelerated when reactant concentrations are increased. However, even adverse effects of high concentrations of Fe^{II} and H_2O_2 must be taken into account, i.e. formation of undesired Fe^{III}-sludge due to limited solubility of Fe^{III} even at pH 3 or •OH-scavenging effects of H_2O_2 and Fe^{II}. Hence, reaction conditions must be optimised for any water treatment scenario. Furthermore, it was shown that Fenton based degradation of BPS without added Fe-complexing ligands is not restricted to acidic pH as frequently reported in the past.[20] Indeed, degradation is slower at pH 7 compared to pH 3 but ~ 80% of the applied BPS concentration are degraded in ultrapure water within 15 minutes, and common hydraulic residence times for oxidative treatment of wastewater can be up to 30 minutes. However, in presence of bicarbonate autoxidation of Fe^{II} may become a limiting factor. Additionally, experiments conducted in presence of *t*-BuOH gave rise to the assumption that in case of the applied reaction conditions •OH are the only oxidant involved in the degradation of BPS or *p*CBA. Consequently, degradation in presence of •OH-scavenging matrix components is drastically slowed down or levelled off after a certain time.

Thus, further research is required with respect to processes occurring in presence of real matrix components in order to improve Fenton based degradation of BPS in real samples (e.g. influence of bicarbonate/carbonate induced Fe^{II}-autoxidation). Another important aspect would be the investigation of degradation products, since identification of degradation products is relevant for ecotoxicological reasons. Furthermore, a study covering degradation of BPS by

means of different AOPs under comparable conditions would be helpful in order to evaluate the best method for BPS degradation.

5.5 SUPPORTING INFORMATION

5.5.1 HPLC-METHOD FOR PARALLEL QUANTIFICATION OF BISPHENOL A AND BISPHENOL S

An Agilent 1100 Series HPLC-UV was used for quantification of bisphenol A and bisphenol S in parallel. A 5 µm EVO C18 100 Å (50 × 2.1 mm) column (Phenomenex, Germany) was used for separation.

As eluent a gradient of pH 2 H_2O (acidified with HCl) and MeOH was applied according to Table 5.1.

Table 5.1: Gradient composition used for quantification of BPA and BPS by HPLC-UV.

Time [min]	Fraction of MeOH [%]
0 – 7	40
7 – 16	Progressively increased to 65

For BPS λ = 258 nm was chosen as detection wavelength, for BPA it was set to λ = 225 nm.

A representative chromatogram is shown in Figure 5.5.

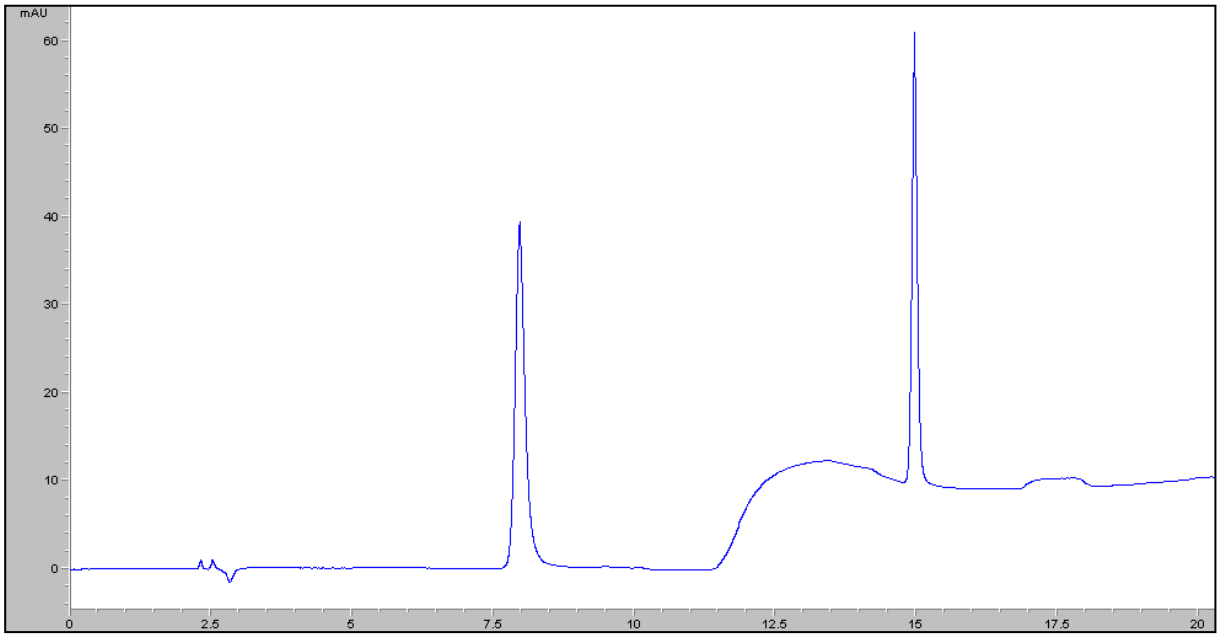

Figure 5.5: Representative chromatogram showing a peak of BPS (ca. 8 min) and a peak of BPA (ca. 15 min).

5.5.2 RELEVANT REACTION RATE CONSTANTS

Table 5.2 compiles relevant reaction rate constants used for calculations of required concentrations to achieve scavenging of a distinct •OH-fraction or of the •OH-fraction available for the reaction with BPS at certain reaction conditions.

Table 5.2: Relevant reaction rate constants used for various calculations.

Reaction	**Reaction rate constant (*k*) [M^{-1} s^{-1}]**	**Reference**
BPS + •OH	1.2×10^{10}	This study
Cl^- + •OH	pH 7: 1.0×10^{3} pH 3: 1.0×10^{7}	von Gunten (2003)[35]
DMSO + •OH	7.0×10^{9}	Buxton, *et al.* (1988)[40]
Fe^{II} + •OH	3.0×10^{8}	Buxton, *et al.* (1988)[40]
H_2O_2 + •OH	2.7×10^{7}	Buxton, *et al.* (1988)[40]
***t*-BuOH + •OH**	6.0×10^{8}	Buxton, *et al.* (1988)[40]
SRFA + •OH	1.4×10^{4}	Lutze, *et al.* (2015)[41]
***p*CBA + •OH**	5.0×10^{9}	Dao and De Laat (2011)[42]

5.5.3 EFFECT OF Fe^{II}-CONCENTRATION ON BPS DEGRADATION

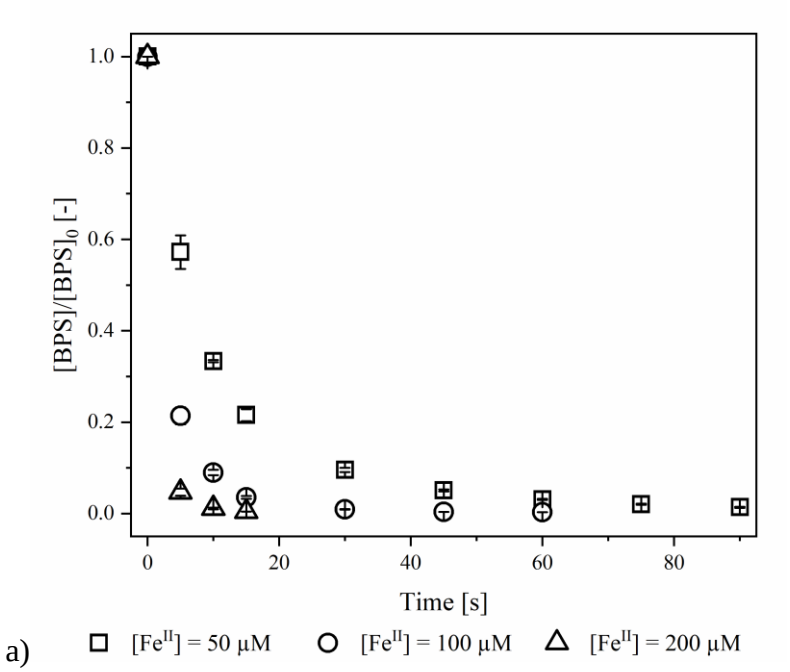

a)

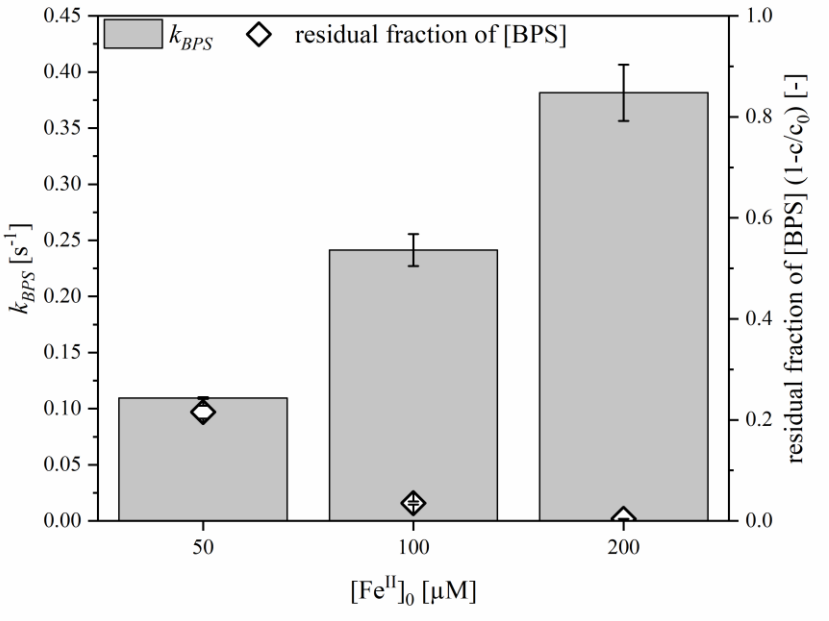

b)

Figure 5.6: a) BPS degradation measured at increasing $[Fe^{II}]_0$ and constant $[H_2O_2]/[Fe^{II}]$-ratio of 25 at pH 3. Errors are depicted as error bars representing standard deviations of triplicates. b) First order reaction rate constants for initial BPS degradation (15 s reaction time) and residual fractions of BPS after 15 s of degradation at increasing $[Fe^{II}]_0$, constant $[H_2O_2]/[Fe^{II}]$-ratios of 25 and pH 3. Errors are depicted as error bars representing standard deviations of triplicates.

5.5.4 EFFECT OF H_2O_2-CONCENTRATION ON BPS DEGRADATION

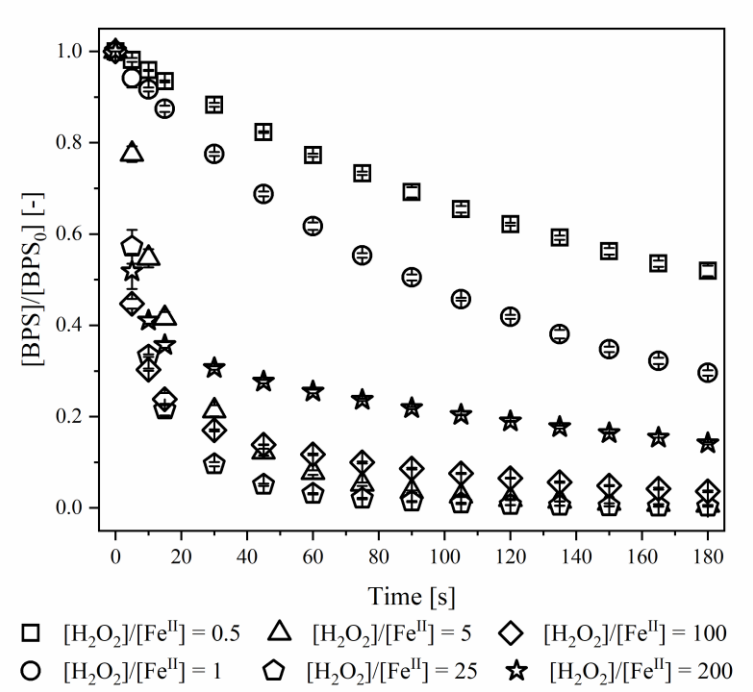

Figure 5.7: BPS degradation measured at increasing $[H_2O_2]/[Fe^{II}]$-ratios, applying constant $[Fe^{II}]_0$ of 50 µM at pH 3. Errors are depicted as error bars representing standard deviations of triplicates.

5.5.5 EFFECT OF PH ON BPS DEGRADATION

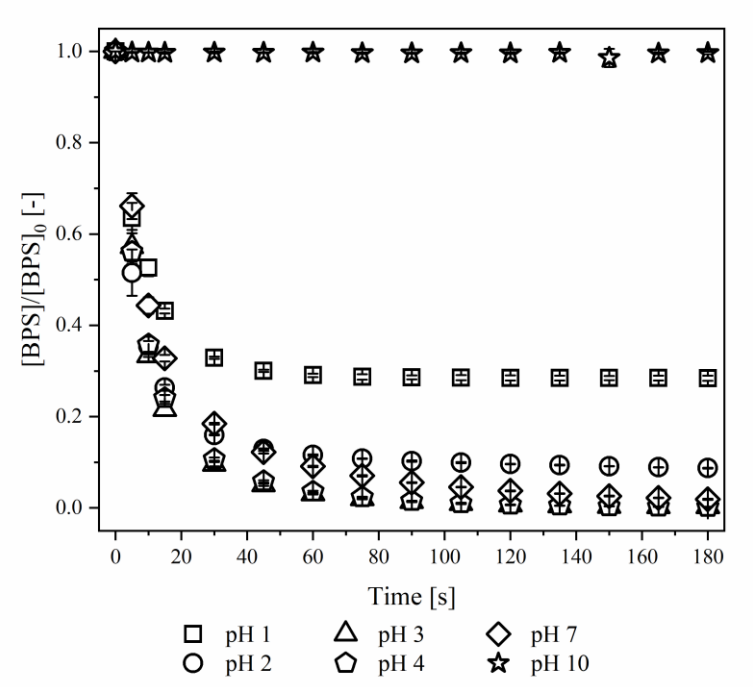

Figure 5.8: BPS degradation measured at increasing pH and constant $[H_2O_2]/[Fe^{II}]_0$-ratio of 25 ($[Fe^{II}]_0$ = 50 µM). Errors are depicted as error bars representing standard deviations of triplicates.

At pH 1 and 2 BPS degradation levels off after about 90 s after 70 and 90% degradation, respectively. As H_2O_2 was dosed in excess over Fe^{II} it was assumed that incomplete degradation at pH 1 and 2 occurs due to lacking Fe^{II}. In order to confirm this assumption experiments were repeated but with addition of another 50 µM Fe^{II} after 90 s of degradation. Figure 5.9 shows respective BPS degradation curves. It can be derived from the figure that BPS degradation restarts after the addition of another 50 µM Fe^{II}.

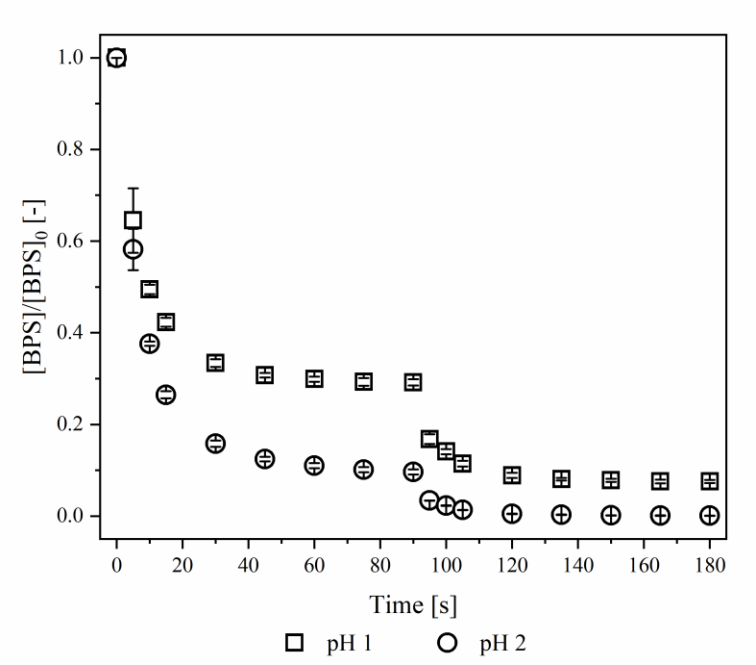

Figure 5.9: BPS degradation measured at a constant $[H_2O_2]/[Fe^{II}]_0$-ratio of 25 ($[Fe^{II}]_0$ = 50 µM) at pH 1 and 2. After 90 s another 50 µM Fe^{II} were added. Errors are depicted as error bars representing standard deviations of triplicates.

Experiments to investigate the influence of the Fenton-like reaction on BPS degradation were conducted applying 50 µM Fe^{II} and 1.25 mM H_2O_2 at pH 1 – 3 and 7. Degradation was observed for three minutes.

5.5.6 FENTON-BASED DEGRADATION OF *PARA*-CHLOROBENZOIC ACID (*P*CBA)

Degradation of *p*CBA by means of Fenton chemistry was studied applying a $[H_2O_2]/[Fe^{II}]_0$-ratio of 1 ($[Fe^{II}]_0$ = 50 µM) at pH 3 and 7 in presence of increasing concentrations of *t*-BuOH. [*t*-BuOH] was calculated according to equation I of the main paper so that 25, 50, 75, or 90% of generated •OH will be scavenged by *t*-BuOH ($k_{pCBA + \bullet OH}$ = 5.0 × 10^9 M^{-1} s^{-1}). Figure 5.10 shows respective *p*CBA degradation curves. It can be derived from the figure that regardless of pH *p*CBA degradation is increasingly inhibited with increasing fraction of •OH scavenged by *t*-BuOH. However, the extent of inhibition differs with pH. At pH 3 scavenging of 90% •OH causes an increase of the residual fraction of *p*CBA remaining after a reaction time of 900 s to

85%; without *t*-BuOH no *p*CBA is left after 900 s. In contrast, at pH 7 residual *p*CBA increases from ~ 25% without scavenger to ~ 90% in case of 90% of generated $^{\bullet}OH$ being scavenged.

As mentioned above, this effect might be ascribed to the formation of $HO_2^{\bullet}/O_2^{\bullet -}$ from the reaction of $^{\bullet}OH$ with *t*-BuOH. According to these results formation of Fe^{IV} at pH 7, as it is suggested in literature,[30-31] can be excluded. In case of exclusive Fe^{IV} formation no degradation of *p*CBA should have been observed, as Fe^{IV} is supposed to be an even more selective oxidant than ozone, which is not capable to degrade *p*CBA.

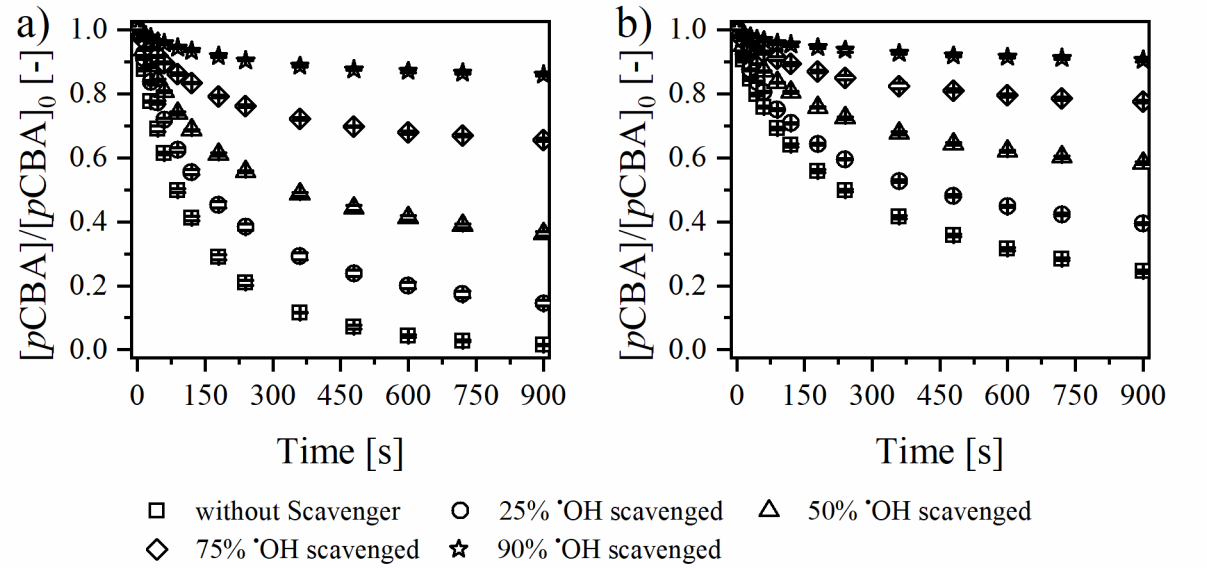

Figure 5.10: pCBA degradation measured at constant $[H_2O_2]/[Fe^{II}]_0$-ratio of 1 ($[Fe^{II}]_0$ = 50 µM) at pH 3 (a) and 7 (b) in presence of various concentrations of t-BuOH. Errors are depicted as error bars representing standard deviations of triplicates.

5.5.7 DEGRADATION OF BISPHENOL S IN TREATED WASTEWATER

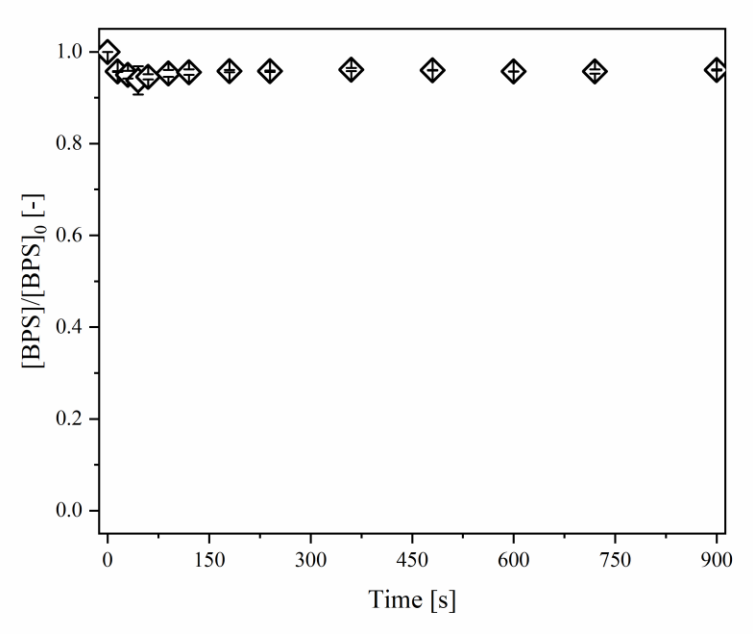

Figure 5.11: BPS degradation measured at constant $[H_2O_2]/[Fe^{II}]_0$-ratio of 1 ($[Fe^{II}]_0$ = 50 µM). As matrix treated wastewater of a municipal wastewater treatment plant was used. Errors are depicted as error bars representing standard deviations of triplicates.

5.6 REFERENCES

1. Liao, C.; Liu, F.; Kannan, K., Bisphenol S, a new bisphenol analogue, in paper products and currency bills and its association with bisphenol a residues. *Environ. Sci. Technol.* **2012,** *46* (12), 6515-6522.

2. EFSA, Opinion of the Scientific Panel on Food Additives, Flavourings, Processing Aids and Materials in Contact with Food on a request from the Commision related to 2,2-Bis(4-Hydroxylphenyl)propane (Bisphenol A). *The EFSA Journal* **2006,** *428*.

3. Pivnenko, K.; Laner, D.; Astrup, T. F., Dynamics of bisphenol A (BPA) and bisphenol S (BPS) in the European paper cycle: Need for concern? *Resour. Conserv. Recycl.* **2018,** *133*, 278-287.

4. Chen, M. Y.; Ike, M.; Fujita, M., Acute toxicity, mutagenicity, and estrogenicity of bisphenol-A and other bisphenols. *Environ. Toxicol.* **2002,** *17* (1), 80-86.

5. Wu, L. H.; Zhang, X. M.; Wang, F.; Gao, C. J.; Chen, D.; Palumbo, J. R.; Guo, Y.; Zeng, E. Y., Occurrence of bisphenol S in the environment and implications for human exposure: A short review. *Sci. Total Environ.* **2018,** *615*, 87-98.

6. Rochester, J. R.; Bolden, A. L., Bisphenol S and F: A systematic review and comparison of the hormonal activity of bisphenol a substitutes. *Environ. Health Perspect.* **2015,** *123* (7), 643-650.

7. Yu, X.; Xue, J.; Yao, H.; Wu, Q.; Venkatesan, A. K.; Halden, R. U.; Kannan, K., Occurrence and estrogenic potency of eight bisphenol analogs in sewage sludge from the U.S. EPA targeted national sewage sludge survey. *J. Hazard. Mater.* **2015,** *299*, 733-739.

8. Bolz, U.; Hagenmaier, H.; Körner, W., Phenolic xenoestrogens in surface water, sediments, and sewage sludge from Baden-Württemberg, south-west Germany. *Environ. Pollut.* **2001,** *115* (2), 291-301.

9. Fromme, H.; Küchler, T.; Otto, T.; Pilz, K.; Müller, J.; Wenzel, A., Occurrence of phthalates and bisphenol A and F in the environment. *Water Res.* **2002,** *36* (6), 1429-1438.

10. Danzl, E.; Sei, K.; Soda, S.; Ike, M.; Fujita, M., Biodegradation of bisphenol A, bisphenol F and bisphenol S in seawater. *Int. J. Environ. Res. Public Health* **2009,** *6* (4), 1472-1484.

11. Ike, M.; Chen, M. Y.; Danzl, E.; Sei, K.; Fujita, M., Biodegradation of a variety of bisphenols under aerobic and anaerobic conditions. *Water Sci. Technol.* **2006,** *53* (6), 153-159.

12. Glaze, W. H.; Kang, J. W.; Chapin, D. H., The chemistry of water treatment processes involving ozone, hydrogen peroxide and ultraviolet radiation. *Ozone Sci. Eng.* **1987,** *9* (4), 335-352.

13. von Sonntag, C., Advanced oxidation processes: Mechanistic aspects. *Water Sci. Technol.* **2008,** *58* (5), 1015-1021.

14. Katsumata, H.; Kawabe, S.; Kaneco, S.; Suzuki, T.; Ohta, K., Degradation of bisphenol A in water by the photo-Fenton reaction. *J. Photochem. Photobiol. A Chem.* **2004,** *162* (2-3), 297-305.

15. Ioan, I.; Wilson, S.; Lundanes, E.; Neculai, A., Comparison of Fenton and sono-Fenton bisphenol A degradation. *J. Hazard. Mater.* **2007,** *142* (1-2), 559-563.

16. Huang, W.; Brigante, M.; Wu, F.; Mousty, C.; Hanna, K.; Mailhot, G., Assessment of the Fe(III)-EDDS complex in Fenton-like processes: From the radical formation to the degradation of bisphenol A. *Environ. Sci. Technol.* **2013,** *47* (4), 1952-1959.

17. Pérez-Moya, M.; Kaisto, T.; Navarro, M.; del Valle, L. J., Study of the degradation performance (TOC, BOD, and toxicity) of bisphenol A by the photo-Fenton process. *Environ. Sci. Pollut. Res.* **2017,** *24* (7), 6241-6251.

18. Mehrabani-Zeinabad, M.; Langford, C. H.; Achari, G., Advanced oxidative degradation of bisphenol A and bisphenol S. *J. Environ. Eng. Sci.* **2016,** *10* (4), 92-102.

19. Mehrabani-Zeinabad, M.; Achari, G.; Langford, C. H., Degradation of Bisphenol S Using O_3 and/or H_2O_2 with UV in a Flow-Through Reactor. *Journal of Environmental Engineering (United States)* **2016,** *142* (8).

20. Pignatello, J. J.; Oliveros, E.; MacKay, A., Advanced oxidation processes for organic contaminant destruction based on the Fenton reaction and related chemistry. *Crit. Rev. Environ. Sci. Technol.* **2006,** *36* (1), 1-84.

21. Bautista, P.; Mohedano, A. F.; Casas, J. A.; Zazo, J. A.; Rodriguez, J. J., An overview of the application of Fenton oxidation to industrial wastewaters treatment. *J. Chem. Technol. Biotechnol.* **2008,** *83* (10), 1323-1338.

22. Oturan, M. A.; Aaron, J. J., Advanced oxidation processes in water/wastewater treatment: Principles and applications. A review. *Crit. Rev. Environ. Sci. Technol.* **2014,** *44* (23), 2577-2641.

23. von Sonntag, C.; Schuchmann, H. P., UV-disinfection of drinkting water and by-product formation - some basic considerations. *Journal of water supply: Research and Technology - AQUA* **1992,** *41* (2), 67-74.

24. Staehelln, J.; Hoigne, J., Decomposition of Ozone in Water in the Presence of Organic Solutes Acting as Promoters and Inhibitors of Radical Chain Reactions. *Environ. Sci. Technol.* **1985,** *19* (12), 1206-1213.

25. Wiegand, H. L.; Orths, C. T.; Kerpen, K.; Lutze, H. V.; Schmidt, T. C., Investigation of the iron-peroxo-complex in the Fenton reaction: Kinetic indication, decay kinetics and hydroxyl radical yields. *Environ. Sci. Technol.* **2017,** *51* (24), 14321-14329.

26. Sehested, K.; Bjergbakke, E.; Rasmussen, O. L.; Fricke, H., Reactions of H_2O_3 in the pulse-irradiated Fe(II)-O_2 system. *J. Chem. Phys.* **1969,** *51* (8), 3159-3166.

27. Morgan, B.; Lahav, O., The effect of pH on the kinetics of spontaneous Fe(II) oxidation by O_2 in aqueous solution - basic principles and a simple heuristic description. *Chemosphere* **2007,** *68* (11), 2080-2084.

28. von Sonntag, C.; Dowideit, P.; Fang, X.; Mertens, R.; Pan, X.; Schuchmann, M. N.; Schuchmann, H. P., The fate of peroxyl radicals in aqueous solution. In *Proceedings of the*

1996 International Conference on Oxidation Technologies for Water and Wastewater Treatment, Vogelpohl, A.; Geissen, S. U., Eds. Clausthal-Zellerfeld, Ger, 1997; Vol. 35, 9-15.

29. Rush, J. D.; Bielski, B. H. J., Pulse radiolytic studies of the reactions of $HO_2^{\bullet}/O_2^{\bullet -}$ with Fe(II)/Fe(III) ions. The reactivity of $HO_2^{\bullet}/O_2^{\bullet -}$ with ferric ions and its implication on the occurrence of the Haber-Weiss reaction. *J. Phys. Chem.* **1985,** *89* (23), 5062-5066.

30. Hug, S. J.; Leupin, O., Iron-catalyzed oxidation of arsenic(III) by oxygen and by hydrogen peroxide: pH-dependent formation of oxidants in the Fenton reaction. *Environ. Sci. Technol.* **2003,** *37* (12), 2734-2742.

31. Bataineh, H.; Pestovsky, O.; Bakac, A., pH-induced mechanistic changeover from hydroxyl radicals to iron(IV) in the Fenton reaction. *Chem. Sci.* **2012,** *3* (5), 1594-1599.

32. Rosenfeldt, E. J.; Linden, K. G.; Canonica, S.; von Gunten, U., Comparison of the efficiency of $^{\bullet}OH$ radical formation during ozonation and the advanced oxidation processes O_3/H_2O_2 and UV/H_2O_2. *Water Res.* **2006,** *40* (20), 3695-3704.

33. Koppenol, W. H.; Liebman, J. F., The oxidizing nature of the hydroxyl radical - a comparison with the ferryl ion (FeO^{2+}). *J. Phys. Chem.* **1984,** *88* (1), 99-101.

34. Miller, C. J.; Rose, A. L.; Waite, T. D., Hydroxyl radical production by H_2O_2-mediated oxidation of Fe(II) complexed by suwannee river fulvic acid under circumneutral freshwater conditions. *Environ. Sci. Technol.* **2013,** *47* (2), 829-835.

35. von Gunten, U., Ozonation of drinking water: Part II. Disinfection and by-product formation in presence of bromide, iodide or chlorine. *Water Res.* **2003,** *37* (7), 1469-1487.

36. Huie, R. E.; Clifton, C. L., Temperature dependence of the rate constants for reactions of the sulfate radical, SO4-, with anions. *J. Phys. Chem.* **1990,** *94* (23), 8561-8567.

37. Fang, G. D.; Dionysiou, D. D.; Wang, Y.; Al-Abed, S. R.; Zhou, D. M., Sulfate radical-based degradation of polychlorinated biphenyls: Effects of chloride ion and reaction kinetics. *J. Hazard. Mater.* **2012,** *227-228*, 394-401.

38. Grebel, J. E.; Pignatello, J. J.; Mitch, W. A., Effect of halide ions and carbonates on organic contaminant degradation by hydroxyl radical-based advanced oxidation processes in saline waters. *Environ. Sci. Technol.* **2010,** *44* (17), 6822-6828.

39. King, D. W.; Farlow, R., Role of carbonate speciation on the oxidation of Fe(II) by H_2O_2. *Mar. Chem.* **2000,** *70* (1-3), 201-209.

40. Buxton, G. V.; Greenstock, C. L.; Helman, W. P.; Ross, A. B., Critical review of rate constants for reactions of hydrated electrons, hydrogen atoms and hydroxyl radicals ($^{\bullet}OH/^{\bullet}O^{-}$) in aqueous solution. *J. Phys. Chem. Ref. Data* **1988,** *17* (2), 513-886.

41. Lutze, H. V.; Bircher, S.; Rapp, I.; Kerlin, N.; Bakkour, R.; Geisler, M.; Von Sonntag, C.; Schmidt, T. C., Degradation of chlorotriazine pesticides by sulfate radicals and the influence of organic matter. *Environ. Sci. Technol.* **2015,** *49* (3), 1673-1680.

42. Dao, Y. H.; De Laat, J., Hydroxyl radical involvement in the decomposition of hydrogen peroxide by ferrous and ferric-nitrilotriacetate complexes at neutral pH. *Water Res.* **2011,** *45* (11), 3309-3317.

Chapter 6 -

FORMATION OF AN AQUATED FERRYL SPECIES IN THE REACTION OF Fe^{II} WITH O_3?

6.1 ABSTRACT

Tetra-valent iron has been published to be generated in the reaction of divalent iron (Fe^{II}) with ozone (O_3) and frequently discussed as reactive species generated in the Fenton reaction at certain conditions. However, also $^{\bullet}OH$ are discussed as such and even if the Fenton reaction is known for more than a century, the Fenton mechanism is not yet entirely understood. An approach to resolve the identity of the reactive Fenton intermediate would be to compare reactivity data obtained from Fenton degradation of electron-rich substrates with reactivity data of the latter when treated with a combination of Fe^{II} and O_3.

Absorbance at 320 nm was followed spectrophotometrically during the reaction of Fe^{II} and O_3 at pH 3. At a constant Fe^{II}-concentration different O_3-concentrations were applied in order to cover different scenarios: Fe^{II} in excess over O_3, O_3 in excess over Fe^{II}, and equal concentrations of both. As reference also absorbance of Fe^{III} and O_3 was recorded at the same wavelength.

Regardless of the applied O_3-concentration, absorbance detected during the reaction of Fe^{II} and O_3 first increases but plateaus in the following and finally stagnates at a constant value. Thereby, finally reached absorbance increases with increasing O_3-concentration from 0.05 AU to 0.38 AU. Compared to constant absorbance of 0.38 AU detected for the combination of Fe^{III} and O_3, these results do not show any evidence for the formation of an aquated ferryl species in the reaction of Fe^{II} and O_3. Instead, results indicate direct formation of Fe^{III}. However, it cannot be unambiguously ruled out that Fe^{IV} is too reactive and thus, too unstable to be detected at investigated reaction conditions with the applied method as Fe^{III} is also described to be the product of consecutive reaction of Fe^{IV} with Fe^{II} or of its decay in water.

However, in summary obtained results let formation of aquated ferryl species either in Fenton chemistry or in the reaction of Fe^{II} and O_3 seem doubtful.

6.2 INTRODUCTION

Aqueous Fe^{IV} is the simplest and one of the most reactive high-valent iron-oxo-species and has a lifetime of a few seconds at ambient temperature in acidic aqueous solutions.[1] Even though formation of aqueous Fe^{IV} was described to occur in the reaction of Fe^{II} with ozone (O_3) in the early 1990s[2] (reaction 6.1) and already was suggested as reactive intermediate in the Fenton reaction even earlier (reaction 6.2),[3] no decisive spectroscopic data were available until 2005 when Pestovsky, *et al.* (2005)[4] succeeded in the spectroscopic identification of $[(H_2O)_5Fe^{IV}=O]^{2+}$. Furthermore, they characterised Fe^{IV} chemically as well as theoretically, derived criteria to distinguish between $^{\bullet}OH$ and aqueous iron-oxo-species.[4]

$$Fe^{II} + O_3 \rightarrow FeO^{2+} + O_2 \qquad (6.1)$$

$$Fe^{II} + H_2O_2 \rightarrow FeO^{2+} + H_2O \qquad (6.2)$$

Since Fenton's discovery that organic matter can effectively be oxidised by ferrous iron (Fe^{II}) in the presence of hydrogen peroxide (H_2O_2) in acidic aqueous solutions, the oxidising capacity of iron was frequently discussed. Up to now there is a still ongoing controversial discussion about which reactive species is best suitable to explain all phenomena observed in Fenton chemistry. Many researchers tried to find indications for one of the two mechanisms to be true and unambiguously rule out the other.[4-10] In contrast, more recent publications come to the conclusion that there might be a mechanistic changeover in the Fenton reaction depending on reaction conditions (e.g., pH).[11-14] They based their conclusion on reaction products of e.g.dimethyl sulfoxide (DMSO), which are unlikely generated by $^{\bullet}OH$-induced reactions. This observation can be explained by means of a mechanism involving formation of an intermediate iron-peroxo-complex (reaction 1.18), which is supposed to react via a one-electron transfer

reaction yielding Fe^{III} and $^{\bullet}OH$ in acidic media (reaction 1.19). At neutral to alkaline pH the intermediate is supposed to yield Fe^{IV} via a two-electron transfer (reaction 1.20).[15]

The Fenton mechanism might further be resolved in detail by means of a kinetic approach, i.e. comparison of reactivity data obtained for the reaction of a probe compound with the oxidant generated in the Fenton reaction or Fe^{IV} generated via the reaction of Fe^{II} with O_3. In case of equal reactivity data regardless of whether Fe^{II} and H_2O_2 or Fe^{II} and O_3 were initially applied, this would be a kinetic indication for Fe^{IV} as the active oxidant in Fenton chemistry. Therefore, the present study intends to first generate Fe^{IV} via the reaction of Fe^{II} with O_3.

6.3 MATERIALS AND METHODS

6.3.1 CHEMICALS

Ammonium iron(II) sulfate hexahydrate ($(NH_4)_2Fe(SO_4)_2 \times 6\ H_2O$) (99%) (Sigma Aldrich, Germany) and ammonium iron(III) sulfate dodecahydrate ($(NH_4)Fe(SO_4)_2 \times 12\ H_2O$) (≥ 98.5%) (Carl Roth, Germany) were used as received without further purification. Solutions of $(NH_4)_2Fe(SO_4)_2 \times 6\ H_2O$ were prepared by dissolution of an appropriate amount in ultrapure water (PURELAB ultra, ELGA, Germany). Sulfuric acid (H_2SO_4) (> 95%) (Fischer Chemicals, Switzerland), perchloric acid ($HClO_4$) (70%, p.a.) (AppliChem, Germany) and sodium hydroxide solution (NaOH) (1 M) (Bernd Kraft, Germany) were used to adjust the pH to 3.

Ozone stock solutions were prepared by generating gaseous ozone by means of an oxygen-fed ozone generator BMT 802X (MBT Messtechnik, Germany). Gaseous ozone was passed through ice-cooled ultrapure water, as solubility of ozone increases with decreasing temperature. Concentrations of ozone stock solutions were measured spectrophotometrically at λ = 258 nm using a molar absorption coefficient (ε_{258}) of 2950 $M^{-1}\ cm^{-1}$.

6.3.2 EXPERIMENTAL SETUP

Formation of Fe^{IV} was followed spectrophotometrically by means of a spectrophotometer (UV-1650PC UV-Visible Spectrom, Shimadzu, Germany) or a stopped-flow system (SFM-20, Biologic, France) equipped with a diode array detector (TIDAS S 300K, j & m Analytics AG, Germany) enabling investigation of fast kinetics.

Samples measured at the spectrophotometer were prepared directly within the cuvette, which has a total volume of 3 mL (d = 1 cm). An appropriate volume of the O_3 stock solution was added to Fe^{II} or Fe^{III} solution and carefully mixed by inverting the cuvette a few times. For two minutes absorbance at 320 nm was recorded every second. This wavelength was chosen as it was described to be suitable to observe formation of Fe^{IV}.[2] Additionally spectra of Fe^{III} in H_2SO_4 or $HClO_4$ were recorded ranging from 190 to 500 nm.

The stopped-flow system worked with two 10-mL syringes, one of them containing ozone solution and the other a solution of Fe^{II} or Fe^{III}. Simultaneously 100 µL per syringe were injected for each measurement applying a total flow rate of 7.0 mL min^{-1} (3.5 mL min^{-1} per syringe). After injection both solutions were rapidly mixed in a mixing chamber before they reached the measurement cell – a 10-µL quartz cuvette (1 × 1 × 10 mm). This led to a dead time of 6.4 ms. 2-Dimensional spectroscopic data were recorded every millisecond for 2.5 s. Due to turbulent flow within the cuvette recorded data of the first 11 ms had to be skipped.

A schematic figure of the stopped-flow setup can be found elsewhere.[16]

6.3.3 EXPERIMENTAL CONDITIONS

Experiments using the spectrophotometer were performed using an iron concentration of 300 µM in the cuvette. Three different ozone concentrations – 30 µM, 300 µM, and 900 µM – were used.

Stopped-flow experiments were conducted applying a total iron concentration of 250 µM in the cuvette of the stopped-flow system. Three different ozone concentrations – 25 µM, 250 µM, and 750 µM – were used. Spectra ranging from 190 – 700 nm were recorded; absorbance detected at 320 nm was used to follow formation of Fe^{IV}.

6.4 RESULTS AND DISCUSSION

Experiments were conducted in analogy to Løgager, *et al.* (1992)[2]. Absorbance developing within 120 s during the reaction of Fe^{II} and ozone was investigated at λ = 320 nm (Figure 6.1). Different ozone concentrations were applied in order to cover different scenarios: iron in excess over ozone, ozone in excess over iron, and equal concentrations of both. The dashed line represents absorbance of equal concentrations of Fe^{III} and ozone. This measurement was conducted in order to deduce whether absorbance observed is really caused by Fe^{IV} or possibly by Fe^{III}.

It can be derived from the figure that regardless of the applied ozone concentration absorbance recorded at 320 nm remains almost constant over the entire reaction time but increases with increasing ozone concentration. In parallel, no difference can be observed between absorbance caused by the combination of Fe^{II} and a surplus of ozone and that one caused by Fe^{III} and O_3. It was expected to observe a fast build-up step followed by a slow decay of the compound being responsible for detected absorbance in analogy to results described earlier by Løgager, *et al.* (1992)[2]. However, the fast build-up was described to occur during the first milliseconds of the reaction, a time which could not be monitored by means of the applied equipment. Hence, experiments were repeated using a stopped-flow system suitable to follow fast kinetics.

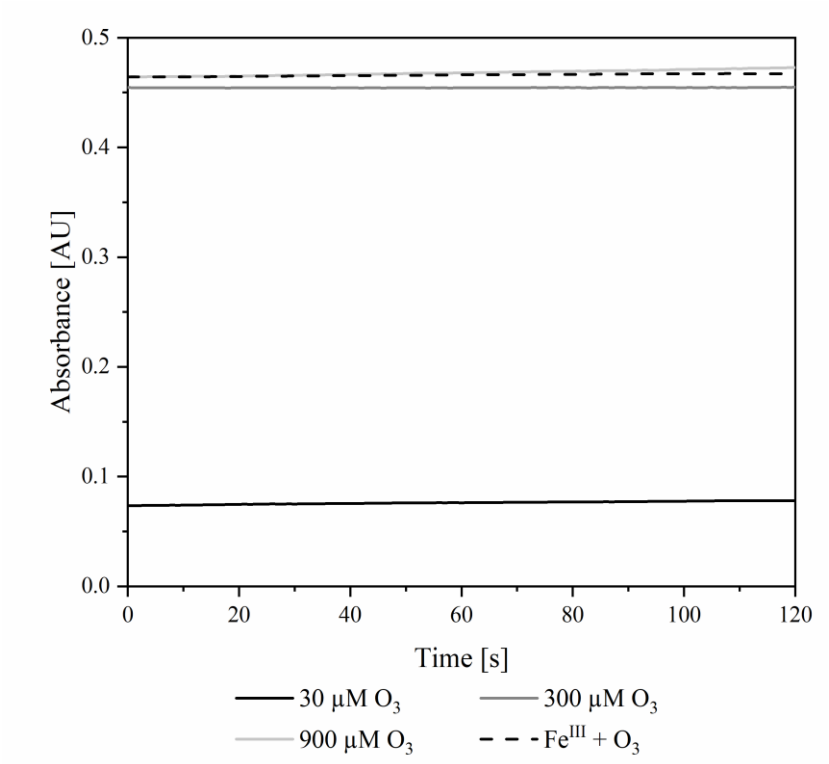

Figure 6.1: Absorbance detected within 120 s at 320 nm during the reaction of 300 µM ferrous iron and various concentrations of ozone. The dashed line illustrates absorbance of 300 µM ferric iron and ozone.

As shown in Figure 6.2, absorbance first increases but plateaus in the following and finally stagnates at a constant value in the first 2.5 seconds of reaction regardless of the applied O_3 concentration. Nevertheless, with increasing O_3 concentration finally reached absorbance increases from about 0.05 AU (25 µM O_3) to 0.38 AU (750 µM). Even in that shorter timeframe absorbance detected for the reaction of Fe^{III} and O_3 does not considerably change but remains constant at a level of 0.38 AU, thus indicating that no reaction takes place.

Comparison of absorbance developing during the reaction of Fe^{II} with 750 µM O_3 with absorbance recorded for the combination of Fe^{III} and O_3 led to the assumption that Fe^{III} is the product of the reaction of Fe^{II} and O_3 as there is no difference in finally reached absorbance. Lower absorbance, which was detected in presence of 25 µM or 250 µM O_3, indicates that these O_3 concentrations are not sufficient to fully oxidise provided Fe^{II}. Considering reaction

equations provided in literature for ozone induced oxidation of Fe^{II} a stoichiometry of 1:1 can be assumed. Hence, 250 µM O_3 should be sufficient to fully oxidise 250 µM Fe^{II}. However, loss of O_3 must be taken into account during transfer of the O_3 stock solution until the final measurement so that obtained results are reasonable.

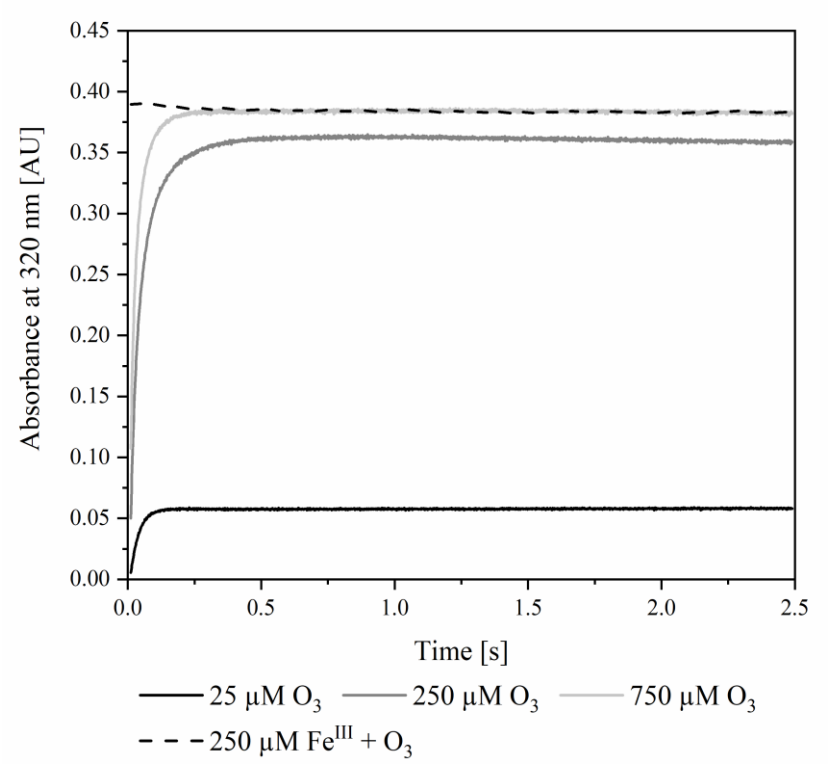

Figure 6.2: Absorbance detected within 2.5 s at 320 nm during the reaction of 250 µM ferrous iron and various concentrations of ozone. The dashed line illustrates absorbance of 250 µM ferric iron and ozone.

Without presenting a spectrum of pure Fe^{III} or the combination of Fe^{III} and O_3, Løgager, *et al.* (1992)[2] ascribed absorbance measured at 320 nm to formation of Fe^{IV}. Their explanation was based on absorbance spectra obtained from computer modelling for FeO^{2+}, Fe^{3+}, O_3, and H_2O_2 in 1 M $HClO_4$. According to these modelled spectra FeO^{2+} is the only compound showing absorbance at 320 nm.[2] However, this explanation is doubtful and could not be confirmed by experiments presented here. Instead, Fe^{III} was found to show strong absorbance at the wavelength of interest. Indeed, the fact that equal absorbances are detected for ozone with Fe^{II}

or Fe^{III}, respectively, does not unambiguously rule out formation of Fe^{IV} in the reaction of Fe^{II} and O_3 as absorbance of Fe^{IV} might also by overlaid by absorbance of Fe^{III}. Furthermore, it might be possible that differences in obtained Fe^{III} spectra might be ascribed to the matrix composition. Whereas spectra derived by computer modelling by Løgager, *et al.* (1992)[2] considered 1 M $HClO_4$ as matrix, recent measurements were conducted in ultrapure water acidified with H_2SO_4. In order to exclude the influence of the used acid on Fe^{III} absorbance, additionally, a spectrum of 300 µM Fe^{III} solution acidified with $HClO_4$ was recorded (Figure 6.3).

It can be derived from Figure 6.3 that there is no considerable difference in the Fe^{III} absorption spectra regardless of the acid used to adjust the sample pH to pH = 3.

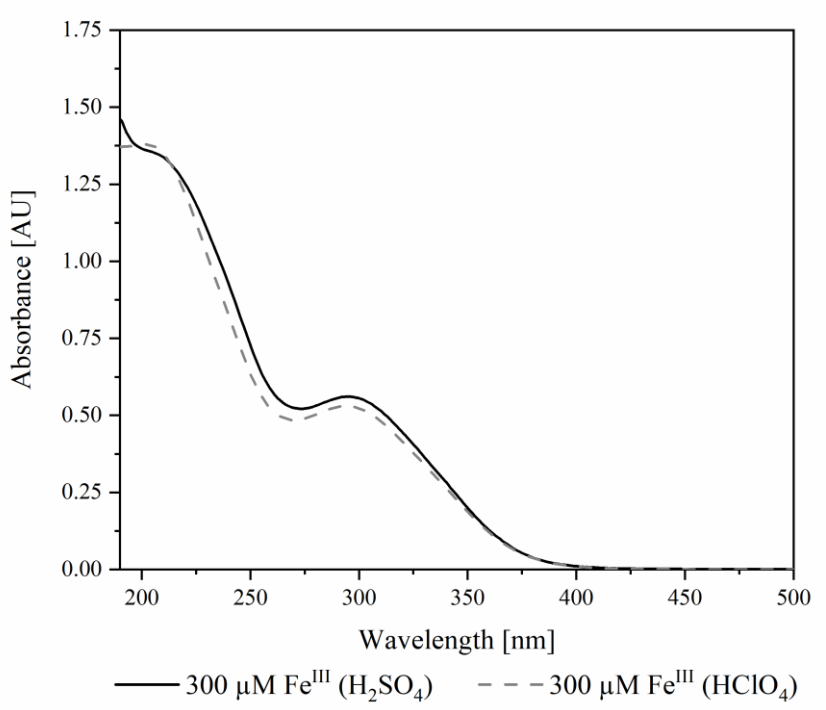

Figure 6.3: Fe^{III}-absorbance spectra in ultrapure water acidified with H_2SO_4 (black) or $HClO_4$ (grey) to pH = 3.

Beside the fast build-up of a compound causing absorbance at 320 nm at the beginning, Løgager, *et al.* (1992)[2] observed a slow decay of the same. They ascribed this effect to

consecutive reactions of Fe^{IV} with Fe^{II} (reaction 3.5) or its decay in water (reaction 3.4), respectively, depending on whether Fe^{II} or O_3 was dosed in excess. They could not obtain any evidence for reactions of FeO^{2+} with O_3 or with itself.

In contrast, recent results did not show any decay over the entire timeframe observed. This confirms the above made assumption that Fe^{III} is directly generated during the reaction of Fe^{II} and O_3 at recent reaction conditions. Based on our experiments, results presented by Løgager, *et al.* (1992)[2] cannot be understood. Indeed, considering consecutive reactions of Fe^{IV} with Fe^{II} or its decay in water, decreasing absorbance of Fe^{IV} seems reasonable. However, this interpretation is based on a modelled Fe^{III} spectrum showing no absorbance at 320 nm, which could not be confirmed experimentally.

In summary, presented results did not show any indication for the formation of an aquated ferryl species as product of the reaction between Fe^{II} and O_3, neither in H_2SO_4 nor in $HClO_4$ media. Hence, further aspects of the study, i.e. the reactivity of Fe^{IV} with electron-rich substrates compared to the reactivity of the latter with the reactive species generated during the Fenton reaction in order to obtain further information about the identity of the Fenton-oxidant could not be assessed.

Possibly, certain ligands could be used in order to complex iron and thus, stabilise Fe^{IV} either in Fenton chemistry or when generated from Fe^{II} and O_3. In the last two decades, tetra-valent iron was found to be stable as low-molecular-weight ferryl-complexes and in non-heme iron-enzymes.[17-19] Ligands described in this regard have in common that complexation occurs via N-atoms. Thereby it was reported that at ambient temperatures lifetime of such complexes increases with increasing denticity of the respective ligand.[18-19] Even those complexes are described to be highly reactive[1] thus, it seems reasonable to assume that if it is really generated, Fe^{IV} might be too reactive to be detected using the experimental setup described above.

In that case, at least when O_3 is applied in excess over Fe^{II}, quantification of $^{\bullet}OH$ would be useful to further elucidate whether Fe^{IV} is generated. As mentioned in reaction 3.4, FeO^{2+} decays in water when O_3 is dosed overstoichiometrically leading to formation of Fe^{III}, OH^-, and $^{\bullet}OH$. The latter can be trapped by a selective $^{\bullet}OH$-scavenger like e.g. dimethyl sulfoxide and resulting reaction products can then be used for quantification. When Fe^{II} is used in excess this approach will not be successful as reaction 6 does not yield any $^{\bullet}OH$.

6.5 REFERENCES

1. Pestovsky, O.; Bakac, A., Reactivity of aqueous Fe(IV) in hydride and hydrogen atom transfer reactions. *J. Am. Chem. Soc.* **2004,** *126* (42), 13757-13764.

2. Løgager, T.; Holcman, J.; Sehested, K.; Pedersen, T., Oxidation of ferrous ions by ozone in acidic solutions. *Inorg. Chem.* **1992,** *31* (17), 3523-3529.

3. Bray, W. C.; Gorin, M. H., Ferryl ion, a compound of tetravalent iron. *J. Am. Chem. Soc.* **1932,** *54*, 2124-2125.

4. Pestovsky, O.; Stoian, S.; Bominaar, E. L.; Shan, X.; Münck, E.; Que Jr, L.; Bakac, A., Aqueous FeIV=O: Spectroscopic identification and oxo-group exchange. *Angewandte Chemie - International Edition* **2005,** *44* (42), 6871-6874.

5. Kremer, M. L., Mechanism of the Fenton reaction. Evidence for a new intermediate. *Phys. Chem. Chem. Phys.* **1999,** *1* (15), 3595-3605.

6. Kremer, M. L., Is $^{\bullet}OH$ the active Fenton intermediate in the oxidation of ethanol? *J. Inorg. Biochem.* **2000,** *78* (3), 255-257.

7. Goldstein, S.; Meyerstein, D., Comments on the mechanism of the "Fenton like" reaction. *Acc. Chem. Res.* **1999,** *32* (7), 547-550.

8. Bossmann, S. H.; Oliveros, E.; Göb, S.; Siegwart, S.; Dahlen, E. P.; Payawan Jr, L.; Straub, M.; Wörner, M.; Braun, A. M., New evidence against hydroxyl radicals as reactive intermediates in the thermal and photochemically enhanced Fenton reactions. *J. Phys. Chem. A* **1998,** *102* (28), 5542-5550.

9. Walling, C., Intermediates in the reactions of Fenton type reagents. *Acc. Chem. Res.* **1998,** *31* (4), 155-157.

10. Walling, C., Fentons reagent revisited. *Acc. Chem. Res.* **1975,** *8* (4), 125-131.

11. Hug, S. J.; Leupin, O., Iron-catalyzed oxidation of arsenic(III) by oxygen and by hydrogen peroxide: pH-dependent formation of oxidants in the Fenton reaction. *Environ. Sci. Technol.* **2003,** *37* (12), 2734-2742.

12. Katsoyiannis, I. A.; Ruettimann, T.; Hug, S. J., pH dependence of Fenton reagent generation and As(III) oxidation and removal by corrosion of zero valent iron in aerated water. *Environ. Sci. Technol.* **2008,** *42* (19), 7424-7430.

13. Bataineh, H.; Pestovsky, O.; Bakac, A., pH-induced mechanistic changeover from hydroxyl radicals to iron(IV) in the Fenton reaction. *Chem. Sci.* **2012,** *3* (5), 1594-1599.

14. Lee, H.; Lee, H. J.; Sedlak, D. L.; Lee, C., pH-Dependent reactivity of oxidants formed by iron and copper-catalyzed decomposition of hydrogen peroxide. *Chemosphere* **2013,** *92* (6), 652-658.

15. von Sonntag, C., Advanced oxidation processes: Mechanistic aspects. *Water Sci. Technol.* **2008,** *58* (5), 1015-1021.

16. Wiegand, H. L.; Orths, C. T.; Kerpen, K.; Lutze, H. V.; Schmidt, T. C., Investigation of the iron-peroxo-complex in the Fenton reaction: Kinetic indication, decay kinetics and hydroxyl radical yields. *Environ. Sci. Technol.* **2017,** *51* (24), 14321-14329.

17. Comba, P.; Kerscher, M.; Krause, T.; Schöler, H. F., Iron-catalysed oxidation and halogenation of organic matter in nature. *Environmental Chemistry* **2015,** *12* (4), 381-395.

18. Kaizer, J.; Klinker, E. J.; Oh, N. Y.; Rohde, J. U.; Song, W. J.; Stubna, A.; Kim, J.; Münck, E.; Nam, W.; Que Jr, L., Nonheme $Fe^{IV}O$ Complexes That Can Oxidize the C-H Bonds of Cyclohexane at Room Temperature. *J. Am. Chem. Soc.* **2004,** *126* (2), 472-473.

19. Rohde, J. U.; In, J. H.; Lim, M. H.; Brennessel, W. W.; Bukowski, M. R.; Stubna, A.; Münck, E.; Nam, W.; Que Jr, L., Crystallographic and spectroscopic characterization of a Nonheme Fe(IV)=O complex. *Science* **2003,** *299* (5609), 1037-1039.

Chapter 7 -

GENERAL CONCLUSION AND OUTLOOK

7.1 GENERAL CONCLUSION

Even though the Fenton reaction is already known for more than a century, mechanistic aspects, especially the identity of the involved reactive species, could not unambiguously be elucidated yet. Thus, this thesis focussed on the investigation of the Fenton mechanism and the characterisation of the active oxidant generated during the reaction of ferrous iron (Fe^{II}) with hydrogen peroxide (H_2O_2) at certain reaction conditions.

This thesis provides the first kinetic indication for the formation of an intermediate iron-peroxo-complex ($Fe(H_2O_2)^{2+}$) in the Fenton reaction at pH 1 to 4. The formation of this intermediate was widely accepted in the past, even though experimental evidence for its existence was missing.[1] Presented results confirmed that the reaction between Fe^{II} and H_2O_2 occurs via an inner sphere electron transfer[2] by exchanging one of the coordinated water molecules by H_2O_2 as an outer sphere electron transfer would require the formation of $H_2O_2^{-\bullet}$ as transient radical ion,[3] which could not be observed. Furthermore, quantification of hydroxyl radicals ($^{\bullet}OH$) revealed that the decay of the intermediate complex exclusively yields $^{\bullet}OH$ at pH 1 – 4, which was also found by Bataineh, *et al.* (2012)[4]. Second order reaction rate constants for the Fenton reaction were determined in the same range as already published ones.[5-7] Experiments conducted in presence of organic chelating ligands (DTPA, EDTA, HEDTA, and NTA) revealed that the mechanism of the Fenton reaction remains unaffected by these ligands. Indeed, primary reactions of the Fenton mechanism were shown to be strongly accelerated with increasing pH (from 2 to 6), but the decay of the intermediate $Fe(H_2O_2)^{2+}$-complex again yields $^{\bullet}OH$ as final oxidant regardless of applied conditions. Especially in ligand-assisted Fenton reactions the type of oxidant is a subject of strong debate and strongly depends on experimental conditions.[8-20]

This thesis comprises the first study dealing with the Fenton-based degradation of bisphenol S (BPS). BPS is a compound of interest as it is increasingly used as substitute of bisphenol A, a compound, which is known to exhibit adverse health effects and thus, was proposed to be banned from 2020.[21] Hitherto, studies dealing with oxidative treatment of BPS are scarce. In the present study BPS was shown to be efficiently degraded by means of Fenton chemistry at various conditions in ultrapure water. Degradation efficiency strongly depended on reaction conditions. Whereas increasing iron concentrations resulted in accelerated degradation of BPS within the investigated concentration range, BPS degradation slowed down when very high concentrations of H_2O_2 were applied due to $^{\bullet}OH$-scavenging by H_2O_2. However, even $^{\bullet}OH$-scavenging by Fe^{II} must be considered in case of very high Fe^{II}-concentrations. Additionally, the applicable Fe^{II}-concentration is restricted by the limited solubility of Fe^{III}, which is generated in the Fenton reaction. Precipitation of Fe^{III} would terminate Fenton-based contaminant degradation due to insufficient Fe^{II}-recycling.[2] Furthermore, the pH strongly affected degradation efficiency. The optimum pH was shown to be around pH 3 as it is frequently described in literature.[2] Hitherto, it was widely accepted that efficient Fenton-based degradation of contaminants is restricted to acidic pH due to limited solubility of Fe^{III} at pH > 3. In contrast, in this thesis it was shown that BPS can successfully be degraded at neutral pH. Indeed, degradation of BPS was decelerated at pH 7 compared to pH 3. However, complete degradation could be achieved within common hydraulic residence times of oxidative water treatment steps, which can be up to 30 minutes. Hitherto, a mechanistic changeover was described to occur in the Fenton process when the pH is increased from acidic to neutral or alkaline leading to formation of $^{\bullet}OH$ at acidic and generation of Fe^{IV} at neutral to alkaline pH.[4, 22-24] Comparison of degradation behaviour of BPS and *para*-chlorobenzoic acid (*p*CBA), a compound, which is supposed to be non-degradable by Fe^{IV},[25-26] during Fenton treatment in presence of tertiary butanol (*t*-BuOH) revealed no indication for formation of Fe^{IV}, neither at

pH 3 nor at pH 7, but instead indicated that •OH are exclusively responsible for observed degradation. Hence, it is reasonable that degradation efficiency is decreased by presence of •OH-scavenging matrix components (*t*-BuOH). In a more complex matrix containing e.g. natural organic matter and/or chloride, also complexation of Fe and formation of secondary oxidants must be considered as both influence degradation efficiency of contaminants.

Overall, results presented in chapters 3 to 5 could not reveal any indication for the formation of Fe^{IV} in Fenton chemistry. Additionally, even in the reaction of Fe^{II} with O_3, which was described in literature to yield aquated Fe^{IV} with a lifetime of several seconds,[27-28] no indication for the formation of Fe^{IV} was found. However, available literature reporting Fe^{IV}-formation in this context seems doubtful as basic interpretation of results was based on computer modelling of Fe^{III}-absorbance, which could not be confirmed experimentally in this thesis. Hitherto, reliable literature published evidence for formation of Fe^{IV} only in presence of special ligands, which are required to stabilise iron in that high oxidation state. These include formation of Fe^{IV}-ligand-complexes in Fenton chemistry as well as in other reactions.[29-31]

7.2 OUTLOOK

The knowledge gained on mechanistic aspects of Fenton chemistry in this thesis could be used to integrate the Fenton process in the treatment process of industrial wastewaters or the remediation of contaminated sites and optimise respective treatment conditions. Fenton chemistry reveals a large potential in this regard as compared to other treatment options it has a low energy demand and required chemicals are comparably cheap, easy to store and non-threatening to the environment. Furthermore, degradation efficiency of Fenton processes

reveals potential to be simply enhanced by modification like, e.g. applied in photo-, sono-, or electro-Fenton reactions.[32-39]

Kinetic indication for the formation of the hitherto postulated intermediate iron-peroxo-complex is important with respect to kinetic modelling. The more reactions are known and can be taken as a basis of the model, the more precise kinetic modelling becomes. In order to determine optimal conditions enabling high treatment efficiencies coincidently with low cost when applying a certain AOP for the treatment of a specific wastewater kinetic modelling has to be performed.[40-42]

In order to further investigate mechanistic aspects of Fenton chemistry, further research is required with respect to the influence of matrix components on contaminant degradation as it was on the one hand shown that degradation efficiency is considerably reduced in presence of $^{\bullet}OH$-scavenging matrix components. On the other hand, previous literature suggests an influence of iron-complexing matrix on the finally generated oxidant. Independent of the type of reactive species the presence of ligands enhances the Fenton process. At first, ligands are known to accelerate the reaction of Fe^{II} with H_2O_2 leading to an active oxidant. Secondly, generated Fe^{III} can be kept dissolved due to complex formation and hence, enable Fenton-based treatment of wastewater even at neutral or alkaline pH.

Additionally, further evaluation of factors leading to formation of Fe^{IV} as reactive species in Fenton reactions are required. In this regard research should focus on the influence of nitrogen-based ligands as these are described to stabilise Fe^{IV}.[29-31, 43] Formation of Fe^{IV} can on the one hand be unfavourable as it is considerably more selective compared to $^{\bullet}OH$ and thus, lowers degradation efficiency. Hence, in cases a wastewater reveals such conditions leading to formation of Fe^{IV} another AOP could be considered in order to enhance degradation. On the other hand, in cases where the Fenton reaction occurs unintentionally, e.g., in fuel cells where

•OH can attack and finally degrade membranes inside the fuel cells, formation of Fe^{IV} can be advantageous in order to avoid undesired reactions.[44]

With respect to formation of Fe^{IV} in the reaction of Fe^{II} with O_3 besides the spectroscopic approach to identify Fe^{IV} via absorbance at a certain wavelength also consecutive reactions of Fe^{IV} can be used for indirect identification. On the one hand, e.g., dimethyl sulfoxide (DMSO) is supposed to form dimethyl sulfone ($DMSO_2$) when reacting with Fe^{IV} in contrast to methanesulfinic acid (MSIA) and methanesulfonic acid (MSOA), which are generated from DMSO in •OH-based reactions.[4] On the other hand, as described in chapter 6, when a surplus of O_3 is applied FeO^{2+} decays in water and yields Fe^{III}, OH^-, and •OH, i.e. the same products described as products in the classical Fenton reaction formulated by Barb, *et al.* (1951)[45, 1951)[46]. However, detection of •OH in the reaction of Fe^{II} with a surplus of O_3 in absence of matrix components leading to •OH-formation when reacting with O_3, would indirectly indicate formation of Fe^{IV}.

Further insight in mechanistic aspects, i.e. the identity of the generated reactive species of the Fenton reaction, might also be achieved by evaluation of transformation products of different contaminants as degradation pathways strongly depend on the involved oxidant.

For an effective and efficient on-site application of the Fenton reaction in terms of wastewater treatment or remediation of contaminated sites, effects of matrix components other than organic •OH-scavengers or complexing agents must be investigated. Especially the influence of bicarbonate (HCO_3^-) should be addressed. In presence of HCO_3^- Fe^{II}-autoxidation if drastically accelerated and thus, outcompetes the reaction of Fe^{II} with H_2O_2. A better understanding of these processes would enable more efficient Fenton remediation.

7.3 REFERENCES

1. von Sonntag, C., Advanced oxidation processes: Mechanistic aspects. *Water Sci. Technol.* **2008,** *58* (5), 1015-1021.

2. Pignatello, J. J.; Oliveros, E.; MacKay, A., Advanced oxidation processes for organic contaminant destruction based on the Fenton reaction and related chemistry. *Crit. Rev. Environ. Sci. Technol.* **2006,** *36* (1), 1-84.

3. Goldstein, S.; Meyerstein, D.; Czapski, G., The Fenton reagents. *Free Radical Biol. Med.* **1993,** *15* (4), 435-445.

4. Bataineh, H.; Pestovsky, O.; Bakac, A., pH-induced mechanistic changeover from hydroxyl radicals to iron(IV) in the Fenton reaction. *Chem. Sci.* **2012,** *3* (5), 1594-1599.

5. Rigg, T.; Taylor, W.; Weiss, J., The rate constant of the reaction between hydrogen peroxide and ferrous ions. *J. Chem. Phys.* **1954,** *22* (4), 575-577.

6. Truong, G. L.; de Laat, J.; Legube, B., Effects of chloride and sulfate on the rate of oxidation of ferrous ion by H_2O_2. *Water Res.* **2004,** *38* (9), 2383-2393.

7. Wells, C. F.; Salam, M. A., Complex formation between iron(II) and inorganic anions. Part II. The effect of oxyanions on the reaction of iron(II) with hydrogen peroxide. *J. Chem. Soc. A* **1968**, 308-315.

8. Yamazaki, I.; Piette, L. H., EPR spin-trapping study on the oxidizing species fomed in reaction of the ferrous ion with hydrogen peroxide. *J. Am. Chem. Soc.* **1991,** *113* (20), 7588-7593.

9. Cohen, G.; Sinet, P. M., The Fenton reaction between ferrous-diethylenetriaminepentaacetic acid and hydrogen peroxide. *FEBS Lett.* **1982,** *138* (2), 258-260.

10. Graf, E.; Mahoney, J. R.; Bryant, R. G.; Eaton, J. W., Iron-catalyzed hydroxyl radical formation. Stringent requirement for free iron coordination site. *J. Biol. Chem.* **1984,** *259* (6), 3620-3624.

11. Sutton, H. C.; Winterbourn, C. C., Chelated iron-catalyzed $^{\bullet}OH$ formation from paraquat radicals and H_2O_2: Mechanism of formate oxidation. *Arch. Biochem. Biophys.* **1984,** *235* (1), 106-115.

12. Koppenol, W. H., The reaction of ferrous EDTA with hydrogen peroxide: Evidence against hydroxyl radical formation. *J. Free Radic. Biol. Med.* **1985,** *1* (4), 281-285.

13. Sutton, H. C., Efficiency of chelated iron compounds as catalysts for the Haber-Weiss reaction. *J. Free Radic. Biol. Med.* **1985,** *1* (3), 195-202.

14. Rush, J. D.; Koppenol, W. H., Oxidizing intermediates in the reaction of ferrous EDTA with hydrogen peroxide. Reactions with organic molecules and ferrocytochrome c. *J. Biol. Chem.* **1986,** *261* (15), 6730-6733.

15. Rahhal, S.; Richter, H. W., Reduction of hydrogen peroxide by the ferrous iron chelate of diethylenediamine-N,N,N',N'',N''-pentaacetate. *J. Am. Chem. Soc.* **1988,** *110* (10), 3126-3133.

16. Rahhal, S.; Richter, H. W., Reaction of hydrogen peroxide with low molecular weight iron complexes. *International Journal of Radiation Applications and Instrumentation. Part* **1988,** *32* (1), 129-135.

17. Rush, J. D.; Koppenol, W. H., Reactions of Fe^{II}NTA and Fe^{II}EDDA with hydrogen peroxide. *J. Am. Chem. Soc.* **1988,** *110* (15), 4957-4963.

18. Croft, S.; Gilbert, B. C.; Lindsay Smith, J. R.; Whitwood, A. C., An E.S.R. investigation of the reactive intermediate generated in the reaction between Fe^{II} and H_2O_2 in aqueous solution. Direct evidence for the formation of the hydroxyl radical. *Free Radical Res.* **1992,** *17* (1), 21-39.

19. Egan, T. J.; Barthakur, S. R.; Aisen, P., Catalysis of the Haber-Weiss reaction by iron-diethylenetriaminepentaacetate. *J. Inorg. Biochem.* **1992,** *48* (4), 241-249.

20. Šnyrychová, I.; Pospíšil, P.; Nauš, J., The effect of metal chelators on the production of hydroxyl radicals in thylakoids. *Photosynth. Res.* **2006,** *88* (3), 323-329.

21. Pivnenko, K.; Laner, D.; Astrup, T. F., Dynamics of bisphenol A (BPA) and bisphenol S (BPS) in the European paper cycle: Need for concern? *Resour. Conserv. Recycl.* **2018,** *133*, 278-287.

22. Hug, S. J.; Leupin, O., Iron-catalyzed oxidation of arsenic(III) by oxygen and by hydrogen peroxide: pH-dependent formation of oxidants in the Fenton reaction. *Environ. Sci. Technol.* **2003,** *37* (12), 2734-2742.

23. Katsoyiannis, I. A.; Ruettimann, T.; Hug, S. J., pH dependence of Fenton reagent generation and As(III) oxidation and removal by corrosion of zero valent iron in aerated water. *Environ. Sci. Technol.* **2008,** *42* (19), 7424-7430.

24. Lee, H.; Lee, H. J.; Sedlak, D. L.; Lee, C., pH-Dependent reactivity of oxidants formed by iron and copper-catalyzed decomposition of hydrogen peroxide. *Chemosphere* **2013,** *92* (6), 652-658.

25. Rosenfeldt, E. J.; Linden, K. G.; Canonica, S.; von Gunten, U., Comparison of the efficiency of •OH radical formation during ozonation and the advanced oxidation processes O_3/H_2O_2 and UV/H_2O_2. *Water Res.* **2006,** *40* (20), 3695-3704.

26. Koppenol, W. H.; Liebman, J. F., The oxidizing nature of the hydroxyl radical - a comparison with the ferryl ion (FeO^{2+}). *J. Phys. Chem.* **1984,** *88* (1), 99-101.

27. Løgager, T.; Holcman, J.; Sehested, K.; Pedersen, T., Oxidation of ferrous ions by ozone in acidic solutions. *Inorg. Chem.* **1992,** *31* (17), 3523-3529.

28. Pestovsky, O.; Bakac, A., Reactivity of aqueous Fe(IV) in hydride and hydrogen atom transfer reactions. *J. Am. Chem. Soc.* **2004,** *126* (42), 13757-13764.

29. Comba, P.; Kerscher, M.; Krause, T.; Schöler, H. F., Iron-catalysed oxidation and halogenation of organic matter in nature. *Environmental Chemistry* **2015,** *12* (4), 381-395.

30. Kaizer, J.; Klinker, E. J.; Oh, N. Y.; Rohde, J. U.; Song, W. J.; Stubna, A.; Kim, J.; Münck, E.; Nam, W.; Que Jr, L., Nonheme $Fe^{IV}O$ Complexes That Can Oxidize the C-H Bonds of Cyclohexane at Room Temperature. *J. Am. Chem. Soc.* **2004,** *126* (2), 472-473.

31. Rohde, J. U.; In, J. H.; Lim, M. H.; Brennessel, W. W.; Bukowski, M. R.; Stubna, A.; Münck, E.; Nam, W.; Que Jr, L., Crystallographic and spectroscopic characterization of a Nonheme Fe(IV)=O complex. *Science* **2003,** *299* (5609), 1037-1039.

32. Faust, B. C.; Hoigné, J., Photolysis of Fe (III)-hydroxy complexes as sources of OH radicals in clouds, fog and rain. *Atmospheric Environment Part A, General Topics* **1990,** *24* (1), 79-89.

33. Pignatello, J. J., Dark and photoassisted Fe^{3+}-catalyzed degradation of chlorophenoxy herbicides by hydrogen peroxide. *Environ. Sci. Technol.* **1992,** *26* (5), 944-951.

34. Neppolian, B.; Jung, H.; Choi, H.; Lee, J. H.; Kang, J. W., Sonolytic degradation of methyl tert-butyl ether: The role of coupled fenton process and persulphate ion. *Water Res.* **2002,** *36* (19), 4699-4708.

35. Liang, J.; Komarov, S.; Hayashi, N.; Kasai, E., Improvement in sonochemical degradation of 4-chlorophenol by combined use of Fenton-like reagents. *Ultrason. Sonochem.* **2007,** *14* (2), 201-207.

36. Adityosulindro, S.; Barthe, L.; González-Labrada, K.; Jáuregui Haza, U. J.; Delmas, H.; Julcour, C., Sonolysis and sono-Fenton oxidation for removal of ibuprofen in (waste)water. *Ultrason. Sonochem.* **2017,** *39*, 889-896.

37. Pratap, K.; Lemley, A. T., Electrochemical Peroxide Treatment of Aqueous Herbicide Solutions. *J. Agric. Food. Chem.* **1994,** *42* (1), 209-215.

38. Oturan, M. A.; Aaron, J. J.; Oturan, N.; Pinson, J., Degradation of chlorophenoxyacid herbicides in aqueous media, using a novel electrochemical method. *Pestic. Sci.* **1999,** *55* (5), 558-562.

39. Foller, P. C.; Bombard, R. T., Processes for the production of mixtures of caustic soda and hydrogen peroxide via the reduction of oxygen. *J. Appl. Electrochem.* **1995,** *25* (7), 613-627.

40. Scott, J. P.; Ollis, D. F., Integration of chemical and biological oxidation processes for water treatment: Review and recommendations. *Environ. Prog.* **1995,** *14* (2), 88-103.

41. Oller, I.; Malato, S.; Sánchez-Pérez, J. A., Combination of Advanced Oxidation Processes and biological treatments for wastewater decontamination-A review. *Sci. Total Environ.* **2011,** *409* (20), 4141-4166.

42. Balanosky, E.; Herrera, F.; Lopez, A.; Kiwi, J., Oxidative degradation of textile waste water. Modeling reactor performance. *Water Res.* **2000,** *34* (2), 582-596.

43. Bautz, J.; Bukowski, M. R.; Kerscher, M.; Stubna, A.; Comba, P.; Lienke, A.; Münck, E.; Que Jr, L., Formation of an aqueous oxoiron(IV) complex at pH 2-6 from a nonheme iron(II) complex and H_2O_2. *Angewandte Chemie - International Edition* **2006,** *45* (34), 5681-5684.

44. Zedda, M.; Tuerk, J.; Peil, S.; Schmidt, T. C., Determination of polymer electrolyte membrane (PEM) degradation products in fuel cell water using electrospray ionization tandem mass spectrometry. *Rapid Commun. Mass Spectrom.* **2010,** *24* (24), 3531-3538.

45. Barb, W. G.; Baxendale, J. H.; George, P.; Hargrave, K. R., Reactions of ferrous and ferric ions with hydrogen peroxide. Part I. - The ferrous ion reaction. *Trans. Faraday Soc.* **1951,** *47*, 462-500.

46. Barb, W. G.; Baxendale, J. H.; George, P.; Hargrave, K. R., Reactions of ferrous and ferric ions with hydrogen peroxide. Part II. - The ferric ion reaction. *Trans. Faraday Soc.* **1951,** *47*, 591-616.

Chapter 8 -

SUPPLEMENTS

8.1 LIST OF FIGURES

8.2 LIST OF TABLES

8.3 LIST OF ABBREVIATIONS

$(NH_4)_2Fe(SO_4)_2 \times 6\ H_2O$	ammonium iron(II) sulfate hexahydrate
$(NH_4)Fe(SO_4)_2 \times 12\ H_2O$	ammonium iron(III) sulfate dodecahydrate
$[Fe^{II}]_0$	initial ferrous iron concentration
$[Fe^{II}]_t$	ferrous iron concentration at a certain time (t)
$[Fe^{III}]_{max}$	maximum ferric iron concentration
$^{\bullet}CH_3$	methyl radical
$^{\bullet}OH$	hydroxyl radical
AOPs	advanced oxidation processes
BDE	bond dissociation energy
BP	bisphenol
BPA	bisphenol A, 4,4'-dimethylmethane diphenol
BPS	bisphenol S, 4,4'-sulfonyldiphenol
cf.	confer
CH_2O	formaldehyde
Cl^-	chloride
$Cl^{\bullet}$	chlorine atom
$Cl_2^{\bullet-}$	chlorine radical
DAD	diode array detector
DCTA	*trans*-1,2-diaminecyclohexanetetraacetic acid
DMPO	5,5-dimethyl-1-pyrrolidine-N-oxide
DMSO	dimethyl sulfoxide
$DMSO_2$	dimethylsulfone
DNA	deoxyribonucleic acid
DNPH	2,4-dinitrophenylhydrazine
DOC	dissolved organic carbon
DTPA	diethylenetriaminepentaacetic acid
e^-	electron
e.g.	for example
E^0	standard oxidation-reduction potential
EDTA	ethylenediaminetetraacetic acid
EPR	electron spin resonance

f(x + y)	fraction of x reacting with y
Fe^{0}	zerovalent iron
ZVI	zerovalent iron
Fe^{II}	ferrous iron
Fe^{III}	ferric iron
Fe^{IV}	tetravalent iron
FeO^{2+}	ferryl ion
$FeOOH^{+}$	iron-peroxo-complex
$Fe(H_2O_2)^{2+}$	iron-peroxo-complex
$Fe(H_2O)(H_2O_2)^{2+}$	iron-peroxo-complex
H	Planck constant
H^{+}	proton
H_2O_2	hydrogen peroxone
H_2SO_4	sulfuric acid
HCl	hydrochloric acid
HEDTA	hydroxyethylenediaminetriacetric acid
$HO_2^{\bullet}$	perhydroxyl radical
$HOCl^{\bullet-}$	hyperchlorous acid
$HOCl_4$	perchloric acid
HPLC	high performance liquid chromatography
i.e.	id est
IC	ion chromatography
K	reaction rate constant
K	equilibrium constant
k'	observed pseudo first order reaction rate
k_{2nd}	second order reaction rate constant
K_{sp}	solubility product
L	ligand
MeOH	methanol
MSIA	methane sulfinic acid
MSOA	methansulfonic acid
CH_4O_3S	methansulfonic acid
n.d.	not determined

Na_2CO_3	disodiumcarbonate
$NaCH_3O_2S$	sodium methanesulfinate
NaCl	sodium chloride
$NaHCO_3$	sodiumhydrogencarbonate
NaOH	sodium hydroxide
No.	number
NOM	natural organic matter
NTA	nitrilotriacetic acid
O_2	molecular oxygen
$O_2^{\bullet-}$	superoxide
O_3	ozone
$O_3^{\bullet-}$	ozonide radical anion
OH^-	hydroxide ion
OM	organic matter
*p*CBA	*para*-chlorobenzoic acid
pK_a	acid dissociation constant
SI	supporting information
SO_4^{2-}	sulfate
SR NOM	Suwannee river natural organic matter
SRFA	Suwannee river fulvic acid
t-BuOH	tertiary butanol
US	ultrasound
)))	ultrasound
UV	ultraviolet
WFD	water framework directive
ε	molar absorption coefficient
λ	wavelength
ν	Frequency

8.4 LIST OF PUBLICATIONS

8.4.1 ARTICLES PUBLISHED IN PEER-REVIEWED JOURNALS

Wiegand, H.L., Kerpen, K., Lutze, H.V., Schmidt, T.C., Response to Comment on „Investigation of the iron-peroxo-complex in the Fenton reaction: Kinetic indication, decay kinetics and hydroxyl radical yields". *Environ. Sci. Technol.* **2018,** DOI: 10.1021/acs.est.8b00982

Wiegand, H.L., Orths, C.T., Kerpen, K., Lutze, H.V., Schmidt, T.C., Investigation of the iron-peroxo-complex in the Fenton reaction: Kinetic indication, decay kinetics and hydroxyl radical yields. *Environ. Sci. Technol.* **2017,** 51 (24), 14321-14329, DOI: 10.1021/acs.est.7b03706

Zscheppank, C., **Wiegand, H.L.**, Lenzen, C., Wingender, J., Telgheder, U., Investigation of volatile metabolites during growth of Escherichia coli and Pseudomonas aeruginosa by needle trap-GC-MS, *Anal. Bioanal. Chem.*, **2014**, 406(26), 6617-6628, DOI 10.1007/s00216-014-8111-2

Wiegand, H.L., Hupperich, K., Lüling, M., Orths, C.T., Lutze, H.V., Schmidt, T.C., Influence of organic chelating agents on the Fenton reaction – Reaction kinetics and $^{\bullet}OH$-yields. Submitted for publication in *Chemosphere*.

Wiegand, H.L., Jütte,M., Hupperich, K., Kranefuß, A., Lutze, H.V., Schmidt, T.C., Investigation of Factors influencing Fenton-based degradation of Bisphenol S. Submitted for publication in *Chemical Engineering Journal*.

8.4.2 ORAL & POSTER PRESENTATIONS AT NATIONAL AND INTERNATIONAL CONFERENCES

Wiegand, H.L., Jütte, M., Hupperich, K., Kranefuß, A., Lutze, H.V., Schmidt, T.C., Abbau von Bisphenol S im Fenton System. Wasser 2018, Jahrestagung der Wasserchemischen Gesellschaft, Papenburg, Germany (oral presentation)

Wiegand, H.L., Orths, C.T., Lutze, H.V., Schmidt, T.C., Charakterisierung des Eisenperoxokomplexes in der Fenton-Reaktion. Wasser 2015, Jahrestagung der Wasserchemischen Gesellschaft, Schwerin, Germany (poster presentation)

Wiegand, H.L., Orths, C.T., Hupperich, K., Lutze, H.V., Schmidt, T.C., Nachweis und Charakterisierung eines intermediären $FeOOH^+$-Komplexes in der Fenton-Reaktion. Wasser 2016, Jahrestagung der Wasserchemischen Gesellschaft, Bamberg, Germany (poster presentation)

Wiegand, H.L., Hupperich, K., Orths, C.T., Lutze, H.V., Schmidt, T.C., Kinetic evidence and characterisation of an intermediate $FeOOH^+$-complex in the Fenton reaction. 1st International conference on sustainable water processing (ICSWaP), Sitges, Spain, 2016 (poster presentation)

Wiegand, H.L., Hupperich, K., Lüling, M., Orths, C.T., Lutze, H.V., Schmidt, T.C., Influence of organic ligands on formation and stability of the intermediate $FeOOH^+$-complex and $^{\bullet}OH$-yield in the Fenton reaction. Wasser 2017, Jahrestagung der Wasserchemischen Gesellschaft, Donaueschingen, Germany (poster presentation)

8.5 CURRICULUM VITAE

Aus Gründen des Datenschutzes ist in der Online-Version kein Lebenslauf enthalten.

8.6 DECLARATION OF SCIENTIFIC CONTRIBUTIONS

This thesis includes work that was published in cooperation with co-authors. My own contributions are declared in the following:

Chapter 3:

Hanna Laura Wiegand, Christian Timon Orths, Klaus Kerpen, Holger Volker Lutze, Torsten Claus Schmidt

Investigation of the iron peroxo-complex in the Fenton reaction: Kinetic indication, decay kinetics and hydroxyl radical yields, Environ. Sci. Technol., 2017, 51(24), pp.14321 - 14329

Declaration of own contribution: Experiments were performed by HLW with support of CTO. CTO conducted some of the experiments during a practical course. Planning and evaluation of experiments was done by HLW. KK was involved in the discussion of kinetic data. The manuscript was drafted and corrected by HLW. HVL and TCS revised the manuscript.

Chapter 4:

Hanna Laura Wiegand, Katharina Hupperich, Michelle Lüling, Christian Timon Orths, Holger Volker Lutze, Torsten Claus Schmidt

Influence of organic chelating agents on the Fenton reaction – Reaction kinetics and $^{\bullet}$OH-yields, submitted for publication in Chemosphere.

Declaration of own contributions: Experiments were conducted by HLW supported by KH, ML, and CTO. Experimental design as well as data interpretation was performed by HLW. The draft of the manuscript was written and corrected by HLW. HVL and TCS supervised the study and revised the manuscript.

Chapter 5:

Hanna Laura Wiegand, Mischa Jütte, Katharina Hupperich, Annika Kranefuß, Holger Volker Lutze, Torsten Claus Schmidt

Investigation of Factors influencing Fenton-based Degradation of Bisphenol S, submitted for publication in Chemical Engineering Journal.

Declaration of own contributions: Degradation experiments were performed by HLW, MJ, KH, and AK. HPLC measurements were conducted by MJ, KH, and AK. Recorded data were analysed by HLW. The draft of the manuscript was prepared and corrected by HLW. Revisions of the manuscript were done by HVL and TCS.

Chapter 6:

Hanna Laura Wiegand, Katharina Hupperich, Michelle Lüling, Holger Volker Lutze, Torsten Claus Schmidt

Formation of an aquated ferryl species in the reaction of Fe^{II} with O_3?

Declaration of own contributions: Experiments were planned by HLW and performed by HLW supported by KH and ML. HLW analysed recorded data and prepared the draft of the manuscript. Corrections of the manuscript were done by HLW. HVL and TCS revised the manuscript

8.7 ERKLÄRUNG

Hiermit versichere ich, dass ich die vorliegende Arbeit mit dem Titel:

“Characterisation of reactive species in the Fenton reaction - ˙OH vs. Fe^{IV}”

selbst verfasst und alle verwendeten Quellen und Hilfsmittel vollständig angegeben habe. Die vorliegende Arbeit wurde in dieser oder ähnlicher Form bei keiner anderen Universität eingereicht.

Essen, im Dezember 2018

_____

Laura Wiegand